

IntechOpen

Path Planning for Autonomous Vehicles

Ensuring Reliable Driverless Navigation
and Control Maneuver

*Edited by Umar Zakir Abdul Hamid,
Volkan Sezer, Bin Li, Yanjun Huang
and Muhammad Aizzat Zakaria*



Path Planning for Autonomous Vehicles - Ensuring Reliable Driverless Navigation and Control Maneuver

*Edited by Umar Zakir Abdul Hamid,
Volkan Sezer, Bin Li, Yanjun Huang
and Muhammad Aizzat Zakaria*

Published in London, United Kingdom



IntechOpen





Supporting open minds since 2005



Path Planning for Autonomous Vehicles – Ensuring Reliable Driverless Navigation and Control
Maneuver

<http://dx.doi.org/10.5772/intechopen.77593>

Edited by Umar Zakir Abdul Hamid, Volkan Sezer, Bin Li, Yanjun Huang and Muhammad Aizzat Zakaria

Contributors

Boyuan Li, Haiping Du, Bangji Zhang, Alfredo Toriz Palacios, Abraham Sánchez López, Alexander Cerón, Flavio Prieto, Luis Mejias, Mohamad T. Shahab, Moustafa Elshafei, Jaroslav Kozubek, Zdenek Flasar, Ivo Dumisinec, Agoston Restas, Jan Nohel, Petr Stodola, Umar Zakir Abdul Hamid

© The Editor(s) and the Author(s) 2019

The rights of the editor(s) and the author(s) have been asserted in accordance with the Copyright, Designs and Patents Act 1988. All rights to the book as a whole are reserved by INTECHOPEN LIMITED. The book as a whole (compilation) cannot be reproduced, distributed or used for commercial or non-commercial purposes without INTECHOPEN LIMITED's written permission. Enquiries concerning the use of the book should be directed to INTECHOPEN LIMITED rights and permissions department (permissions@intechopen.com).

Violations are liable to prosecution under the governing Copyright Law.



Individual chapters of this publication are distributed under the terms of the Creative Commons Attribution 3.0 Unported License which permits commercial use, distribution and reproduction of the individual chapters, provided the original author(s) and source publication are appropriately acknowledged. If so indicated, certain images may not be included under the Creative Commons license. In such cases users will need to obtain permission from the license holder to reproduce the material. More details and guidelines concerning content reuse and adaptation can be found at <http://www.intechopen.com/copyright-policy.html>.

Notice

Statements and opinions expressed in the chapters are those of the individual contributors and not necessarily those of the editors or publisher. No responsibility is accepted for the accuracy of information contained in the published chapters. The publisher assumes no responsibility for any damage or injury to persons or property arising out of the use of any materials, instructions, methods or ideas contained in the book.

First published in London, United Kingdom, 2019 by IntechOpen

IntechOpen is the global imprint of INTECHOPEN LIMITED, registered in England and Wales,

registration number: 11086078, The Shard, 25th floor, 32 London Bridge Street

London, SE19SG – United Kingdom

Printed in Croatia

British Library Cataloguing-in-Publication Data

A catalogue record for this book is available from the British Library

Additional hard and PDF copies can be obtained from orders@intechopen.com

Path Planning for Autonomous Vehicles – Ensuring Reliable Driverless Navigation and Control
Maneuver

Edited by Umar Zakir Abdul Hamid, Volkan Sezer, Bin Li, Yanjun Huang and Muhammad Aizzat Zakaria
p. cm.

Print ISBN 978-1-78923-991-1

Online ISBN 978-1-78923-992-8

eBook (PDF) ISBN 978-1-83962-285-4

We are IntechOpen, the world's leading publisher of Open Access books Built by scientists, for scientists

4,300+

Open access books available

116,000+

International authors and editors

130M+

Downloads

151

Countries delivered to

Our authors are among the
Top 1%

most cited scientists

12.2%

Contributors from top 500 universities



WEB OF SCIENCE™

Selection of our books indexed in the Book Citation Index
in Web of Science™ Core Collection (BKCI)

Interested in publishing with us?
Contact book.department@intechopen.com

Numbers displayed above are based on latest data collected.
For more information visit www.intechopen.com



Meet the editors



Umar Zakir Abdul Hamid, PhD, is one of the pioneering researchers in the autonomous vehicle (AV) field in Malaysia. Dr. Hamid was a member of the Intelligent Drive Team of the Vehicle System Engineering Research Group at the Universiti Teknologi Malaysia. The team researches Advanced Driver Assistance Systems (ADAS) and autonomous vehicles in Malaysia; previous collaborators include PROTON Holdings Berhad and the Smart Mobility Research Center (Tokyo). Dr. Zakir served as an AV Scientist with Moovita (Singapore and Malaysia) from 2017 to 2018, before embarking on a new journey as an AV Senior Engineer with Sensible 4 in Espoo, Finland. He is a reviewer for several prestigious journals and conferences in the automotive and robotics field.



Dr. Volkan Sezer received a BSc in Electronics and Telecommunication Engineering from Yildiz Technical University, Istanbul, Turkey, in 2005, and an MSc in Mechatronics Engineering and a PhD in Control and Automation Engineering from Istanbul Technical University, Istanbul, Turkey, in 2008 and 2012, respectively. His research covers mostly robotics and automotive technology. During his undergraduate studies, he founded and managed a student team in alternative energy vehicles. They developed a solar car and fuel cell car and were awarded in Turkey's national competitions. He also worked on a hybrid electric vehicle development project. He designed and applied a new energy management strategy to a real hybrid electric vehicle. During his graduate studies, he continued his research on hybrid and electric vehicles together with autonomous robots. He founded and managed the first autonomous vehicle project team and developed, along with three of his students, the first fully autonomous vehicle in Turkey. Dr. Sezer developed and applied several new methods in obstacle avoidance, speed planning, and low-level control of the vehicle. After obtaining his PhD, he worked as a researcher in Singapore for the Massachusetts Institute of Technology (MIT) in its Future Urban Mobility (FM) group. His fields of interest are autonomous/semi-autonomous ground vehicles, mobile robots, control of hybrid electric vehicles, trajectory planning, obstacle/collision avoidance, active safety in road vehicles, machine learning, control of hybrid electric vehicles, and energy efficiency.



Bin Li, PhD, is currently working with Aptiv PLC, USA, as Lead Algorithm Engineer, focusing on system architecture and algorithm development and verification of motion planning and control of autonomous vehicles. He received a PhD in Mechanical Engineering from Shanghai Jiao Tong University, Shanghai, China, in 2010. Dr. Li has more than 15 years' research experience in vehicle dynamics and control, electric vehicles, active safety, and autonomous driving. He has published more than 50 papers and chapters. He was a researcher on active safety control for commercial vehicles at Concordia University, a research engineer on mobile robotic control at McGill University, Montreal, Quebec, and a research fellow on next-generation electric vehicle at the University of Waterloo, Ontario, Canada. Dr. Li has been an active organizer for SAE World Congress and ASME conferences since 2015.



Yanjun Huang is a postdoctoral fellow at the Department of Mechanical and Mechatronics Engineering at the University of Waterloo, Ontario, Canada, where he received his PhD in 2016. His research interest is mainly on vehicle holistic control in terms of safety, energy savings, and intelligence, including vehicle dynamics and control, HEV/EV optimization and control, motion planning and control of connected and autonomous vehicles, and human-machine cooperative driving. Dr. Huang is also an associate editor for several international journals.



One of the pioneering researchers in the field of autonomous vehicles in Malaysia, Dr. Muhammad Aizzat Zakaria is a senior lecturer at Universiti Malaysia Pahang. His current research focuses on intelligent vehicle navigation. Dr. Zakaria has worked on the intelligent mobile robot systems of autonomous vehicles. He is also interested in working with robotic system modelling and mechatronic systems for robotic intelligent control applications.

Contents

Preface	XIII
Section 1 Path Planning for Autonomous Vehicles	1
Chapter 1 Introductory Chapter: Roles of Path Planning in Providing Reliable Navigation and Control for Autonomous Vehicles and Robots <i>by Umar Zakir Abdul Hamid, Volkan Sezer, Bin Li, Yanjun Huang and Muhammad Aizzat Zakaria</i>	3
Chapter 2 Military Factors Influencing Path Planning <i>by Jaroslav Kozůbek, Zdeněk Flasar and Ivo Dumišinec</i>	9
Section 2 Path Planning in Varied Environments	27
Chapter 3 Path Planning for Autonomous Vehicle in Off-Road Scenario <i>by Boyuan Li, Haiping Du and Bangji Zhang</i>	29
Chapter 4 Vision-Based Path Finding Strategy of Unmanned Aerial Vehicles for Electrical Infrastructure Purpose <i>by Alexander Cerón, Flavio Prieto and Luis Mejias</i>	51
Chapter 5 Extending the Limits of the Random Exploration Graph for Efficient Autonomous Exploration in Unknown Environments <i>by Alfredo Toriz Palacios and Abraham Sánchez López</i>	63
Section 3 Towards an Optimal Path Planning	77
Chapter 6 Model of the Optimal Maneuver Route <i>by Jan Nohel, Petr Stodola and Zdeněk Flasar</i>	79

Chapter 7	101
Path Planning Optimization with Flexible Remote Sensing Application <i>by Agoston Restas</i>	
Chapter 8	119
Distributed Optimization of Multi-Robot Motion with Time-Energy Criterion <i>by Mohamad T. Shahab and Moustafa Elshafei</i>	

Preface

The full implementation of autonomous vehicles on a large scale, despite appearing to be far off, is inevitable. One of the biggest challenges for autonomous vehicle navigation and manoeuvrability is to assure the vehicle's ability to react instantaneously to potential hazards in its environment. This requires the formulation of a dependable path planning strategy. Path planning re-plans the autonomous vehicle's original reference trajectory based on the environmental information provided by the vehicle's perception modules. Despite the amount of work done in the areas of autonomous vehicles and mobile robots, real-time implementation still faces some challenges. This is due to the dynamic nature of the real world. For example, a commonly traversable road can suddenly be subject to continuous changes in its landscape due to reconstruction, thus creating hindrances for driverless navigation. This requires dependable planning modules for the driverless platform to provide reliable reference routes for the vehicle. Regarding autonomous mobile robots, manoeuvring in a narrow and scattered environment is also a challenge. Thus path planning is a challenge to be addressed in many fields.

This book is based on our combined experiences in the fields of automated driving and vehicle controls. The editors are experienced researchers from Finland, Turkey, the United States, Canada, and Malaysia who have worked extensively in the field of autonomous vehicles and mobile robots. We would like to thank all of the reviewers and authors involved in creating this volume.

In this book, we provide introductory ideas on the topic of 'path planning' to not only researchers but interested readers alike. The content is not limited to path planning algorithm formulation for road vehicles; it also explores the topic in the context of mobile robots, off-road scenarios, multi-robot motion, and unmanned aerial vehicles (UAVs).

The book is divided into three sections. The first section, 'Path Planning for Autonomous Vehicles' provides the introduction to the book. It includes a discussion of the factors that influence path planning for autonomous military vehicles. The second section, 'Path Planning in Varied Environments', discusses path planning as it relates to different use cases, such as off-road vehicles and UAVs, and the themes of unknown environment exploration. The final section, 'Towards an Optimal Path Planning', explores path planning in the off-road scenario, followed by a discussion of optimizing driverless navigation by integrating path planning and control strategies.

In conclusion, for wide implementation of autonomous vehicles to come to fruition, the question is not 'Can it be done?' but rather 'How do we do it safely?' The first

step in answering this question is a discussion of path planning as presented in this book.

Dr. Umar Zakir Abdul Hamid

Sensible 4 Oy,
Finland

Dr. Volkan Sezer

Associate Professor,
Istanbul Technical University,
Turkey

Dr. Bin Li

Aptiv PLC,
United States of America

Dr. Yanjun Huang

University of Waterloo,
Canada

Dr. Muhammad Aizzat Zakaria

Universiti Malaysia Pahang,
Malaysia

Section 1

Path Planning for Autonomous Vehicles

Introductory Chapter: Roles of Path Planning in Providing Reliable Navigation and Control for Autonomous Vehicles and Robots

*Umar Zakir Abdul Hamid, Volkan Sezer, Bin Li,
Yanjun Huang and Muhammad Aizzat Zakaria*

1. Introduction

Shared, connected, and driverless vehicles have been the discussion of many researchers, and autonomous vehicle (AV) itself is considered as a highly disruptive emerging technology. One of the examples of its disrupting feature is when 11 major automotive companies which include BMW, Daimler and Volkswagen have collaborated and published a white paper entitled “Safety First for Automated Driving” in 2019 to address the topic [1]. With the predicted market value of US\$7 Trillion by 2050 for the automated driving segments, it is hard to ignore the highly disruptive effects that the AV will deliver [2, 3]. In addition to the ongoing development of the autonomous vehicles’ platforms, to complement for its expanding advancement, the discussion is also now reaching other topics such as the mobility-as-a-service (MaaS), city infrastructures as well as policy-making [4–6].

2. How does autonomous vehicle work?

Generally, in addition to the hardware requirements, a high-level autonomous vehicle software module comprises of the perception and vision, localization and mapping as well as the guidance, navigation and control modules (**Figure 1**). The combination of these modules yields an ability to compensate for the driver’s absence during the navigation. AV, in any case, should possess the ability to measure the risk surrounding its environment as well as guiding the vehicle motion. In addition, a driverless vehicle is also expected to compensate for the absence of a human driver by possessing the required intelligence to mimic the human driving behavior of the vehicle.

The smooth and comfortable automated driving experience requires the expertise of interdisciplinary fields, which includes the development of required hardware and software integration. In the case of road navigation of an autonomous vehicle, the vehicle is typically expected to navigate independently during the entire

driving process. This implies that the vehicle is fully responsible for preventing any unwanted incidents.

In a controlled environment, the use of predefined information of the environment is usually sufficient. However, in the risky scenario that demands the AV to react to its environment, the usage of dependable path planning strategies to replan its current reference or trajectory is demanded.

3. Path planning

Path planning (PP) is the computation of a maneuverable path from an initial point to a terminal point, which the host vehicle or robots tracks and follows [8, 9]. Despite much of the works done in the PP fields for autonomous robots and vehicles, real-time implementation still possesses some challenges. This is due to the dynamic nature of the environment of the real world. For example, a road that is usually traversable can abruptly be having a continuous change in a construction site. This requires dependable PP for AV to provide reliable reference path for the vehicle. In addition, for the discussion of autonomous mobile robots, the maneuver in the narrow scattered environment is also a challenge. Thus, PP does not only revolve on the topics of moving from point A to B, but instead, the challenges are of large scales.

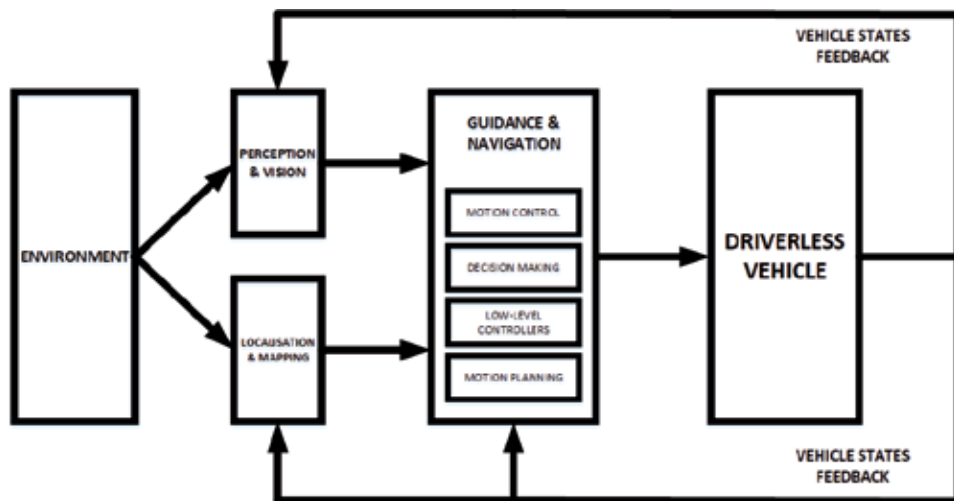


Figure 1. Modules of driverless vehicles [7].

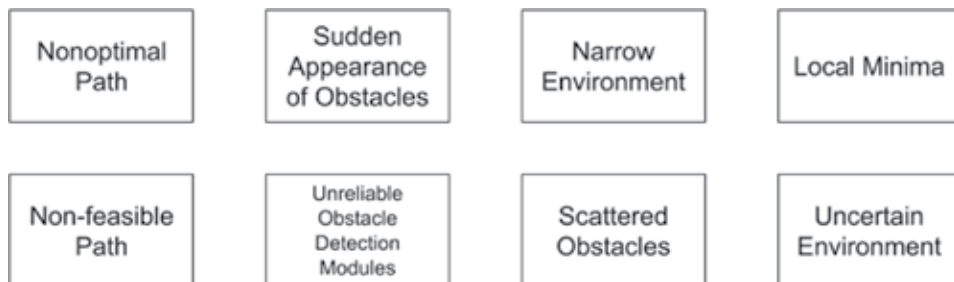


Figure 2. Challenges and issues for path planning of autonomous vehicles [12–14].

3.1 Challenges of path planning

Due to the rapid progress of works done in recent years, the implementation and validation of AV development have been performed in varied environments, which include harsh-weather conditions and city environment, among many others [10, 11]. These studies have led to the identification of previously known and new issues in the path planning topics, with some of them being highlighted in **Figure 2**. For brevity, details of the listed issues can be found in the following references [12–14]. Thus, to ensure reliable and safe navigation by AV and autonomous robots, it is evident the necessity to understand the topics of PP.

4. Aim of the book and its organization

Realizing the importance of the path planning topic for autonomous vehicles and robots, this book is written. With the open-access publication concept, the book is hoped to give the introductory ideas to the researchers and the general audience about the topics. It is co-edited by researchers who have worked extensively in the field of autonomous vehicles and robots from Finland, Turkey, USA, Canada as well as Malaysia.

It is important to be mentioned that this book does not aim to solve and highlight each of the available PP issues. But instead, it tries to present as many topics and issues as possible to give the wide idea of path planning. As automation of the vehicles does not only cover the road vehicles, the book will also cover the autonomous vehicle for the off-road, military, and unmanned aerial vehicles (UAV). Despite the different type of vehicle and robot, the ethos of the discussions can still be adapted to the varied platforms.

5. Conclusion and expectations

We hope this introductory chapter and the book will be able to indicate and give ideas on the issues related to PP topics, where the authors explore the topics of PP in the context of road vehicles, robots, off-road scenario, multi-robot motion, and UAVs.

For further reading following the discussions in this book (which serve as the introductory ideas for new researchers), we are recommending the topics of path planning as an active safety feature of AV, which includes the collision avoidance theme, among many others. We believe the knowledge of path planning will help researchers in developing safer collision avoidance system for AV.

Concluding, for a wide implementation of AV to be seen, the questions are not limited to “Can it be done?” but instead, the real question is “How do we do it safely?”. And the discussion of PP is one of the prerequisites of a safe AV. With the open access nature of the book, it is hoped that the discussion reaches as much as possible audience.

Acknowledgements

The editors would like to thank all the reviewers and authors involved in the works.

Author details

Umar Zakir Abdul Hamid^{1*}, Volkan Sezer², Bin Li³, Yanjun Huang⁴
and Muhammad Aizzat Zakaria⁵

1 Sensible 4 Oy, Finland

2 Istanbul Technical University, Turkey

3 Aptiv PLC, United States of America

4 University of Waterloo, Canada

5 Universiti Malaysia Pahang, Malaysia

*Address all correspondence to: umar.hamid@sensible4.fi

IntechOpen

© 2019 The Author(s). Licensee IntechOpen. This chapter is distributed under the terms of the Creative Commons Attribution License (<http://creativecommons.org/licenses/by/3.0>), which permits unrestricted use, distribution, and reproduction in any medium, provided the original work is properly cited. 

References

- [1] Safety First for Automated Driving. Bmw Group. 2019. Available from: <https://www.press.bmwgroup.com/global/article/detail/T0298103EN/automotive-and-mobility-industry-leaders-publish-first-of-its-kind-framework-for-safe-automated-driving-systems> [Cited July 09, 2019]
- [2] Lanctot R. Accelerating the Future: The Economic Impact of the Emerging Passenger Economy. Intel & Strategy Analytics; 2017. Available from: <https://newsroom.intel.com/newsroom/wp-content/uploads/sites/11/2017/05/passenger-economy.pdf>
- [3] Ab Rahman A, Hamid UZA, Chin TA. Emerging technologies with disruptive effects: A review. *Perintis e-Journal*. 2017;7(2):111-128
- [4] Coppola P, Silvestri F. Autonomous vehicles and future mobility solutions. In: *Autonomous Vehicles and Future Mobility*. Elsevier; 2019. p. 1. Available from: <https://www.elsevier.com/books/autonomous-vehicles-and-future-mobility/coppola/978-0-12-817696-2>
- [5] Bojic I, Braendli R, Ratti C. What will autonomous cars do to the insurance companies? In: *Autonomous Vehicles and Future Mobility*. Elsevier; 2019. p. 69
- [6] Hawkins J, Nurul Habib K. Integrated models of land use and transportation for the autonomous vehicle revolution. *Transport Reviews*. 2019;39(1):66-83
- [7] Maurer M, Gerdes JC, Lenz B, Winner H. *Autonomous Driving*. Vol. 10. Berlin, Germany: Springer Berlin Heidelberg; 2016. pp. 978-983
- [8] Patle BK, Babu LG, Pandey A, Parhi DRK, Jagadeesh A. A review: On path planning strategies for navigation of mobile robot. *Defence Technology*. 2019. DOI: 10.1016/j.dt.2019.04.011. Available from: <https://www.sciencedirect.com/science/article/pii/S2214914718305130>
- [9] Mohanan MG, Salgoankar A. A survey of robotic motion planning in dynamic environments. *Robotics and Autonomous Systems*. 2018;100:171-185
- [10] GACHA—Self-driving Shuttle Bus for All Weather. *Sensible4*. 2019. Available from: <https://www.sensible4.fi/gacha/> [Cited: July 09, 2019]
- [11] Caesar H, Bankiti V, Lang AH, Vora S, Liong VE, Xu Q, et al. nuScenes: A multimodal dataset for autonomous driving. *arXiv preprint arXiv:1903.11027*; 2019
- [12] Trigatti G, Boscarriol P, Scalera L, Pillan D, Gasparetto A. A new path-constrained trajectory planning strategy for spray painting robots-rev. 1. *The International Journal of Advanced Manufacturing Technology*. 2018;98(9-12):2287-2296
- [13] Wang W, Zuo L, Xu X. A learning-based multi-RRT approach for robot path planning in narrow passages. *Journal of Intelligent and Robotic Systems*. 2018;90(1-2):81-100
- [14] Noreen I, Khan A, Habib Z. Optimal path planning using RRT* based approaches: a survey and future directions. *International Journal of Advanced Computer Science and Applications*. 2016;7(11):97-107

Military Factors Influencing Path Planning

Jaroslav Kozůbek, Zdeněk Flasar and Ivo Dumišinec

Abstract

The chapter discussed and considered the factors that influence the path planning for military purposed autonomous vehicles. The planning of movement (path planning) for autonomous vehicles is complex process influenced by many categories of factors. The complexity of autonomous vehicles path planning is dramatically increasing in military operational environment when the confrontation with enemy is expected. From operational point of view, it is necessary to be considered in which military domain the autonomous vehicles will operate, for example, in Land domain, Air domain or Sea domain. From tactical point of view, there will be group of common factors for each domains and group of different factors for specific domain. As much as possible factors which will be included in consideration of path planning as the part of mathematical algorithms will increase the prerequisite for successful fulfilling of assigned tasks and missions.

Keywords: path planning, military factors, domains, operation environment

1. Introduction

Within last decade the utilization of autonomous vehicles during waged military operations significantly increased in importance. The main factor of their utilization was protection and safe lives of own soldiers or contributors. This trend will surely continue and become relevant in the future as well.

In military operations the decision support systems for utilization of autonomous vehicles have become an integral part of the commander's decision-making process [1]. One of the models of autonomous vehicles are Unmanned Aerial Systems (UAS) mainly utilize for reconnaissance which is the part of the Tactical Decision Support Systems (TDSS) developed at University of Defence, Czech Republic [2]. This system aims at supporting commanders of the Czech Army with their Military Decision-Making Process (MDMP). More detailed information about the integration of TDSS into commander's Troop Leading Procedures (TLP) can be found in [3]. Reconnaissance is one of the crucial parts of intelligence support. Intelligence support is the one of the essential part of MDMP to find a solution for a specific problem allowing to fulfil the assigned mission. It consists of models of military tactics. Each model can solve the corresponding task.

One of many important models in military tactics is the optimal cooperative reconnaissance which is a problem when an area of interest needs to be searched (observed) by multiple military elements (scouts, UAVs, UGVs) as quickly as possible [4].



Figure 1.
Military domains in operational environment.

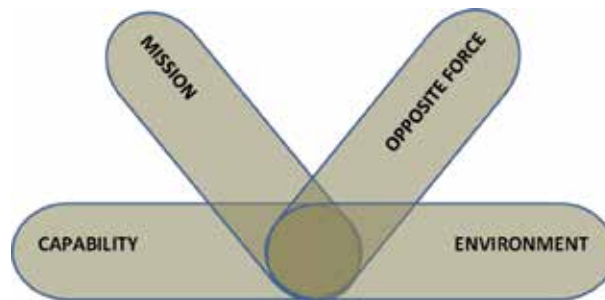


Figure 2.
Categories of factors-steps for consideration and planning.

The operational environment¹ generally consists of factors and conditions that must be understood to successfully apply military capabilities protect the force and complete the mission. It influences the completion of a single mission as well as an entire campaign and its constituent elements [5]. The operational environment includes the sea, land, air and space, the enemy, neutral, friendly and other actors, facilities, weather, terrain, electromagnetic spectrum (EMS) CBRN threats and hazards, and the information environment (e.g., **Figure 1**).

The operational environment of the armed conflicts was, is and will be very diverse and it is involving many aspects. The armed forces must be able to perform a wide range of tactical activities in different domains as Land, Air, Sea, Cosmic and Cyber [5].

Both (all) fighting parties will strive to achieve their goals in the most effective way, including minimizing their loss of life and deployed resources. One of the ways to minimize the loss of lives is the utilization of modern technical means-as autonomous vehicles could be.

Nowadays the predominant domain where fighting parties operate by soldiers is Land. But the most significant domain to gain domination by forces is Air. The multiplier of requested armed forces capabilities to effectively operate in each domain is electromagnetic spectrum.

Focusing on solving issues the Land domain is the most demanding for autonomous vehicles path planning. For ground autonomous vehicles path planning

¹ According to Allied Administrative Publication 6 (AAP-6) the operational environment is defined as: *A composite of the conditions, circumstances and influences that affect the employment of capabilities and bear on the decisions of the commander.*

is possible to apply the analogical approaches as for military units movement planning.

Movement can be understood in broad terms as relocating someone from point to point in order to create conditions for and to be capable carry out particular planned activities after the move is over.

There has to be considered amount of factors that affect the move and the goals set for it (e.g., **Figure 2**). The first step in movement consideration is capability (parameters, technical data) of the autonomous vehicle itself, the second step is the autonomous vehicles mission (recce, destroy, cooperate, transport, refuel, etc.), the third step is opposite acting force and the last step is complexity of environment (terrain, weather, temperature, visibility, etc.).

2. Capability of autonomous vehicles

Most modern armies, assessing, in particular, combat vehicles and its combat capability, evaluate four basic parameters:

1. combat power/special purpose ability,
2. protection (if applicable) of the crew (subsystems),
3. mobility,
4. signal and command.

The utilization of autonomous vehicles for military purposes can be considered in two basic missions, as lethal or non-lethal assets. Within both types of mission the opposite side tries to eliminate autonomous vehicle or to capture it. For development of autonomous vehicle to be used by military purpose should be considered the same approach as for development of the combat vehicles operated by soldiers. The parameters of autonomous vehicles have to meet maximum of factors which are influencing its movement.

According to author's long-life military experiences and deep and comprehensive analysis of the facts in the Army of the Czech Republic Lessons Learned Databases [6] the capabilities of autonomous vehicles can be considered in following ways.

The combat power of the autonomous vehicle will consist of the ability to meet the desired goal. This goal can be "only" to carry out monitoring and to find out the required information about the enemy, the task environment and their transfer to appropriate locations, detect the presence of undesirable substances in the area of operation, and warn troops about the presence of such substances until possible destruction of the enemy and its objects. Autonomous vehicle will be equipped with appropriate sensors and devices for special sub-tasks.

It is necessary to consider the degree of autonomy of the resource for the **issue of protecting** the crew of an autonomous vehicle. Fully autonomous vehicle will be equipped with an artificial intelligence that will enable him to perform the task without any human intervention (collaboration), from his deployment to the fulfilment of the task, including eventual return to assigned assembly area. Partial autonomy may consist in the necessity or only the possibility of intervening in the selected phases of the autonomous vehicle implementation by the operator. The operator may, depending on the specific conditions on the battlefield and their change over the autonomous vehicle deployment planning phase, correct and control selected functions and their interdependence.

Partly autonomous means can be considered as a means of transporting directly to this device, although some of the required functions will be automated and autonomous vehicle operators will either not influence at all or will be able to correct them. Under the declared crew protection (operator), we can understand the “only” protection of the entire device and its component components and sensors in the case of autonomous vehicle.

Like a standard combat vehicle, the autonomous vehicle should be able to withstand the effects of the environment (weather conditions, fulfillment of the task within the required temperature range, in dusty and other environments, etc.) as well as enemy effects in the form of explosive firefighting systems, enemy fire interventions to a certain caliber, contamination or ignition of autonomous vehicle area of operation, etc. An important role in the area of autonomous vehicle resilience and its ability to move and perform tasks in a particular environment will play the location of its components and sensors on the “base” of autonomous vehicle. It can be said that the autonomous vehicle as a whole will be so resistant to environmental influences (both natural and caused by human factor), how least its component, component, sensor will be resistant. Both in the profile (overlapping the sensor above the “base” of the autonomous vehicle) and attaching this sensor to the “base” of the autonomous vehicle and its cabling.

The autonomous vehicles should have the required **mobility parameters**, the ability to perform tasks in the widest possible sense of the word mobility. For most moving assets, and not only for the vehicles used by the army, the following parameters are listed:

- the average speed of the resource depending on the specific communication-on the road, on the ground, etc.,
- maximum travel speed,
- acceleration (usually from zero to desired or maximum),
- ability to overcome climb/descent (usually expressed as a percentage),
- side tilt (usually in degrees),
- crossing the obstacle and pitch,
- consumption and necessity of refueling,
- range,
- the height, width and weight,
- ability to overcome water barriers and a number of other parameters.

Mobility is also related to **terrain throughput**. A tactical view of terrain patency typically features three stages-through terrain (where no action is needed to move the device), partially through terrain (in which action must be taken towards the device or field so that it can be (although some radical measures could be taken to penetrate the terrain, but these measures would be inefficient for time or other reasons). The landing area of autonomous vehicle also relates to its undercarriage. There are terrains that are more suitable for wheeled chassis and on the contrary are terrains that can be easily overcome with tracked chassis. The ideal autonomous vehicle, which would be deployed in different terrain, could have a combined bogie

(wheel and belt) where it would autonomously (based on artificial intelligence) evaluate the most suitable variant of the chassis and “deploy” itself (it would move from one platform to second, or the process could be managed by the operator. Similarly, the problem of adhesion conditions could be solved in the sense of increasing or decreasing the contact surface of the undercarriage with the terrain, or an automatic or operator controlled change of autonomous vehicle aperture. For example, in the Russian army some combat vehicles have been introduced, which can change the clearance by up to 30 cm during the movement.

If the vehicle’s clearance (vehicle) changes during movement, logically this will change the position of the center of gravity of the device. Due to the generally small dimensions of autonomous vehicle compared to other combat vehicles, the change in autonomous vehicle center of gravity may radically change (as a rule reduce) some other mobility-related features such as side tilt, climb/descending, etc. But this problem is technically feasible for autonomous vehicle. It can be envisaged that by changing the autonomous vehicle’s aperture and thus increasing the center of gravity of the device, the autonomous vehicle could either autonomously or by an operator’s intervention modify the axle or half-axle of the undercarriage so that on one side of the bottom of the “hull” the second is lower, and the original offshore characteristics can be achieved. With mobility, the dimensions, profile and weight of the autonomous vehicle and its parts, components and sensors are logically related.

The parameters in the **area of signal and command** can be included:

- source sufficiency of the autonomous vehicle as a whole and its individual components (to fulfill their functions),
- the reach of command and control means in case the autonomous vehicle is not completely autonomous (will be operated by the operator),
- transferring data and information obtained by the autonomous vehicle in real-time tasks, various data paths, or even confidentially,
- resistance to interference with the autonomous vehicle control and information transmission system and more.

To fulfill task in any mode of autonomy, the device must be equipped with the most accurate information, parameters and programs. Ideally, autonomous vehicle would be able to “retrieve” real-world information (such as changing the terrain and the terrain, etc.) into its software and, if necessary, by the operator to correct the data and update it.

Among autonomous vehicle requirements that can be perceived as borderline between “combat power” and “mobility”, views such as:

- in what environment, in terms of an unfriendly/friendly atmosphere, the autonomous vehicle will move and perform tasks;
- whether their mission will be demonstrative or will be interested in secrecy (until the possible use of lethal weapons) and some others.

3. Mission of autonomous vehicles

Autonomous vehicles (ground or air) are especially valuable in environments where immediate information feedback is needed, manned ground or air vehicles

are unavailable or excessive risk or other conditions render use of manned vehicles less than deliberate. The autonomous vehicles can conduct day and night operations to support units.

The autonomous vehicle missions can include:

- Route, area, object and zone reconnaissance,
- Surveillance of named areas of interest (NAIs),
- Adjusting indirect fire weapons, close air support (CAS), and close-in fire support (CIFS),
- Support to:
 - Combat search and rescue (C-SAR),
 - Target acquisition (TA),
 - Battle damage assessment (BDA),
 - Rear area security,
 - Situation awareness (SA) development,
 - Intelligent preparation of battlefield (IPB),
 - Electronic warfare (EW),
 - Communications relay,
 - Mine and chemical detection,
 - Mine cleaning,
 - Weather surveillance,
 - Material and munition resupply,
 - Casualty evacuation.

In case of that autonomous vehicle is equipped by a weapon system (considered as a combat vehicle) it can fulfill combat missions to destroy enemy in open terrain, in vehicles or covered in shelters or in buildings.

Special consideration for mission planning is if autonomous vehicle act independently (alone) or act in cooperation with other vehicle or with units (soldiers) or act in swarming collaboration (dozens of vehicles).

4. Opposite force

The basic factor in the use of the autonomous vehicle will be the possibility of a conflict with the enemy. This factor is based on all other factors and, in particular, on autonomous vehicle technology. In the case of a high probability of a conflict with the enemy it will put demands on the protection of the autonomous vehicle,

weapon system, observation systems and autonomous vehicle cloaking. The enemy's factor will further affect the mobility and speed of the autonomous vehicle, which also affects its navigation on the battlefield.

Factors affecting autonomous vehicle movement within conflict with the enemy:

- audio concealment of the enemy movement,
- thermal confidentiality of movement before the enemy,
- vulnerability to air strikes and other enemy means,
- opportunity to observe and conduct fire,
- the ability and speed of capturing advantageous lines or firing positions on the battlefield,
- way of recognizing the enemy,
- start and firing time,
- selection of an effective weapon system to destroy the enemy,
- setting elements for shooting to effectively destroy the enemy,
- possibilities of camouflage,
- the possibility of protection by using space-saving,
- ability to overcome obstacles (see below),
- ability to move at night and under reduced visibility.

5. Environment

Last but not least, the type of autonomous vehicle will influence the intent to use in a specific environment in which the autonomous vehicle fulfills and performs the desired activity. Completely different requirements for autonomous vehicle design, parameters and technology will have an urbanized, hilly and wooded environment and other desert or arctic environment.

The limitations set out help us to specify what type of autonomous vehicle is best for our purposes in order to efficiently use and meet the desired goals of the operation. The following list of factors applies without limitation to all autonomous vehicles. Which factor and level of its impact on the move depends on the choice of the type of autonomous vehicle.

5.1 Geographical factors

One of the basic groups of factors influencing autonomous vehicle movement are factors of a geographical nature. Area of operation will fundamentally affect the process of planning and executing autonomous vehicle moves. Combined with another factor such as weather, these factors are no less important as an opposite force (enemy).

For autonomous vehicle used out of the contact with the enemy for supporting and logistic operations, a set of geographic and hydro meteorological factors are more important than tactical factors.

Geographic factors affecting autonomous vehicle path planning are:

- incline of the terrain relief,
- terrain throughput,
- elevation of the terrain,
- terrain load capacity,
- hide and cover options,
- ability to evaluate key terrain for maneuver,
- frequency of roads and their type (paved, unpaved, forest, etc.)
- the width and clear height when moving along roads,
- characteristics of shores (banks) of waterways and streams,
- the width and depth of rivers, streams and waterways,
- nature of water areas,
- water flow and river flow rate,
- ability to overcome artificially created obstacles.

5.1.1 Terrain relief

The relief of the terrain is the most important element of the physical-geographic conditions at the theater (area of operation). It has an impact on the preparation and conduct of the fighting activities of the troops and especially on their mobility. The fragmentation of the terrain in specific areas of operation determines the choice of the most appropriate directions of the autonomous vehicle activities, its correct evaluation and the use of the peculiarities of the types and shapes of the relief can contribute to the surprising maneuver or to the complete concealment of the movements. The significance of the relief increases with growing fragmentation and altitude.

5.1.2 Terrain throughput

The effect on throughput (cross-country) or activity in the area of operation has obstructions that are either natural or created by human activity. The examples of effects which are obstructing movement of autonomous vehicles are mentioned in Section 5.1.5.

Another aspect of the terrain throughput when moving troops on unpaved roads and in the open terrain is the assessment of their condition, taking into account parameters of the physical condition of the subsoil, which vary depending on the season and the hydro-meteorological conditions.

In the case of forestry throughput, the main factor influencing the use of autonomous vehicle is its inclination. In the case of openness, open-air space will be

influenced by the types of vegetation (shrubs, grasses or trees), their density and the space among trees.

5.1.3 Shelters and covers

Evaluating and optimizing the use of terrain shelters and covers will provide autonomous vehicle high level of protection as well as confidentiality of movement. It also makes it possible to estimate possible access routes to the mission area, and the intended gathering points or directions of action of enemy units.

Hidden access and free movement create, depending on the mission in a military operation, so-called key areas. Their knowledge provides a significant advantage in realizing the intentions of who controls the given key space.

5.1.4 Terrain load capacity

The decisive influence on the behavior of autonomous vehicle has the properties of the earth surface with which the vehicle meets its wheels (belts). This surface can be divided into “pavements” (suitably treated surface) and “terrain” (modified only partially-forest or field roads-or not modified at all).

Defining the surface type (grass, asphalt, sand, etc.) characterized by a certain degree of adhesion and rolling resistance is another sub-parameter that will affect autonomous vehicle shifts.

Soil conditions, along with current meteorological conditions (especially rainfall and air and soil temperatures) are logically another factor that cannot be overlooked when planning autonomous vehicle shifts as they greatly affect the autonomous vehicle rate of movement.

5.1.5 Obstacles

Obstacles generally prevent the maneuver from making or directing it from spaces with more favorable or disadvantageous conditions for its implementation. For autonomous vehicle needs, it is necessary to define the types of major obstacles and the autonomous vehicle activity when dealing with the obstacle. It is also necessary for each autonomous vehicle to be able to evaluate the tactical importance of the obstacle at a certain stage of the combat task and to be able to use the obstacle to its own advantage or against the enemy’s activity.

Natural obstacles:

- vegetation:
 - species and types of forests and wooded areas,
 - shrubs and ravines
 - sets,
 - hop,
- water:
 - rivers,
 - streams,

- water tanks,
- marshes,
- swamps,
- wetlands.

Artificial obstacles:

- communication:
 - road,
 - railways,
 - bridges and bridges,
 - passes,
 - tunnels,
 - fords,
- utilities:
 - power lines,
 - pipelines.
- built up areas:
 - buildings and blocks of buildings,
 - power stations,
 - railway station,
- other objects:
 - chimneys,
 - masts,
 - towers,
 - lookout towers.

5.2 Hydro-meteorological factors

Hydro-meteorological conditions create advantages and disadvantages for both the enemy and the troops. Thanks to good knowledge of conditions and correct weather information, we can streamline our own troops and also minimize their adverse effects.

Weather in conjunction with the terrain forms an inseparable and mutually integrated system. The weather affects the visibility, the function of the sensors and the weapons used, the autonomous vehicle's operability, but and already mentioned terrain passage. An important aspect of the weather is that the effect of changing weather does not have to valid information recorded on maps.

In the summer season, the use of ground autonomous vehicle affects above all high air temperature, high dustiness and difficult driving conditions.

By increasing the humidity in the soil, it becomes more difficult to move the fighting techniques to such an extent that the unpaved roads become unstable. The exception is sandy soils, which are dry in the dry state, they are more solid and passable during the wet season.

In winter, the strength of the soil without the snow cover depends on the degree of freezing of the surface layer. At melting (thaw) the thickness of the thawed layer and the frozen layer below it.

Climate factors affecting autonomous vehicle:

- air temperature,
- air pressure,
- humidity and water vapor,
- cloudiness,
- visibility and visibility,
- wind conditions,
- collisions,
- sunshine and radiation.

5.2.1 Air temperatures

Temperature is one of the basic characteristics of the atmosphere. It characterizes the heat state of the air.

Low air temperature in the winter period causes a change in the physical properties of fuels, lubricants and operating materials. It also reduces the capacity of autonomous vehicle batteries. It also works the temperature of the motors, the power of the electrical triggering device and the degree of mechanical wear.

High ambient air temperature adversely affects engine operation. It also affects engine cooling, when less air is sucked into the cylinders. Water and operating fluids are also rapidly evaporating. Higher temperatures risk engine overheating.

5.2.2 Air pressure

All atmospheric objects and the Earth's surface are affected by the pressure caused by the weight of the atmosphere. Changes in pressure are closely related to the development of basic atmospheric processes. Extremely high or low air pressures can affect the autonomous vehicle control and measurement sensors, observation devices or autonomous vehicle navigation modules.

5.2.3 Humidity

Increased air humidity is manifested especially in winter. For the operation of any technique the optimum relative humidity is around 60%. The functions of all groups and subgroups into which the air is accessible are influenced by the high content of water vapor in the air. In the long run, corrosion can occur, thus rendering any part of autonomous vehicle unnecessary. From a tactical point of view, it is possible to ignite and fog the sighting devices, sighting or significant corrosion of parts of weapon systems.

5.2.4 Visibility

Visibility is the maximum distance to which the contours of the object observed in daylight under normal human eye conditions can still be distinguished. At night, it is the longest distance to which light can be distinguished by steady and dimly changing luminosity. Visibility is most affected by precipitation and fog and is therefore dependent on the presence of solid particles and water condensation products in the atmosphere.

Visibility is one of the most important meteorological elements influencing combat activity.

It has a major impact on the exploration, discovery and recognition of the enemy and its activities, the determination of landmarks, and the effective destruction of the enemy's ground and air targets.

5.2.5 Wind conditions

Wind may be a cause that will not allow the required combat tasks to be accomplished. Due to strong winds, the autonomous vehicle may be delayed. And also when it comes to the side wind to overturn the autonomous vehicle and hence the inability to continue moving. Combined with rain or snow, it may icy optical devices or sensors (sensors) and thus makes it impossible to control the autonomous vehicle or to limit its (combat) capabilities.

5.2.6 Precipitation

Precipitation (rain-fall) are a significant factor and have a great impact on soil conditions and thus the slopes of slopes, roads and terrain especially during winter (snow and deep snow). This is mainly the longest rain, after which the soil is saturated with water and thus decreases its load capacity. Long-term precipitation also causes significant changes in the nature of watercourses and surfaces.

In the case of storms, there is a risk of interference with autonomous vehicle thus the decommissioning of its electronic systems.

6. Military factors evaluation for path planning

Proposed factors were identified as the outputs of complex analysis of the facts in the Army of the Czech Republic Lessons Learned Databases [6] and compared by outputs gained from The Army of the Czech Republic Units Leaders who are using military designed autonomous vehicles for fulfilling the military missions.

Factors should not only be considered as factors that negatively affect autonomous vehicle's movement. The opposing forces (enemy) vs. our own can be stated in a general sense that if something adversely affects the activity of the enemy, it is for the

own forces an advantage, a positive influence and vice versa. Positive influences must be able to use by autonomous vehicle, negatively minimize or completely suppress.

Some of the above aspects and autonomous vehicle requirements may be conceived at the same time as the factors that will movement of the autonomous vehicle both during the planning phase of the movement and during the management phase of the movement. Some aspects (factors) will be influencing ground autonomous vehicle, the same factor can affect the air autonomous vehicle in a radically different way and intensity.

The influence of this factor can be assessed by different approaches:

- has an effect-it does not affect;
- has a major influence-it has influence-it does not affect (possibly a wider range);
- weight of individual influences-percentage (or point) representation of individual influences, etc.

To more precisely the range of effects and the weight of the individual effects on the autonomous vehicle movement will be determined the better equipped autonomous vehicle could be designed (HW and SW) in order to eliminate or reduce the effects of negative influences and will ultimately be higher quality (reliable, faster, with minimizing losses, ...) a combat mission is met. However, the weight of individual influences will likely be variable in relation to the specific task the autonomous vehicle has to fulfill. **The goal to be attained will always be decisive!** And the objective of the mission can be characterized primarily by time, of the type "Fulfill the task even with possible losses, but the decisive criterion is that it must be fulfilled by ..." In another mission, the primary criterion may be an effect on the target area, such as "Detect the enemy and destroy it; until you do, do not return!" If necessary, "Complete the task with minimal losses on your own side!", etc. So it is important and decisive to be aware of the factors that influence the movement of autonomous vehicle in the specific situation and the specific task and then assign these factors their specific weight.

The fulfillment of the autonomous vehicle task with the acceptance of individual factors and their weight can be expressed also mathematically (1), e.g.,

$$Pmf = \frac{fpos1 \cdot kpos1 + fpos2 \cdot kpos2 + \dots + fposn \cdot kposn}{fneg1 \cdot kneg1 + fneg2 \cdot kneg2 + \dots + fnegn \cdot knegn} \quad (1)$$

where:

Pmf , probability of mission fulfilment; $fpos1$ till n , positive factor (1/first/till n/n -th/); $kpos1$ till n , coefficient of positive factor (1/first/till n/n -th/); $fneg1$ till n , negative factor (1/first/till n/n -th/); $kneg1$ till n , coefficient of negative factor (1/first/till n/n -th/).

The coefficient is an integer from one to the value specified by the "assignor of the mission". The coefficients (both positive and negative factors) indicate the weight, the effect of these factors on the fulfillment of the given task. The larger the scale (value) of the coefficients, the more precisely their influence on the task can be defined. The scale can be set, for example, from 1 to 5 (10 and other variants). "Task designer" may even divide these factors into several groups after the factors involved in mission planning, from the point of view of the size of their impact on the task and the individual groups, and their significance separated from each other by a diverse range of coefficients. A group of the most important factors can be evaluated, for

Factors	Influence		Effect weight [number/ order] [*]
	Positive	Negative	
Preparation of autonomous vehicle to be put in place (time required to get ready for task start)			
Complexity/ease of operation of autonomous vehicle in all phases of task fulfillment (especially in the semi-automatic autonomous vehicle controlled by the operator)		x	
Sufficient capacity of source	x		
Functionality of all components (sensors)	x		
Interaction with “control center” at declared distance	x		
Terrain Pass Through	pass through	x	
	partially through		x
	impassable		x
Ability to select the axis of movement without detection by the enemy	x		
Ability to transmit information in the required ways	x		
The existence of enemy means in the transfer space, which can destroy the autonomous vehicle		x	
Autonomous vehicle ability to overtake the enemy in its destruction (to detect and destroy the enemy before he does so)	x		
Heavy detection of autonomous vehicle by enemy means (autonomous vehicle does not produce sounds, smoke, other manifestations, minimizes radiation, etc.)	x		
Easily detection of autonomous vehicle by enemy means		x	
Inapplicability of autonomous vehicle to cooperate with other vehicles in mass deployment		x	
Etc.			

^{*}Specified by the “assignor of the mission”.

Table 1.
Example of evaluation factors influencing autonomous vehicle movement.

example, coefficients ranging from 1 to 10, a group of minor factors, coefficients in the range 1–6, and a group of least significant factors, coefficients in the range 1–3.

The result of calculating the probability of completing a task is either left in a fraction that is adjusted to the “number” on the numerator or denominator side (e.g., 1/3.8 or 2.6/1). Such a fraction shape gives a multiple predominance of the probability of fulfilling/not fulfilling the task.

The possible factors affecting the ground autonomous vehicle (as listed in **Table 1**) to which the “assignor of a particular task” has to assign a specific value before commencing (in the mission planning process).

7. Approach to the maneuver optimization

One of the approach for optimizing the autonomous vehicle maneuver in the conditions of the opposition forces is to utilize advantages of modelling combat activities. During the military decision making process, commander and his staff members use a series of models and programs to accelerate and refine decision-making and operation missions. Example of good practise is exploitation of model of cooperative

reconnaissance as part of Tactical Decision Support System [7]. According to [8], the fundamental approach is based on a sequence of procedures and the weighted integration of discrete layers, where all phases converge to a maneuver optimization issued from modified versions of Floyd-Warshall algorithm. Initial C++ application was designed for a basic experiments, providing relatively fast solution (derived from path-finding algorithms used in autonomous systems), whose task was to verify theoretical approach and the time profile of solution. If it is necessary, application could find alternative routes with more-favorable movement factor.

Fundamental theoretical approach in that case was inspired by Floyd-Warshall algorithm [8]. Original algorithm was pushed throughout several modifications that make it computationally applicable even for a large data structures comprising more than 106 nodes. Basic adjustment lay in elimination of so-called reverse cycles by stopping the 82 calculation on all nodes in its root.

This process is carried out through the main field elements chosen for next phase solution. The status and verification cycle matches the bit position in the bit field with the position of the active element in the default structure. If the element belongs to a root what was modified (attribute is present), the element is excluded from the processing in the following iterative phase because it will be modified in the next steps.

This process is theoretically simple; however, the realization of this step is relatively difficult in practice, because the memory performance P_n achieves (2):

$$P_n = \frac{N^2}{8} \quad (2)$$

where: N is the number of nodes (elements) of the graph.

It means that models which contain more than 106 nodes must allocate over 125 GB memory only for genetic structure of each element. In the case of information transfer into other elements the amount of operations raise to a level that is incompatible neither with the real time application, nor on the fastest nowadays computers. It is therefore necessary to address the sub-problem in a different way and optimize the whole process by other approach. Previously mentioned idea works well but for a wide set of nodes (more than 106) is ineffective.

For the purpose of utilizing autonomous vehicle in role as reconnaissance means is the part of MDMP to plan the reconnaissance operation of the area of interest. For optimization of using more than one air autonomous vehicle so called as Unmanned Air Vehicle (UAV) in one assigned mission was developed model for optimization of using swarm of UAV to effectively reconnaissance the area of interest [2].

The objective of the model is specified in Formula (3) which is to minimize the maximum time of flight of all routes of individual UAS in the fleet. The details of the model along with its complete mathematical formulation can be found in [8].

$$\text{minimize } (\max(T_1, T_2, \dots, T_N)) \quad (3)$$

where T_i is the time of flight of i -th UAS in the fleet, N is the total number of UAS in the fleet.

The model of UAS Reconnaissance is similar to the Multi-Depot Vehicle Routing Problem (MDVRP) [9, 10]. The MDVRP is also about optimization of routes of a set of vehicles originating from multiple depots to visit a number of customers to deliver goods or services. There is, however, the significant difference between the models. While the main objective of the MDVRP is to minimize the total distance travelled by all vehicles which is expressed in Formula (4), the objective of the UAS Reconnaissance is to minimize the time of whole operation as already mentioned in Formula (1).

$$\text{minimize } \left(\sum_{i=1}^N Di \right) \quad (4)$$

where Di is the distance travelled by i -th vehicle, N is the total number of vehicles.

For verification of the proposed UAS Reconnaissance model there were designed two scenarios of tactical situation and applied experiments in real terrain with real UAV's [2, 11].

8. Conclusion

The information mentioned in the text of the chapter could not provide an exhaustive overview of all the factors that may influence the planning of the moving of autonomous vehicles. In the chapter there is presented a view especially on the military factors, respectively, factors from a military perspective when using autonomous vehicles in environments conducting military operations. In the case of the use of autonomous vehicles in military operations, the factory has no influence on whether an enemy will be operating in the environment in order to take measures against the effects of autonomous vehicles and to eliminate their activities to the maximum.

The chapter did not address the issue of methodology when planning the transfer of autonomous vehicles, which goes to the chapter itself.

Mentioned information can be used as a guideline in which detail to contemplate when intending to use autonomous vehicles in military operations.

Acknowledgements


For the Section 6 was utilized research outputs of academics workers of Department of Tactics Faculty of Military Leadership and one former academic worker LTC Assoc. Professor Jan Mazal, Ph.D. who is actually in duty as Head of Education and Training Department NATO Modelling & Simulation Centre of Excellence in Rome. For purposes of verification proposed models of autonomous systems path planning optimization by experiments is used synthetics and virtual environment rendered by tactical virtual simulator Virtual Battlespace [12, 13].

Author details

Jaroslav Kozůbek*, Zdeněk Flasar and Ivo Dumišinec
University of Defence, Brno, Czech Republic

*Address all correspondence to: jaroslav.kozubek@unob.cz

IntechOpen

© 2019 The Author(s). Licensee IntechOpen. This chapter is distributed under the terms of the Creative Commons Attribution License (<http://creativecommons.org/licenses/by/3.0>), which permits unrestricted use, distribution, and reproduction in any medium, provided the original work is properly cited. 

References

- [1] Hodicky J. Autonomous systems operationalization gaps overcome by modelling and simulation. In: Hodicky J, editor. *Modelling and Simulation for Autonomous Systems. MESAS. Lecture Notes in Computer Science*. Cham: Springer; 2016;**9991**:40-47
- [2] Drozd J, Stodola P, Křišťálová D, Kozůbek J. Experiments with the UAS reconnaissance model in the real environment. In: *Modelling and Simulation for Autonomous Systems*. Cham: Springer International Publishing; 2018. pp. 340-349. ISSN 0302-9743. ISBN 978-3-319-76071-1
- [3] Stodola P, Mazal J. Tactical decision support system to aid commanders in their decision-making. In: Hodicky J, editor. *Modelling and Simulation for Autonomous Systems. MESAS. Lecture Notes in Computer Science*. Cham: Springer; 2016;**9991**:396-406
- [4] Stodola P, Mazal J. Model of optimal cooperative reconnaissance and its solution using metaheuristic methods. *Defence Science Journal*. 2017;**67**(5):529-535. ISSN: 0011-748X
- [5] Allied Joint Doctrine for Land Operations (NATO Standard AJP3-2). Brussels: NSO; 2016. pp. 1-1-1-2
- [6] The Army of the Czech Republic Lessons Learned Databases. Prague: The Army of the Czech Republic General Staff; 2018
- [7] Drozd J, Flasar Z, Stodola P. Use of modern technologies for combat units preparation and management. *Military Technical Courier*. 2017;**65**(3): 602-616
- [8] Mazal J, Mašlej M, Stodola P, Mazalová I. Modeling approach to the specific tactical activities. *Ekonomika a Management*. 2013;**2013**(2):76-86. ISSN 1802-3975
- [9] Dantzig GB, Ramser JH. The truck dispatching problem. *Management Science*. 1959;**6**(1):80-91
- [10] Stodola P. Using metaheuristics on the multi-depot vehicle routing problem with modified optimization criterion. *Algorithms*. 2018;**11**(5):1-14. ISSN 1999-4893
- [11] Stodola P, Kozůbek J, Drozd J. Using unmanned aerial systems in military operations for autonomous reconnaissance. In: *Modelling and Simulation for Autonomous Systems*. Cham, Switzerland: Springer; 2019. pp. 514-529. ISSN 0302-9743. ISBN 978-3-030-14983-3
- [12] Kozůbek J, Flasar Z. Possibilities of verification the required capabilities according to NATO network enabled capabilities concept. *Croatian Journal of Education*. 2012;**14**(Spec. Ed. 1/2012):87-98. ISSN 1848-5189
- [13] Kozůbek J, Flasar Z. Quantifiable criteria of simulated combat activities. IN: *The 18th International Conference The Knowledge-Based Organisation, Conference Proceedings*. Vol. 2012, No. 3. 2012. pp. 230-233. ISSN 1843-6722

Section 2

Path Planning in Varied
Environments

Path Planning for Autonomous Vehicle in Off-Road Scenario

Boyuan Li, Haiping Du and Bangji Zhang

Abstract

The road topography information, such as bank angle and road slope, can significantly affect the trajectory tracking performance of the autonomous vehicle, so this information needs to be considered in the trajectory planning and tracking control for off-road autonomous vehicle. In this chapter, a two-level real-time dynamically integrated spatiotemporal-based trajectory planning and control method for off-road autonomous vehicle is proposed. In the upper-level trajectory planner, the most suitable time-parameterised trajectory with the minimum values of road slope and bank angle can be selected from a set of candidate trajectories. In the lower-level trajectory tracking controller, the sliding-mode control (SMC) technique is applied to control the vehicle and achieve the desired trajectory. Finally, simulation results are presented to verify the proposed integrated trajectory planning and control method and prove that the proposed integrated method has better overall tracking control and dynamics control performance than the conventional method both in the highway scenario and off-road scenario. Furthermore, the four-wheel-independent-steering (4WIS) and four-wheel-independent-driving (4WID) vehicle shows better tracking control performance than vehicle based on two-wheel model.

Keywords: trajectory planning, trajectory tracking control, off-road vehicle, vehicle dynamics, optimisation

1. Introduction

Nowadays, the off-road autonomous ground vehicle has been widely applied in various industries, such as military [1, 2] and space applications [3, 4]. Furthermore, this kind of vehicle also received focused attention in mining [5], agriculture and forestry sectors [6].

In order to improve the stability and safety of off-road autonomous vehicles, the path planning of these vehicles should be considered as the priority of current research. The path planning of autonomous vehicle includes two stages: the trajectory planning in the upper-level and trajectory tracking control in the lower-level. The upper-level trajectory planner considers the surrounding environment information according to the various sensors and selects the best desired trajectory, while the lower-level trajectory tracking controller controls the steering and driving actuators to achieve the desired trajectory.

In the current literature, the path planning of autonomous vehicle has attracted focused attention. Particularly, the spatial-based path planning methods are widely

applied, but the time parameter is not considered [7]. For example, for the direct tracking method, the steering system is controlled to follow the pre-planned spatial-based desired path exactly at every time step [8, 9]. In the potential field method proposed in [10], the desired path is planned within a potential field with a tracking error tolerance along the road centreline. In this way, the autonomous vehicle does not need to strictly follow the road centreline, and smaller steering control effort is required compared with the direct tracking method. The spatiotemporal-based trajectory planning concept, on the other hand, considers the kinematic constraints and generates time-parameterised trajectories. Several typical spatiotemporal-based trajectory planning methods, such as the methods proposed in [11–13], aim to find the best suitable time-parameterised trajectory connecting the initial vehicle states with exactly defined goal states. These methods rely on discrete geometric structure, such as the rapidly exploring random trees (RRT) [14] and state lattice [13]. However, the generation of candidate trajectories requires large computational work. When the surrounding environment is unconstructed and complex, these methods may not be computationally efficient. In [15, 16], the proposed trajectory planning strategies utilise ‘deliberated multiple final states’ method. This method deliberately generates multiple alternative final states which can respond to traffic changes very fast. In study [17], based on the concept of ‘deliberated multiple final states’, the combined trajectory planning of the longitudinal and lateral motion of autonomous vehicle are proposed, and the ‘deliberated multiple final states’ are described as the offset error values from the target reference final states. The most suitable trajectory which satisfies the initial and ending states with certain terminal time can be selected from candidate trajectory set, and the kinematic constraints are satisfied.

Motivated by the widely application of the off-road autonomous vehicle in various industries and based on above research studies on path planning, this chapter proposed a two-level real-time dynamically integrated spatiotemporal-based trajectory planning and control method by considering the off-road scenario. The major innovative part of this chapter is the development of the spatiotemporal-based trajectory planning method and considering the off-road topography information in trajectory planning. In the upper-level trajectory planner, a number of candidate spatiotemporal-based trajectories with various terminal times and state-ending conditions are generated. These candidate trajectories also include the road topography information—the bank angle and road slope. The best suitable trajectory can be selected from these candidate trajectories based on the optimised cost function which is used to minimise the tracking error, terminal time spent and the effect of road topography on the vehicle. After that, trajectory tracking controller in the lower-level is proposed based on the sliding-mode technique and vehicle dynamics model in order to track the selected best suitable trajectory. In addition, the vehicle dynamics model of this chapter is based on a four-wheel-independent-steering (4WIS) and four-wheel-independent-driving (4WID) electric vehicle. Due to a large number of available control actuators, the 4WIS-4WID electric vehicle shows advantages over the traditional vehicle. This chapter also discusses the advantage of 4WIS-4WID electric vehicle on trajectory planning and trajectory tracking control over traditional two-wheel vehicle.

In this chapter, Section 2 first discusses the vehicle dynamics model based on 4WIS-4WID electric vehicle. Then Section 3 describes the upper-level trajectory planner, and Section 4 shows the lower-level trajectory tracking control. After that, Section 5 presents the simulation results to verify the proposed trajectory planning and control method. Finally, the conclusion is given in Section 6.

2. Vehicle dynamics modelling

In this section, a 4WIS-4WID vehicle model is utilised first to describe the dynamic motion of an off-road autonomous vehicle [18]. The information of road slope and bank angle is included in the vehicle longitudinal and lateral dynamics equations. Furthermore, vehicle roll dynamics equation and pitch dynamics equation are included in the dynamics model to better present the effect of bank angle and road slope on the vehicle dynamics. The vector diagram of vehicle dynamics model is presented in **Figure 1**.

The equations of motion of this model are described as follows:
 Longitudinal motion:

$$m\dot{v}_x = mv_y r + (F_{xfl} + F_{xfr} + F_{xrl} + F_{xrr}) + mg \sin \theta_s \quad (1)$$

Lateral motion:

$$m\dot{v}_y = -mv_x r + (F_{yfl} + F_{yfr} + F_{yrl} + F_{yrr}) + mg \sin \theta_b \quad (2)$$

Yaw motion:

$$I_z \dot{r} = l_f (F_{yfl} + F_{yfr}) - l_r (F_{yrl} + F_{yrr}) + \frac{b_f}{2} (F_{xfl} - F_{xfr}) + \frac{b_r}{2} (F_{xrl} - F_{xrr}) \quad (3)$$

Roll motion:

$$I_x \ddot{\phi} = -m e_r \dot{v}_y - m e_r v_x r + m g e_r \sin \phi - K_\phi \phi - C_\phi \dot{\phi} \quad (4)$$

Pitch motion:

$$I_y \ddot{\varphi} = -m e_p \dot{v}_x - m e_p v_y r + m g e_p \sin \varphi - K_\varphi \varphi - C_\varphi \dot{\varphi} \quad (5)$$

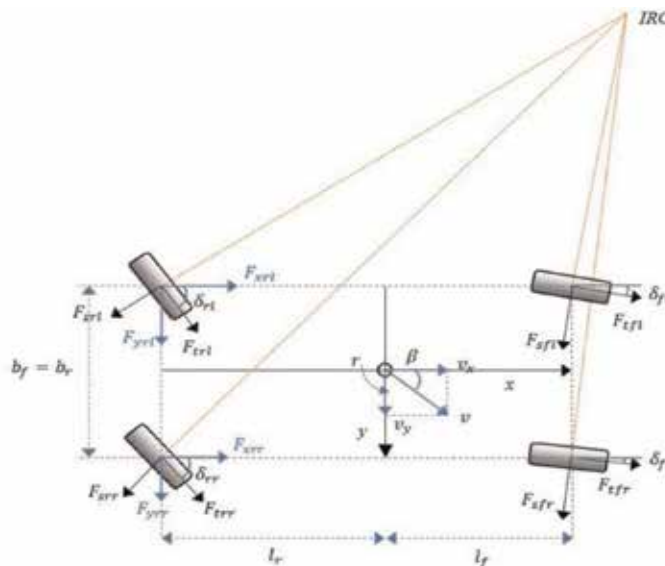


Figure 1.
 The vector diagram of 4WIS-4WID vehicle dynamics model.

where v_x , v_y and r are the vehicle longitudinal velocity, lateral velocity and yaw rate. θ_s shows the road slope, and θ_b represents the road bank angle. b_f and b_r represent the front and rear track width. l_f is the length of front wheel base, and l_r is the length of rear wheel base. I_z represents the moment of yaw inertia, and m is vehicle mass. F_{xfl} and F_{xfr} represent the longitudinal tyre force of front left and front right tyre, while F_{xrl} and F_{xrr} present the longitudinal tyre force of rear left and rear right wheel. F_{yfl} and F_{yfr} present the lateral tyre force of front left and front right tyre, while F_{yrl} and F_{yrr} present the lateral tyre force of rear left and rear right wheel. ϕ and φ represent the vehicle roll angle and pitch angle, respectively. e_r is the distance from the vehicle centre of gravity (CG) to the roll centre, and e_p is the distance from the vehicle CG to the pitch motion centre. K_ϕ is the roll axis torsional stiffness, and C_ϕ is the roll axis torsional damping. K_φ is the pitch axis torsional stiffness, and C_φ is the pitch axis torsional damping.

The tyre side force F_{si} and traction or brake force F_{ti} can be transferred to the longitudinal force F_{xi} and the lateral tyre force F_{yi} as follows:

$$\begin{aligned} F_{xi} &= F_{ti} \cos \delta_i - F_{si} \sin \delta_i \\ F_{yi} &= F_{ti} \sin \delta_i + F_{si} \cos \delta_i \end{aligned} \quad (6)$$

where $i = fl, fr, rl$ and rr , which represents the front left wheel, front right wheel, rear left wheel and rear right wheel.

The non-linear Dugoff tyre model is used in this chapter [19], and tyre traction or brake force and side force of each wheel are described by:

Tyre side force:

$$F_{si} = \frac{C_\alpha \tan \alpha_i}{1 - s_i} f(\lambda_i) \quad (7)$$

Tyre traction or brake force:

$$F_{ti} = \frac{C_s s_i}{1 - s_i} f(\lambda_i) \quad (8)$$

λ_i in Eqs. (7) and (8) can be determined by the following equation:

$$\lambda_i = \frac{\mu F_{zi} \left[1 - \varepsilon_r u_i \sqrt{s_i^2 + \tan^2 \alpha_i} \right] (1 - s_i)}{2 \sqrt{C_s^2 s_i^2 + C_\alpha^2 \tan^2 \alpha_i}} \quad (9)$$

$f(\lambda_i)$ in Eqs. (7) and (8) can be determined by the following equation:

$$f(\lambda_i) = \begin{cases} \lambda_i (2 - \lambda_i) & (\lambda_i < 1) \\ 1 & (\lambda_i > 1) \end{cases} \quad (10)$$

where C_α represents the lateral cornering stiffness and C_s is the longitudinal cornering stiffness. The tyre-road friction coefficient can be represented as μ , and F_{zi} represents the individual wheel vertical load. α_i represents the lateral side-slip angle, and s_i is the longitudinal slip ratio. u_i represents the vehicle longitudinal velocity in the individual wheel plane. ε_r is the road adhesive reduction factor, which is a constant value.

The following equation shows the wheel rotation dynamics:

$$I_\omega \dot{\omega}_i = -R_\omega F_{ti} + T_i \quad (11)$$

where ω_i presents the wheel angular velocity of each wheel and T_i presents the traction or brake torque of each wheel. R_ω is the wheel radius, and I_ω is the wheel moment of inertial.

The load transfer model is considered here by adding the roll and pitch motion to better present the effect of road slope and bank angle on the vehicle vertical load distribution [20]. The vertical load of individual wheel can be presented by the following equations by including the load transfer model:

$$F_{zfl} = \frac{m}{l_f + l_r} \left(\frac{1}{2}gl_r - \frac{1}{2}\dot{v}_x h + \frac{l_r}{b_f} (\dot{v}_y h - ge_r \sin \phi) + \frac{1}{2}ge_p \sin \phi (l_f + l_r)^2 \right) \quad (12)$$

$$F_{zfr} = \frac{m}{l_f + l_r} \left(\frac{1}{2}gl_r - \frac{1}{2}\dot{v}_x h - \frac{l_r}{b_f} (\dot{v}_y h - ge_r \sin \phi) + \frac{1}{2}ge_p \sin \phi (l_f + l_r)^2 \right) \quad (13)$$

$$F_{zrl} = \frac{m}{l_f + l_r} \left(\frac{1}{2}gl_f + \frac{1}{2}\dot{v}_x h + \frac{l_f}{b_r} (\dot{v}_y h - ge_r \sin \phi) - \frac{1}{2}ge_p \sin \phi (l_f + l_r)^2 \right) \quad (14)$$

$$F_{zrr} = \frac{m}{l_f + l_r} \left(\frac{1}{2}gl_f + \frac{1}{2}\dot{v}_x h - \frac{l_f}{b_r} (\dot{v}_y h - ge_r \sin \phi) - \frac{1}{2}ge_p \sin \phi (l_f + l_r)^2 \right) \quad (15)$$

where h is the height of the vehicle CG above the ground.

3. Upper-level trajectory planner

Figure 2 presents the whole structure of the proposed integrated trajectory planning and control method, which mainly includes the upper-level trajectory planner, the lower-level trajectory controller and the vehicle dynamics model [21].

At the beginning, it is assumed that a behaviour layer planner exists and can determine the rough global reference path according to the digital map. This behaviour layer planner consists of a number of modules, such as digital map, perception and localisation system and behaviour level path planner [22]. The digital map provides real-time traffic information, and the real-time vehicle position on the digital map can be determined by the perception and localization system (such as the GPS combined with IMU and wheel encoder). When digital map and vehicle's real-time position on the digital map are available, the behaviour planner can make deliberate manoeuvre task decisions, such as lane following, lane changing, vehicle following and overtaking, in complex street-driving scenario. Based on the manoeuvre task decisions, the global route planner in the behaviour planner can compute the rough reference path. This is a reasonable assumption because many studies in the literature have determined the rough reference path by behaviour level task planner based on digital map [22–24].

In the upper-level trajectory planner, according to the rough desired path determined by the behaviour planner, the desired vehicle initial and ending states of each section of the road along the rough reference path can be assumed to be known in advance.

3.1 Generate the candidate trajectory set

In each section of road, when the initial states are assumed to be available, the multiple target ending states can be defined as a group of offset state values from the reference state values (such as longitudinal position, longitudinal velocity,

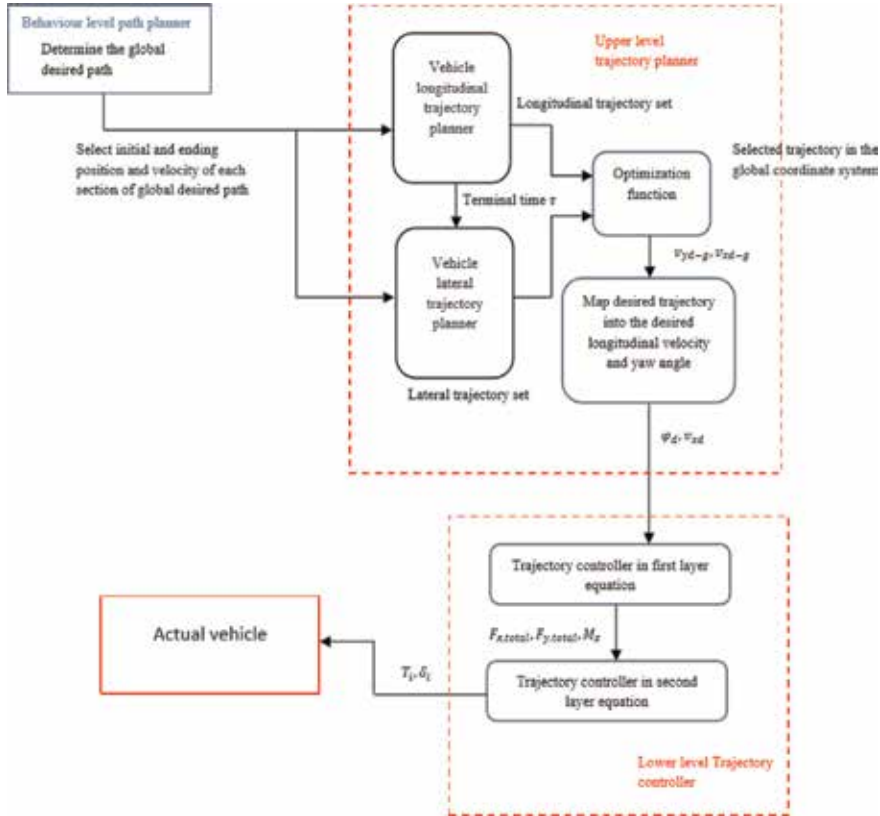


Figure 2.
The whole structure of the proposed integrated trajectory planning and control method.

lateral position and lateral velocity). The start state is assumed as $\begin{bmatrix} d_0 & \dot{d}_0 & \ddot{d}_0 \end{bmatrix}$, and the desired ending state is assumed as $\begin{bmatrix} d_1 & \dot{d}_1 & \ddot{d}_1 \end{bmatrix}$. d_0 is the initial vehicle position, and d_1 is a group of offset positions from reference ending position, and these offset positions are constrained within the road boundary. \dot{d}_0 and \ddot{d}_0 present the initial velocity and acceleration, while \dot{d}_1 and \ddot{d}_1 present the ending velocity and acceleration. For the purpose of the guarantee of the continuities of the planned trajectory between each section of the road, the initial state d_0 in current section of road should be the ending state of previous section.

In each section of the road, when the initial and ending state values are determined, the candidate trajectories with different ending conditions d_{1i} and terminal time τ_j can be generated [17], where i, j means that the number of $i \times j$ trajectories will be generated by the trajectory planner. d_{1i} represents i number of final positions and will close to the target ending position when $d_{1i} \rightarrow d_1$. τ_j represents the j number of candidate terminal time. The optimisation algorithm presented in the later section will choose the best trajectory from these $i \times j$ trajectories.

It can be assumed that the candidate vehicle trajectory $d(\tau)$ in the optimisation of trajectory planning can be described by the following quintic state equations [17]:

For the position of candidate trajectory:

$$d_1 = c_0 + c_1t + c_2t^2 + c_3t^3 + c_4t^4 + c_5t^5 \quad (16)$$

For the velocity of candidate trajectory:

$$\dot{d}_1 = c_1 + 2c_2t + 3c_3t^2 + 4c_4t^3 + 5c_5t^4 \quad (17)$$

For the acceleration of candidate trajectory:

$$\ddot{d}_1 = 2c_2 + 6c_3t + 12c_4t^2 + 20c_5t^3 \quad (18)$$

with $c_0, c_1, \dots, c_5 \in R$ and $t \in [0 \ \tau]$. τ is the terminal time of the candidate trajectory and $\tau \in [0 \ T]$. T is the longest time required to complete the motion.

Eqs. (16)–(18) can be rewritten as the following equation:

$$\xi_t(t) = \mathbf{M}_1(t)\mathbf{c}_{012} + \mathbf{M}_2(t)\mathbf{c}_{345} \quad (19)$$

$$\text{where } \mathbf{M}_1(t) = \begin{bmatrix} 1 & t & t^2 \\ 0 & 1 & 2t \\ 0 & 0 & 2 \end{bmatrix}, \mathbf{M}_2(t) = \begin{bmatrix} t^3 & t^4 & t^5 \\ 3t^2 & 4t^3 & 5t^4 \\ 6t & 12t^2 & 20t^3 \end{bmatrix} \text{ and } \xi_t(t) = \begin{bmatrix} d_1(t) \\ \dot{d}_1(t) \\ \ddot{d}_1(t) \end{bmatrix}.$$

The coefficients \mathbf{c}_{012} and \mathbf{c}_{345} of the quintic state trajectory in Eq. (19) can be calculated as follows:

$$\mathbf{c}_{012} = \begin{bmatrix} c_0 \\ c_1 \\ c_2 \end{bmatrix} = \mathbf{M}_1(0)^{-1}\xi_0 \quad (20)$$

$$\mathbf{c}_{345} = \begin{bmatrix} c_3 \\ c_4 \\ c_5 \end{bmatrix} = \mathbf{M}_2(\tau)^{-1}[\xi_t - \mathbf{M}_1(\tau)\mathbf{c}_{012}] \quad (21)$$

$$\text{where } \mathbf{M}_1(0) = \begin{bmatrix} 1 & 0 & 0 \\ 0 & 1 & 0 \\ 0 & 0 & 2 \end{bmatrix} \text{ and } \xi_0 = \begin{bmatrix} d_0 \\ \dot{d}_0 \\ \ddot{d}_0 \end{bmatrix}.$$

After the coefficients \mathbf{c}_{012} and \mathbf{c}_{345} are calculated, the vehicle trajectory can be described as $d_1(t)$ in Eq. (16). In this way, candidate trajectories in this section of the road can be determined, and the best trajectory can be selected based on the proposed optimisation cost function in the next section.

3.2 Determine the optimisation cost function

After the candidate trajectories have been determined in each section of the road, the next step is to determine the cost function to select the best suitable trajectory. The optimisation cost function is designed as the following equation:

$$\min_{d_1, \tau} J_1 = k_\tau \tau + k_d (d_r - d_1(\tau))^2 \quad (22)$$

where this cost function has two optimization variables, the ending position d_1 and terminal time τ . This cost function also includes two terms, and k_τ and k_d are the scaling factors of each term, which can be used to balance the term of total time cost and the term of offset error from the desired ending state. d_r is the reference vehicle ending state. $d_r - d_1(\tau)$ presents the offset error from the desired reference ending state. The selection of total time cost can greatly affect the vehicle trajectory tracking behaviour: with the small total time cost, the vehicle can reach the final states early, while large time cost will make the vehicle movement slow and stable with late arrival of final states.

Furthermore, the vehicle longitudinal or lateral jerk (presented as $\ddot{d}(\tau)$) should be minimised to improve the smoothness of the trajectory. The total optimisation cost function J_1 of the trajectory planning can be augmented as:

$$\min_{d_1, \tau} J_1 = k_J (\ddot{d}_1(\tau))^2 + k_\tau \tau + k_d (d_r - d_1(\tau))^2 \quad (23)$$

where k_J is the scaling factor of the term related to longitudinal or lateral jerk. It can be noted that the target final velocity \dot{d}_1 or acceleration \ddot{d}_1 can be used in (23) instead of d_1 if the final velocity or acceleration is required to be optimised.

In optimisation cost function (23), the road topography information, such as the road slope and bank angle, has not been considered. However, road topography will greatly affect the trajectory planning and vehicle dynamics performance in off-road scenario. The trajectory planning optimisation cost function should consider the additional optimisation control target of road topography by selecting the trajectory with the smaller road slope and bank angle. Furthermore, in order to prevent the abrupt change of road slope and bank angle, the change of the road slope and bank angle between current and previous time step should be minimised.

The assumption is made that the topography information along each candidate trajectory is already known through various sensors equipped in the intelligent vehicle system. In this chapter, the topography information at a specific point can be obtained from a lookup table. The average road slope $\bar{\theta}_s$ and bank angle $\bar{\theta}_b$ along one particular candidate trajectory could be calculated as the following equation:

$$\bar{\theta}_s = \frac{\sum_{i=1}^n \theta_s(x_i, y_i)}{n} \quad (24)$$

$$\bar{\theta}_b = \frac{\sum_{i=1}^n \theta_b(x_i, y_i)}{n} \quad (25)$$

where $\theta_s(x_i, y_i)$ and $\theta_b(x_i, y_i)$ are the road slope and bank angle at a specific point along the candidate trajectory. n is the total number of discrete points along this candidate trajectory.

After the road topography information is available, the road topography information can be included into the optimal cost function (23) as the following equation:

$$\begin{aligned} \min_{d_1, \tau} J_1 = & k_J (\ddot{d}_1(\tau))^2 + k_\tau \tau + k_d (d_r - d_1(\tau))^2 + k_s \bar{\theta}_s (d_1(\tau)) + k_{sd} \dot{\bar{\theta}}_s (d_1(\tau)) \\ & + k_b \bar{\theta}_b (d_1(\tau)) + k_{bd} \dot{\bar{\theta}}_b (d_1(\tau)) \end{aligned} \quad (26)$$

where this cost function have four additional cost function terms compared with cost function (23). The terms $k_s \bar{\theta}_s (d_1(\tau))$ and $k_b \bar{\theta}_b (d_1(\tau))$ are designed to minimise the road slope and bank angle along the selected trajectory. $k_{sd} \dot{\bar{\theta}}_s (d_{x,y}(\tau))$ and $k_{bd} \dot{\bar{\theta}}_b (d_{x,y}(\tau))$ are designed to prevent the abrupt change of road slope and bank angle. k_s, k_{sd} and k_b, k_{bd} are scaling factors of each term.

When the optimisation values of ending position d_1 and terminal time τ are determined based on (26), the desired best trajectory can be determined according to Eqs. (16)–(18).

It is noted that the trajectory planning in this section can be divided as the longitudinal trajectory planning and lateral trajectory planning. Eqs. (16)–(26) merely provide the common mathematical equations to generate the candidate trajectory set and determine the best suitable trajectory according to optimisation

cost function. These mathematical equations are only corresponding to one section of road. The predefined global desired path can have a number of sections of road, and a number of the optimisation calculations are implemented successively. In the ideal condition, the more sections the desired global path is divided, the more accurate the optimisation results would be. However, a large number of the divided sections of road require intensive computing efforts, and the computational cost will increase a lot.

3.3 Map planned trajectory into vehicle dynamics control targets

After the desired trajectory is planned and determined while satisfying certain position constraints and velocity constraints, the next step is to map the desired trajectory into vehicle dynamics control targets: desired yaw angle and desired longitudinal velocity in the body-fixed coordinate system.

The desired yaw angle φ_d and longitudinal velocity v_{xd} in the body-fixed coordinate system can be determined according to the following optimisation cost function:

$$\min_{\varphi_d, v_{xd}} J_2 = a(v_{xd}(k) - v_{xd-b}(k))^2 + b(v_{xd} \tan \varphi_d(k) - v_{yd-b}(k))^2 + c(\varphi_d(k) - \varphi_d(k-1))^2 \quad (27)$$

where this cost function includes three terms, which are used to achieve the desired longitudinal velocity (the first term), desired lateral velocity (the second term) and avoid the abrupt change of the yaw angle between each time step and improve the smooth of the trajectory (the third term). a , b and c are scaling factors of each term. k represents the time step $t(k)$, and $k-1$ represents the time step $t(k-1)$. v_{xd-b} and v_{yd-b} represent the desired longitudinal velocity and lateral velocity in the body-fixed coordinate system, which can be calculated according to the desired longitudinal velocity v_{xd-g} and lateral velocity v_{yd-g} in the global coordinate system:

$$v_{xd-b} = v_{xd-g} \cos \varphi + v_{yd-g} \sin \varphi \quad (28)$$

$$v_{yd-b} = v_{xd-g} \sin \varphi - v_{yd-g} \cos \varphi \quad (29)$$

where the desired longitudinal velocity v_{xd-g} and lateral velocity v_{yd-g} along the desired trajectory in the global coordinate system can be determined according to Eqs. (17), (26).

After the desired longitudinal velocity and yaw angle in the vehicle body-fixed coordinate system are determined, the desired tyre forces and yaw moment to achieve these desired control targets can be calculated by the lower-level trajectory controller in the next section.

4. Lower-level trajectory tracking controller

In this section, the lower-level two-layer trajectory tracking controller is proposed to control the autonomous vehicle to follow the desired planned trajectory [21]. In the first layer, according to the desired longitudinal velocity, desired zero lateral velocity and desired yaw angle, the desired longitudinal force, lateral force and yaw moment in the vehicle body-fixed coordinate system can be calculated. In

the second layer, the individual steering and driving actuators are optimised and controlled to achieve the desired longitudinal force, lateral force and yaw moment.

4.1 Trajectory tracking controller in the first layer

First, the error dynamics equation of vehicle trajectory tracking including the longitudinal velocity error, lateral velocity error and yaw angle error is presented to calculate the feedback tyre force and moment, which can be presented by the following equation based on [25]:

$$\tilde{v}_y = [v_x \sin \tilde{\varphi} + v_y \cos \tilde{\varphi}] - v_{yd} \quad (30)$$

$$\tilde{v}_x = [v_x \cos \tilde{\varphi} - v_y \sin \tilde{\varphi}] - v_{xd} \quad (31)$$

$$\tilde{\varphi} = \varphi_{act} - \varphi_d \quad (32)$$

where φ_{act} is the actual measurement yaw angle. v_x and v_y are actual measurement feedback longitudinal and lateral velocity. \tilde{v}_x and \tilde{v}_y are longitudinal velocity error and lateral velocity error, respectively. In order to improve the vehicle stability, the desired lateral velocity v_{yd} is assumed as zero value.

The feedback tyre force and moment can be determined according to the tracking error dynamics in Eqs. (30–32):

$$F_{x,feedback} = -K_1 \tilde{v}_x \quad (33)$$

$$F_{y,feedback} = -K_{2p} \tilde{v}_y - K_{2d} \dot{\tilde{v}}_y \quad (34)$$

$$M_{z,feedback} = -K_{3p} \tilde{\varphi} - K_{3d} \dot{\tilde{\varphi}} \quad (35)$$

where K_1 , K_{2p} , K_{2d} , K_{3p} and K_{3d} represent feedback control gains.

The feedforward tyre force and moment can be calculated as:

$$F_{x,forward} = m \dot{v}_{xd} - m \tilde{v}_y \dot{\varphi}_d \quad (36)$$

$$F_{y,forward} = m v_{xd} \dot{\varphi}_d + m \tilde{v}_x \dot{\varphi}_d \quad (37)$$

$$M_{z,forward} = I_z \ddot{\varphi}_d \quad (38)$$

The vehicle total desired longitudinal force $F_{x,total}$, lateral force $F_{y,total}$ and yaw moment $M_{z,total}$ can be determined by adding up feedforward and feedback terms:

$$F_{x,total} = m \dot{v}_{xd} - m \tilde{v}_y \dot{\varphi}_d - K_1 \tilde{v}_x \quad (39)$$

$$F_{y,total} = m v_{xd} \dot{\varphi}_d + m \tilde{v}_x \dot{\varphi}_d - K_{2p} \tilde{v}_y - K_{2d} \dot{\tilde{v}}_y \quad (40)$$

$$M_{z,total} = I_z \ddot{\varphi}_d - K_{3p} \tilde{\varphi} - K_{3d} \dot{\tilde{\varphi}} \quad (41)$$

4.2 Trajectory controller in the second layer

In this section, the individual steering and driving control actuators are allocated and controlled to achieve the desired total longitudinal tyre force, the desired total lateral tyre force and desired yaw moment determined in the first layer of trajectory controller. First the individual tyre forces are optimal allocated by the optimisation cost function, and then the allocated tyre forces can be mapped into the individual steering and driving control actuators.

The mathematical equation of cost function of this control allocation and optimisation problem can be shown as follows:

$$\min_{F_{ti}, F_{si}} J_3 = \frac{F_{tfl}^2 + F_{sfl}^2}{\mu^2 F_{zfl}^2} + \frac{F_{tfr}^2 + F_{sfr}^2}{\mu^2 F_{zfr}^2} + \frac{F_{trl}^2 + F_{srl}^2}{\mu^2 F_{zrl}^2} + \frac{F_{trr}^2 + F_{srr}^2}{\mu^2 F_{zrr}^2} \quad (42)$$

with the constraints of:

$$\mathbf{B}_x \mathbf{F} = F_{x, total} \quad (43)$$

$$\mathbf{B}_y \mathbf{F} = F_{y, total} \quad (44)$$

$$\mathbf{B}_r \mathbf{F} = M_{z, total} \quad (45)$$

where $\mathbf{F} = [F_{tfl} \ F_{tfr} \ F_{trl} \ F_{trr} \ F_{sfl} \ F_{sfr} \ F_{srl} \ F_{srr}]^T$,
 $\mathbf{B}_x = [\cos \delta_{fl} \ \cos \delta_{fr} \ \cos \delta_{rl} \ \cos \delta_{rr} \ -\sin \delta_{fl} \ -\sin \delta_{fr} \ -\sin \delta_{rl} \ -\sin \delta_{rr}]$
 $\mathbf{B}_y = [\sin \delta_{fl} \ \sin \delta_{fr} \ \sin \delta_{rl} \ \sin \delta_{rr} \ \cos \delta_{fl} \ \cos \delta_{fr} \ \cos \delta_{rl} \ \cos \delta_{rr}]$

$$\begin{aligned} \mathbf{B}_r = & [l_f \sin \delta_{fl} + 0.5b_f \cos \delta_{fl} \quad l_f \sin \delta_{fr} - 0.5b_f \cos \delta_{fr} \\ & -l_r \sin \delta_{rl} + 0.5b_r \cos \delta_{rl} \quad -l_r \sin \delta_{rr} - 0.5b_r \cos \delta_{rr} \\ & l_f \cos \delta_{fl} - 0.5b_f \sin \delta_{fl} \quad l_f \cos \delta_{fr} + 0.5b_r \sin \delta_{fr} \\ & -l_r \cos \delta_{rl} - 0.5b_r \sin \delta_{rl} \quad -l_r \cos \delta_{rr} + 0.5b_r \sin \delta_{rr}] \end{aligned}$$

$$F_{ti}^2 + F_{si}^2 \leq \mu F_{zi}^2 \quad (46)$$

where the optimisation variables of this cost function are individual tyre forces F_{ti} , and F_{si} . $F_{x, total}$, $F_{y, total}$ and $M_{z, total}$ are the desired total longitudinal tyre force, lateral tyre force and yaw moment determined in the first layer controller. The effect of tyre friction circle is considered in (46). The constraints (43), (44) and (45) are used to achieve the desired total longitudinal tyre force, lateral tyre force and yaw moment. In order to overcome the model error due to the non-linear characteristic of the vehicle dynamics model, the sliding-mode controller (SMC) is applied and included in constraints (43), (44) and (45) to accurately track the desired total tyre forces and yaw moment. After applying the SMC control law, the following equations are proposed to replace the constraints (43), (44), (45):

$$\mathbf{B}_x \mathbf{F} = F_{x, total} - K_{s1} \operatorname{sgn} S_1 \quad (47)$$

$$\mathbf{B}_y \mathbf{F} = F_{y, total} - K_{s2} \operatorname{sgn} S_2 \quad (48)$$

$$\mathbf{B}_r \mathbf{F} = M_{z, total} - K_{s3} \operatorname{sgn} S_3 \quad (49)$$

where K_{s1} , K_{s2} and K_{s3} are positive control gains of SMC. The sliding surface S_1 , S_2 and S_3 in Eqs. (47)–(49) can be presented as follows:

$$S_1 = \int \mathbf{B}_x \mathbf{F} - F_{x, total} \quad (50)$$

$$S_2 = \int \mathbf{B}_y \mathbf{F} - F_{y, total} \quad (51)$$

$$S_3 = \int \mathbf{B}_r \mathbf{F} - M_{z, total} \quad (52)$$

After the individual tyre forces have been optimised and allocated in (42), the controlled values of individual steering and driving actuators can be mapped from the individual tyre force according to the following equations:

$$T_i = F_{ti}R_\omega \quad (53)$$

$$\delta_{fl} = \frac{F_{sfl}}{C_\alpha} + \frac{l_f r}{v_x} \quad (54)$$

$$\delta_{fr} = \frac{F_{sfr}}{C_\alpha} + \frac{l_f r}{v_x} \quad (55)$$

$$\delta_{rl} = \frac{F_{srl}}{C_\alpha} - \frac{l_r r}{v_x} \quad (56)$$

$$\delta_{rr} = \frac{F_{srr}}{C_\alpha} - \frac{l_r r}{v_x} \quad (57)$$

This controlled actuator values can be input into actual electric vehicle to achieve desired vehicle trajectory.

5. Simulation results

In this section, two sets of simulation results are used to verify the effectiveness of proposed trajectory planner and controller in both highway and off-road scenarios. The simulation parameters are shown in **Table 1**.

In the first set of simulations, the controlled vehicle is overtaking the vehicle ahead in the same lane in the highway scenario. A slow vehicle (with the velocity of

Symbol	Definition	Values
m	Mass	1298.9 kg
l_f	Distance of CG from the front axle	1.3 m
l_r	Distance of CG from the rear axle	1.5 m
b_f	Front track width	1.6 m
b_r	Rear track width	1.6 m
C_s	Longitudinal stiffness of the tyre	50,000 N/unit slip
C_α	Cornering stiffness of the tyre	30,000 N/unit slip
I_z	Vehicle moment of inertial about yaw axle	3900 kgm ²
I_x	Vehicle moment of inertial about longitudinal axle	765 kgm ²
I_y	Vehicle moment of inertial about lateral axle	3477 kgm ²
R_ω	Wheel radius	0.3 m
I_ω	Wheel moment of inertial	4 kgm ²
e	The distance between the vehicle roll centre and CG	0.4 m
h	Height of the vehicle centre of gravity	0.533 m
K_ϕ	The stiffness of roll axis	89,000

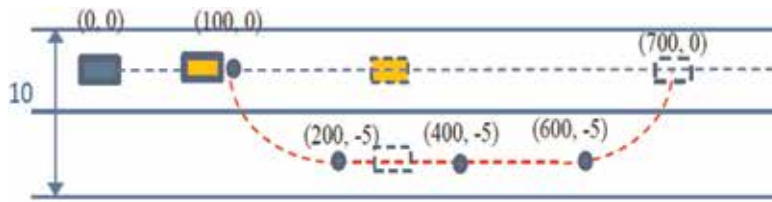
Table 1.
The simulation parameters [18].

15 m/s) is moving 100 metres ahead of the controlled vehicle (with the velocity of 20 m/s). In order to overtake the slow vehicle, the controlled vehicle first decelerates from 20 m/s into 15 m/s and then makes the lane change to the right lane. After that, the controlled vehicle accelerates from 15 m/s into 20 m/s to go ahead of the overtaken vehicle. Finally, the controlled vehicle goes back to the left lane. The details of this scenario are described in **Figure 3(a)**, and the whole global desired path can be divided by 5 sections. For the purpose of comparison, the control performance of the potential field method based on [26] is also presented here. Furthermore, in order to show the advantage of 4WIS-4WID vehicle model, the proposed trajectory planning and control performance based on two-wheel model is presented and compared.

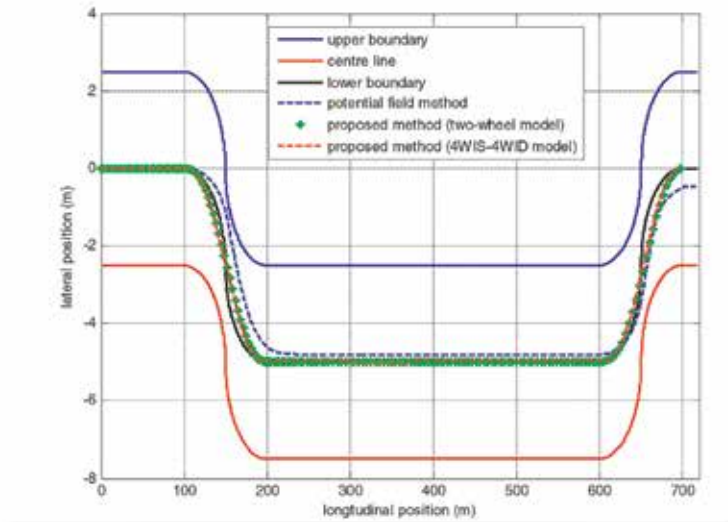
In **Figure 3(b)**, the moving trajectory of the overtaking vehicle controlled by both the potential field method and the proposed method based on two-wheel model and 4WIS-4WID model is compared. The proposed method based on two-wheel model and 4WIS-4WID model shows good control performance, and the controlled vehicle is moving within the road boundary. **Figure 3(c)** shows that the overtaking vehicle and overtaken vehicle maintain the safety distance to avoid collision. **Figure 4** demonstrates that the potential field method shows big lateral tracking error compared with the proposed methods based on two-wheel model and four-wheel model, while the longitudinal tracking error of potential field method is smaller than the proposed method. Since the lateral tracking error is more important than longitudinal tracking error on highway overtaking scenario, the proposed method has better overall tracking performance than potential field method. It is also noted that the tracking error of proposed method based on two-wheel model is larger than four-wheel model, especially for the tracking error of the lateral position. This shows the advantages of 4WIS-4WID model.

In **Figures 5(a)** and **5(b)**, the longitudinal velocity and lateral velocity in the global coordinate system for both the potential field method and the proposed trajectory planning method are presented. V_{xd1} , V_{xd2} , V_{xd3} , V_{xd4} and V_{xd5} are desired longitudinal velocities on each section of road, while V_{yd1} , V_{yd2} , V_{yd3} , V_{yd4} and V_{yd5} are desired lateral velocities on each section of road. The potential field method can only roughly achieve the desired longitudinal velocity and lateral velocity, while the proposed method can accurately achieve desired values. This proves that the proposed method can not only achieve the desired ending positions but also achieve the desired ending velocities. **Figure 5(c)** and **Figure 5(d)** present the vehicle yaw rate and body side-slip angle responses, which proves that the proposed trajectory planning method can achieve much better handling and stability performance compared with potential field method.

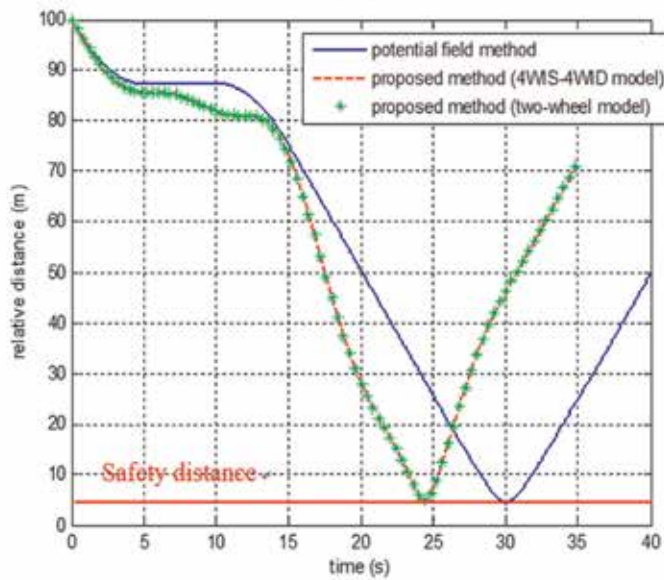
In the second set of simulations, the autonomous vehicle is assumed to move in the off-road scenario, and the road topography should be considered. **Figure 6** presents the scenario in the second set of simulations: in a particular section of the road, the vehicle start position is (0, 0) and the target ending position is constrained by a certain boundary (90–110, 20–30); the initial and ending longitudinal velocity is 5 m/s, and the initial and ending lateral velocity is 0 and 3 m/s, respectively. The bank angle and road slope of this section of road is shown in **Figure 7**. The trajectory planner proposed in Eq. (26) will choose the best suitable ending position and vehicle trajectory by considering the road topography information (minimising the bank angle and road slope). The vehicle dynamics response of the trajectory planner which has not considered the road topography information proposed in Eq. (23) is also shown and compared. It is noted that trajectory planner without considering road topography is briefly called ‘trajectory planner 1’ and trajectory planner considering road topography is briefly called ‘trajectory planner 4’. **Figure 8** compares



(a)



(b)



(c)

Figure 3. (a) Vehicle overtaking scenario in the first set of simulations (unit: m). (b) The vehicle trajectory in the global coordinate system. (c) The relative distance between the overtaking vehicle and overtaken vehicle [21].

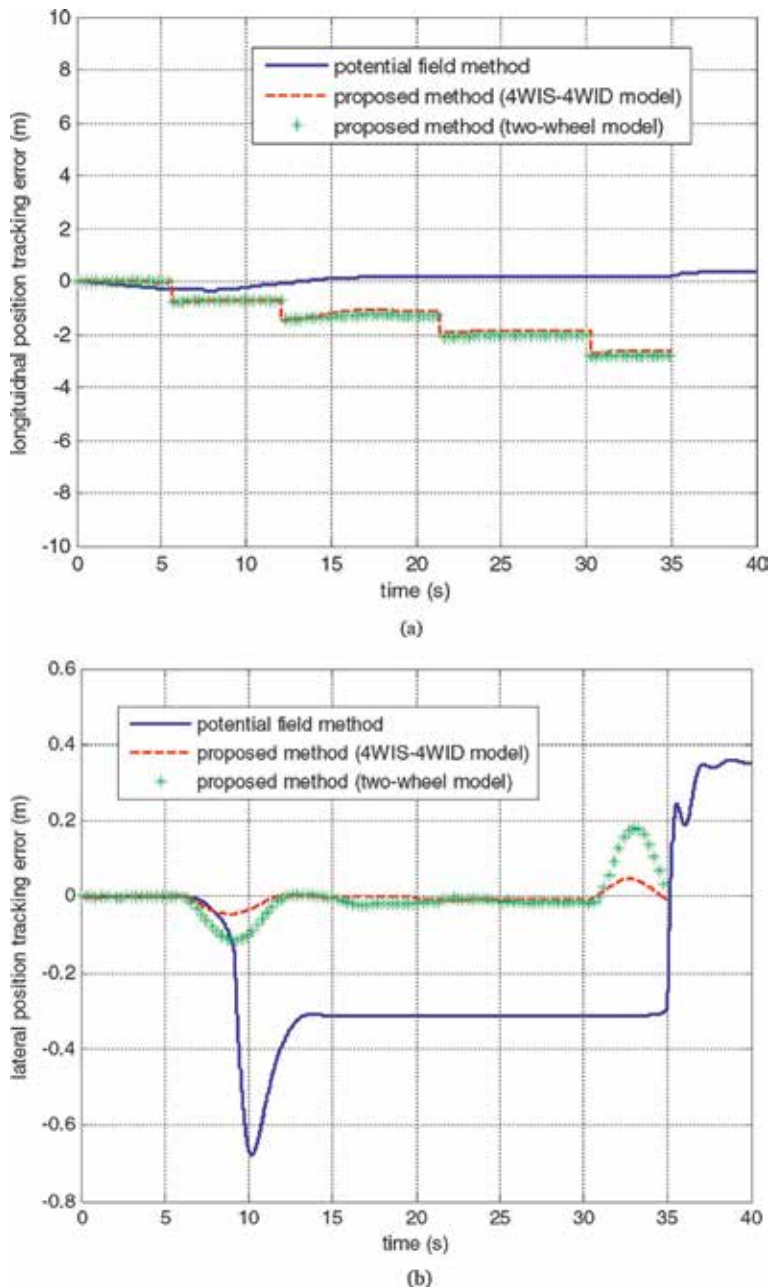


Figure 4. The tracking errors of vehicle trajectory in the first set of simulations: (a) longitudinal position and (b) lateral position [21].

the bank angle and road slope of the desired trajectories planned by trajectory planner 1 and trajectory planner 4 and proves that the trajectory planner 4 can generate the trajectory with smaller bank angle and road slope. **Figure 9** shows the trajectory tracking performance when trajectory planner 4 applied is much improved compared with trajectory planner 1. **Figure 10** shows the dynamics responses between trajectory planner 1 and trajectory planner 4. **Figure 10(a)** suggests that the undesired lateral velocity is reduced a lot when trajectory planner 4 has been applied. **Figure 10(b)** and **Figure 10(c)** prove that the autonomous

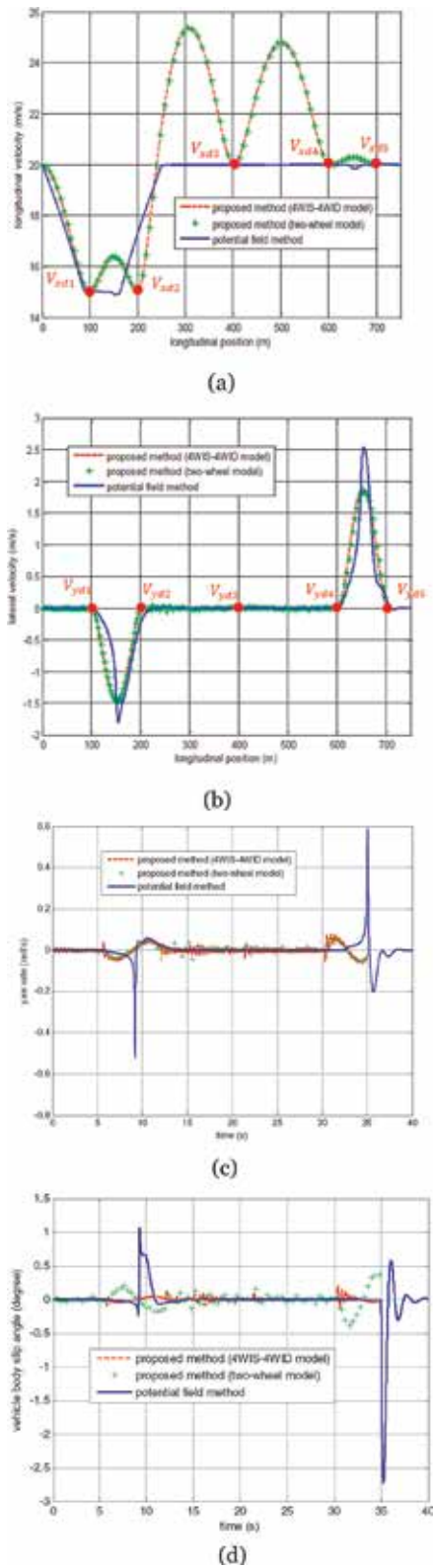


Figure 5. The vehicle state in the first set of simulations: (a) longitudinal velocity in the global coordinate system, (b) lateral velocity in the global coordinate system, (c) yaw rate and (d) body slip angle [21].

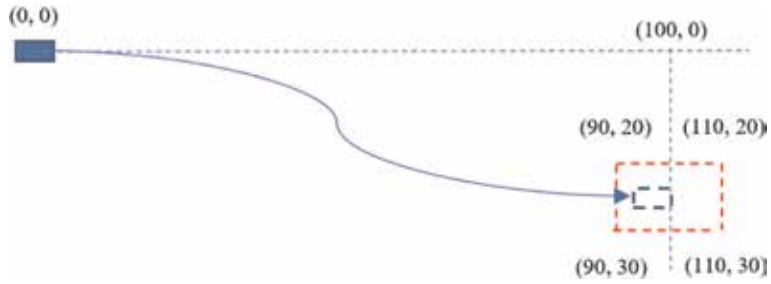
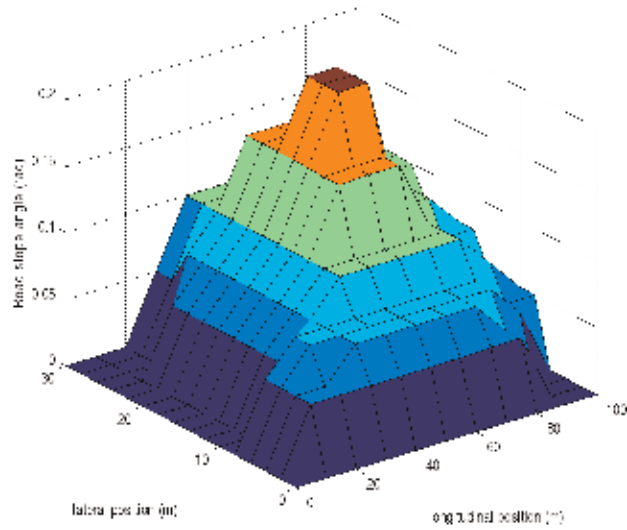
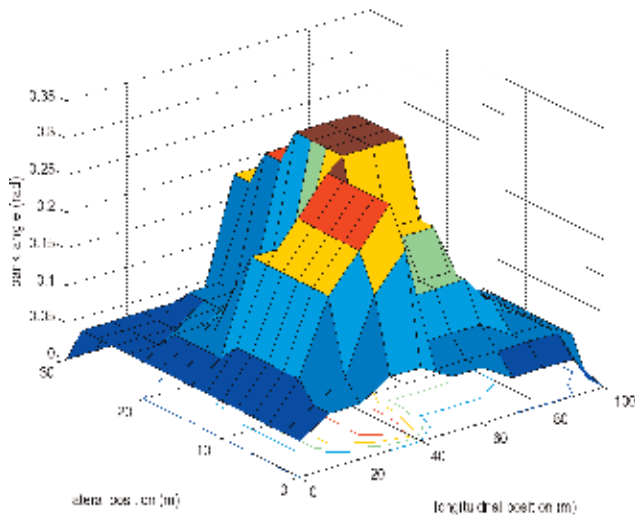


Figure 6.
 The vehicle off-road scenario in the second set of simulations (unit: mm).

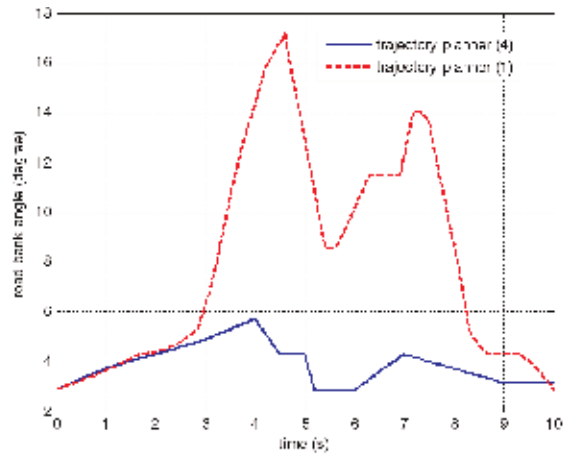


(a)

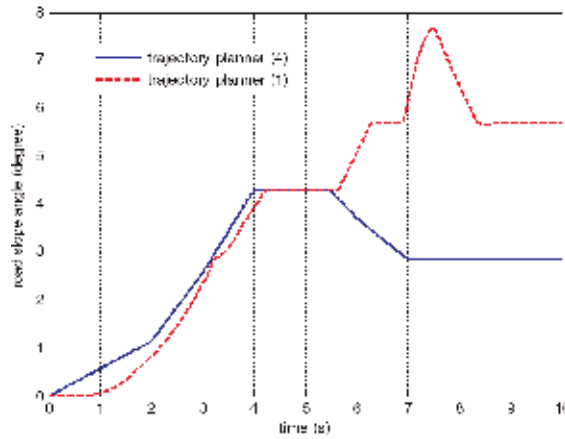


(b)

Figure 7.
 The vehicle (a) road slope and (b) bank angle of the one particular section of uneven road surface in the second set of simulations.



(a)



(b)

Figure 8.
The actual (a) bank angle and (b) road slope in the second set of simulations.

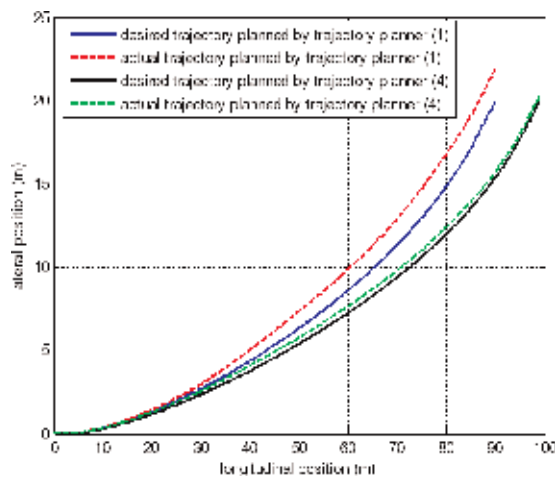


Figure 9.
The desired trajectory tracking performance in the second set of simulations.

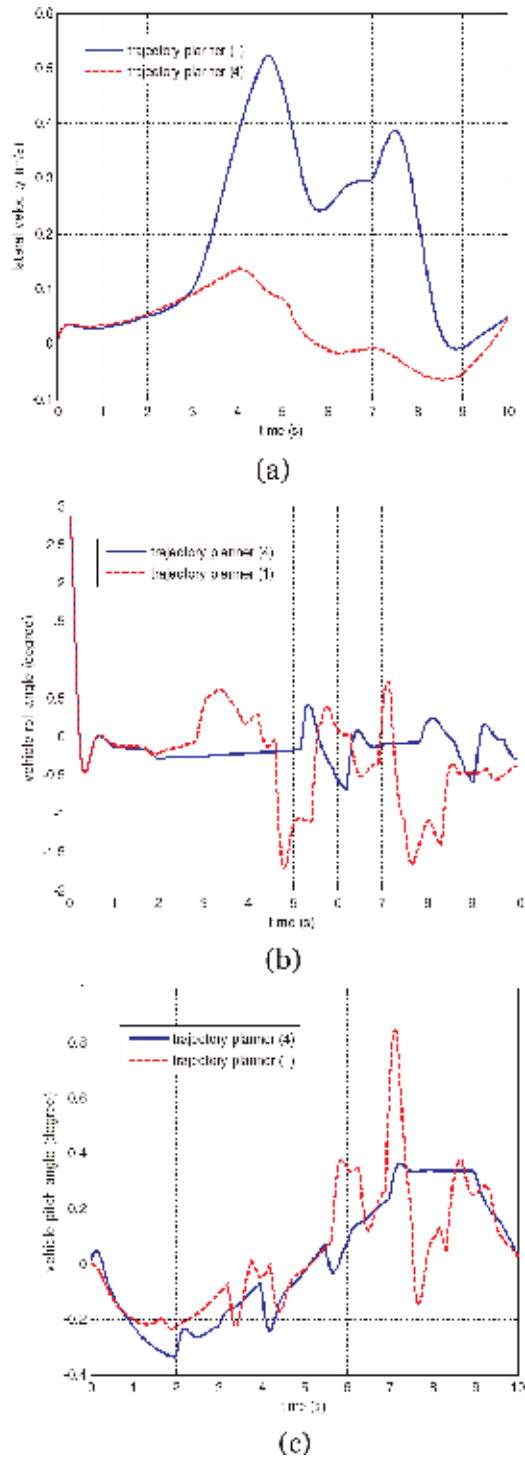


Figure 10. Vehicle dynamics responses in the second set of simulations: (a) lateral velocity, (b) roll angle and (c) pitch angle.

vehicle has smoother roll angle and pitch angle response when trajectory planner 4 is applied since the road bank angle and road slope is minimised compared with the situation when trajectory planner 1 is applied.

6. Conclusion

In this chapter, a dynamically integrated spatiotemporal-based trajectory planning and control method for the off-road autonomous vehicles is proposed. The upper-level trajectory planner can select the best time-parameterised trajectory among a group of the candidate trajectories by considering the road topography information. Then, the lower-level trajectory controller can control the motion of the vehicle and achieve the desired trajectory.

Simulation results have proved that the proposed trajectory planning and control method can successfully control the motion of autonomous vehicles and achieve the spatiotemporal-based desired trajectory while satisfying the target ending position and velocity. In the highway scenario, the proposed method has better overall position tracking control performance and can better achieve the desired longitudinal and lateral velocity compared with the conventional potential field method. In addition, the 4WIS-4WID vehicle shows better tracking control performance than traditional vehicle based on two-wheel model.

In the off-road scenario, the proposed trajectory planning method can successfully find a specific trajectory which can avoid the peak values of bank angle and road slope. Simulation results prove that the proposed trajectory planner when considering the road topography information can generate the trajectory with much smaller bank angle and road slope compared with trajectory generated by traditional trajectory planner. The actual trajectory tracking performance, roll stability and pitch stability performance can be improved by using the proposed trajectory planning method to minimise the effect of road topography on vehicle dynamics.

Conflict of interest

We declare that there is no conflict of interest in this chapter.

Author details

Boyuan Li¹, Haiping Du^{2*} and Bangji Zhang¹

1 State Key Laboratory of Advanced Design and Manufacturing for Vehicle Body, Hunan University, Changsha, China

2 School of Electrical, Computer and Telecommunication Engineering, University of Wollongong, Wollongong, Australia

*Address all correspondence to: hdu@uow.edu.au

IntechOpen

© 2019 The Author(s). Licensee IntechOpen. This chapter is distributed under the terms of the Creative Commons Attribution License (<http://creativecommons.org/licenses/by/3.0>), which permits unrestricted use, distribution, and reproduction in any medium, provided the original work is properly cited. 

References

- [1] Baten S, Luetzeler M, Dickmanns E, Mandelbaum R, Burt P. Techniques for autonomous off-road navigation. *IEEE Intelligent Systems and their Applications*. 1998;**13**(6):57-65. DOI: 10.1109/5254.736003
- [2] Krotkov E, Fish S, Jackel L, McBride W, Perschbacher M, Pippine J. The DAPRA PerceptOR evaluation experiments. *Autonomous Robots*. 2006;**22**(1):19-35. DOI: 10.1007/s10514-006-9000-0
- [3] Andrade G, Amara F, Biduad P, Chatila R. Modelling of robot-soil interaction for planetary rover motion control. In: *Proceedings of IEEE/RSJ International Conference on Intelligent Robots and Systems. Innovations in Theory, Practice and Applications*; 17 October 1998; Victoria, Canada. 1998
- [4] Schenker P, Hunstberger T, Pirjanian P, Dubowski S, Iagnemma K, Sujun V. Rovers for agile intelligent traverse of challenging Terrain. In: *Proceedings of the 7th International Symposium on Artificial Intelligence, Robotics and Automation in Space*; 2003; Nara, Japan. 2003
- [5] Roberts J, Corke P, Winstanley G. Development of a 3,500 tonne field robot. *The International Journal of Robotics Research*. 1999;**18**(7):739-752. DOI: 10.1177/02783649922066547
- [6] Hagrass H, Colley M, Callaghan V, Carr-West M. Online learning and adaptation of autonomous mobile robots for sustainable agriculture. *Autonomous Robots*. 2002;**13**(1):37-52. DOI: 10.1023/A:1015626121039
- [7] Werling M, Gindele T, Jagszent D, Gröll L. A robust algorithm for handling moving traffic in urban scenarios. In: *IEEE Intelligent Vehicles Symposium*; 2008; Eindhoven, The Netherlands. 2008. pp. 1108-1112
- [8] Lapierre L, Zapata R, Lepinay P. Combined path-following and obstacle avoidance control of a wheeled robot. *The International Journal of Robotics Research*. 2007;**26**(4):361-375. DOI: 10.1177/0278364907076790
- [9] Soetanto D, Lapierre L, Pascoal A. Adaptive, nonsingular path following control of dynamic wheeled robot. In: *42nd IEEE Conference on Decision and Control*; 2003; Maui, Hawaii, USA. 2003. pp. 1765-1770
- [10] Ge S, Cui J. Dynamic motion planning for mobile robots using potential field method. *Autonomous Robots*. 2002;**13**:207-222. DOI: 10.1023/A:1020564024509
- [11] Kuwata Y, Fiore G, Teo J, Frazzoli E, How J. Motion planning for urban driving using RRT. In: *International Conference on Intelligent Robots and Systems*; 2008; Nice, France. 2008. pp. 1681-1686
- [12] Likhachev M, Ferguson D. Planning long dynamically feasible maneuvers for autonomous vehicles. *The International Journal of Robotics Research*. 2009; **28**(8):933-945. DOI: 10.1177/0278364909340445
- [13] Pivtoraiko M, Kelly A. Efficient constrained path planning via search in state lattices. In: *International Symposium on Artificial Intelligence, Robotics, and Automation in Space*; September 2005; Munich, Germany. 2005. pp. 1-7
- [14] LaValle M. *Rapidly-Exploring Random Trees: A New Tool for Path Planning* [Technical Report]. Computer Science Department, Iowa State University; 1998
- [15] Howard T, Kelly A. Optimal rough terrain trajectory generation for

- wheeled mobile robots. *The International Journal of Robotics Research*. 2007;**26**(2):141-166. DOI: 10.1177/0278364906075328
- [16] Montemerlo M, Becker J, Bhat S, Dahlkamp H, Dolgov D, Ettinger S, et al. Junior: The Stanford entry in the urban challenge. *Journal of Field Robotics*. 2008;**25**(9):569-597. DOI: 10.1002/rob.20258
- [17] Werling M, Kammel S, Ziegler J, Gröll L. Optimal trajectories for time-critical street scenarios using discretised terminal manifolds. *The International Journal of Robotics Research*. 2011; **31**(3):346-359. DOI: 10.1177/0278364911423042
- [18] Boada B, Boada M, Díaz V. Fuzzy-logic applied to yaw moment control for vehicle stability. *Vehicle System Dynamics*. 2005;**43**:753-770
- [19] Dugoff H, Fancher P, Segel L. An analysis of tyre traction properties and their influence on vehicle dynamic performance. *SAE Transactions*. 1970; **79**(2):1219-1243. Available from: <https://www.jstor.org/stable/44644491>
- [20] Zhao Y, Zhang J. Yaw stability control of a four-independent-wheel drive electric vehicle. *International Journal of Electric and Hybrid Vehicles*. 2009;**2**(1):64-76. DOI: 10.1504/IJEHV.2009.027677
- [21] Li B, Du H, Li W, Zhang B. Dynamically integrated spatiotemporal-based trajectory planning and control for autonomous vehicles. *IET Intelligent Transport Systems*. 2018;**12**(10): 1271-1282. DOI: 10.1049/iet-its.2018.5306
- [22] Li X, Sun Z, Cao D, He Z, Zhu Q. Real-time trajectory planning for autonomous urban driving: Framework, algorithms, and verifications. *IEEE/ASME Transactions on Mechatronics*. 2016;**21**(2):740-753. DOI: 10.1109/TMECH.2015.2493980
- [23] Levinson J, Montemerlo M, Thrun S. Map-based precision vehicle localization in urban environments. In: *Robotics: Science and Systems*; April 2007. Cambridge, MA, USA: MIT Press; 2007. p. 1
- [24] Levinson J, Thrun S. Robust vehicle localization in urban environments using probabilistic maps. In: *Proceedings of IEEE International Conference on Robotics and Automation*; 2010; Anchorage, AK, USA. 2010. pp. 4372-4378
- [25] Park H, Gerdes J. Optimal Tyre force allocation for trajectory tracking with an over-actuated vehicle. In: *2015 IEEE Intelligent Vehicles Symposium (IV)*; 2015; Seoul, Korea. 2015. pp. 1032-1037
- [26] Li B, Du H, Li W. A potential field approach-based trajectory control for autonomous electric vehicles with In-wheel motors. *IEEE Transactions on Intelligent Transportation Systems*. 2017;**18**(8):2044-2055. DOI: 10.1109/TITS.2016.2632710

Vision-Based Path Finding Strategy of Unmanned Aerial Vehicles for Electrical Infrastructure Purpose

Alexander Cerón, Flavio Prieto and Luis Mejias

Abstract

In this chapter we present the development of automated visual inspection systems for electrical infrastructure. The inspection is performed using images acquired with an unmanned aerial vehicle (UAV). Through automated inspection routes, the state of the infrastructure can be evaluated and then the appropriate correcting measures be taken. The monitoring of power lines can be done using passive sensors such as cameras or active sensors such as light detection and ranging (LIDAR) cameras, image processing techniques, computer vision and control systems can then be used. Additionally, a three-dimensional (3D) reconstruction process is possible using images either offline or during the monitoring. An UAV with an onboard embedded computer is used to execute the computer vision and path planning algorithms. The work done shows that the proposed strategy aids in the automation of power line inspection.

Keywords: UAV, power line detection, 3D reconstruction

1. Introduction

There exist numerous applications for UAVs that include autonomous navigation, tracking and 3D reconstruction [1–3]. Electrical infrastructure inspection with aerial robots, especially transmission line inspection, is very important since it can minimize costs, risk and logistic problems that usually are associated with manual inspection [4]. In this context the use of new technologies for power line inspection such as UAVs can bring great benefits. The common methods for power line inspection are manual inspection, manned helicopters and UAVs as shown in **Figure 1**.

In the work presented in [5], three aspects have been shown: (1) strategies for risk administration in high power line corridors, (2) selection of suitable platforms for sensor location and (3) data processing techniques for identifying vegetation.

One of the principal problems to resolve in this field is the image distortion/noise due to camera movement/vibration, which can be mitigated with the use of the gimbal stabilizers and a mechanical vibration isolator under the flight controller.

A path planning process for electrical infrastructure inspection requires to consider the detection of power lines and electrical towers because these elements can generate a corridor where an autonomous system can perform the inspection task [5].



Figure 1.
Example of different methods for power line inspection.

An important aspect of autonomous navigation systems is the collision avoidance [6, 7]. In a path planning process for automatic inspection of electrical infrastructure, it is necessary to be able to avoid electrical towers and power lines. The first task for accomplishing this goal is an object detection process that will be discussed in this chapter.

The access throughout the corridor is very important since it is necessary in order to inspect the area surrounding power lines. It must be free of obstacles and vegetation.

As a part of the inspection process, an important task is the detection of elements of the electrical infrastructure; this is achieved by using computer vision techniques such as object detection. The common objects present in the electrical infrastructure scene are the power lines and electrical towers. An additional task is the 3D reconstruction of the elements of the scene by using the captured images.

2. Power line detection

In this section, we show different methods for the detection of electrical lines through image processing and computer vision, which include methods for detection of rectilinear segments and catenary. Also, the use of machine learning is presented.

2.1 Line detection process

There are different methods for line detection [8–11]. Some of them are based on graphics processing unit (GPU) approaches and geometrical considerations [12–15] that can be used in the context of power line detection. It is important to note that line detection methods based on monocular images present better results in uniform background sceneries.

For the detection of rectilinear long segments from images taken from a top-down view, the process can be composed of the stages shown in **Figure 2**.

As this process cannot differentiate the power lines from other lines presented in the scene, there exists the possibility of using machine learning to reduce detection errors or improving the power line detection.

2.1.1 Machine learning method

The recognition system has to be trained with real power lines; after that the system must be able to recognize or select the power lines in a scene. In the first stage, it is necessary to define what lines are electrical lines. This is done by using an application for labelling as shown in **Figure 3**.

This system operates in two modes, training and detection, as shown in **Figure 4**.

The training mode begins with an edge detector such as Sobel, Prewitt, Canny or Edge drawing. After that, different line detection methods can be used for detecting a representative set of lines present in the scene. The dataset is obtained by labelling

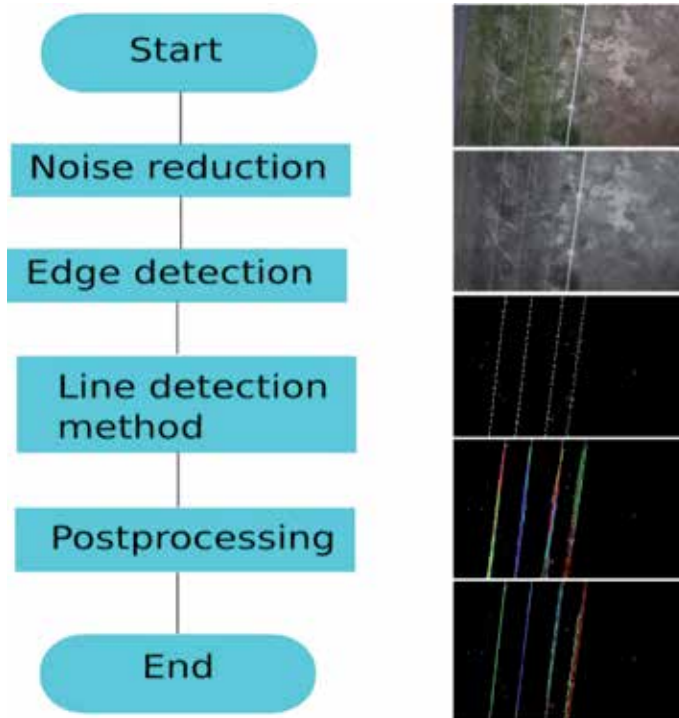


Figure 2.
Stages of a rectilinear process detection.

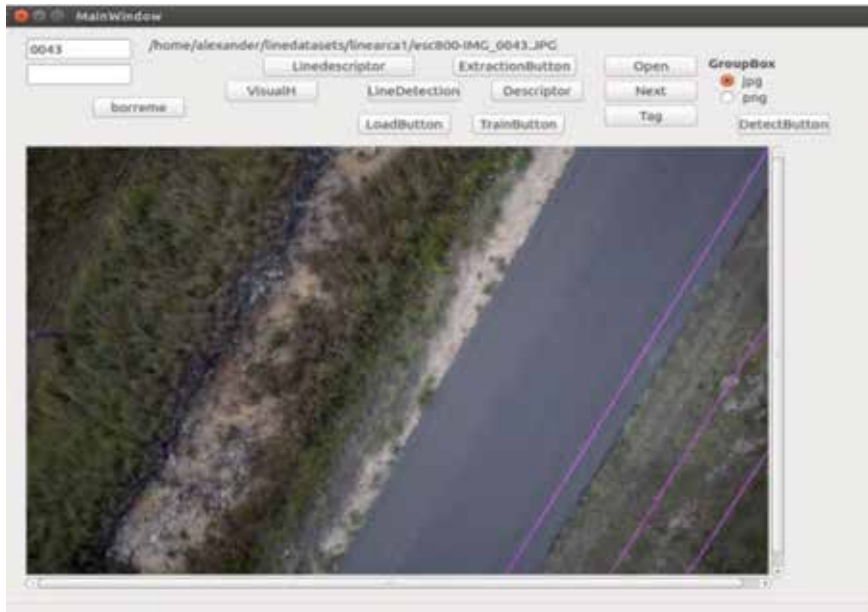


Figure 3.
Power line labelling.

(tagging), manually, the power lines in each image in order to select only the lines that correspond to power lines in the training mode as a true example. For this reason, an application with a graphical user interface (GUI) for selecting lines over a copy of the real image can be used (Figure 3).

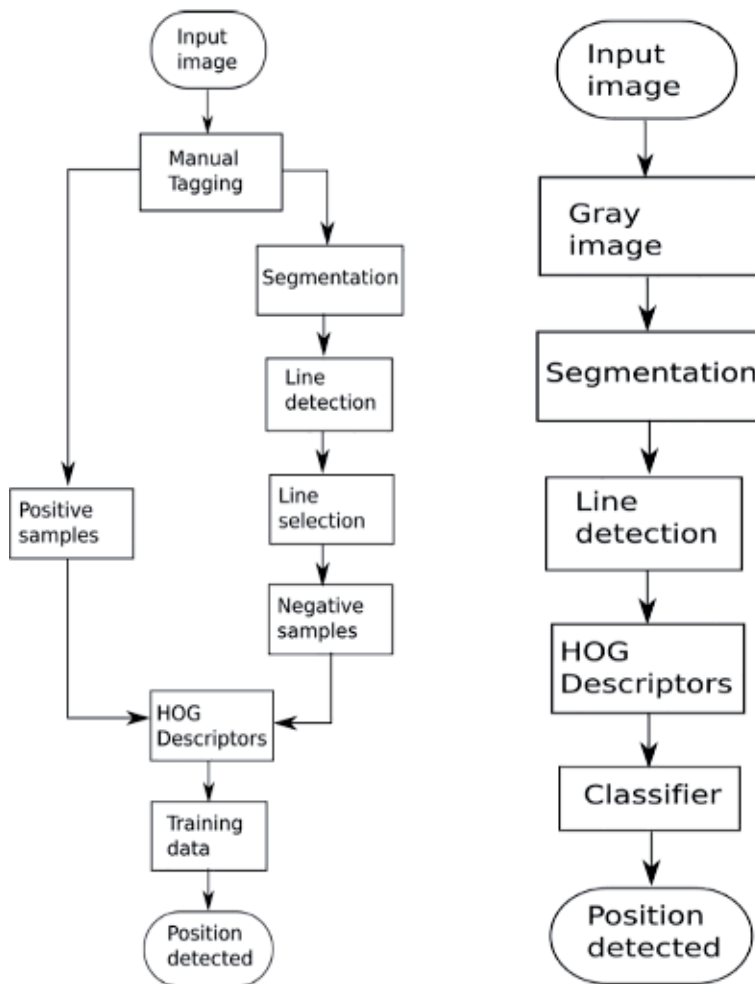


Figure 4. Process for line recognition system, training and detection.

The overall detected lines are compared with the labeled lines in order to differentiate the positive and negative samples. The positive samples are power lines that overlap the previously labeled lines. The negative samples are other lines detected in the scene that are not power lines. This corresponds to lines that have not been tagged.

The overlapping between the tagged lines and detected lines that are not power lines must be zero.

After that, a feature extraction stage is performed by using HOG descriptors [16], which are computed for the selected lines on the labeled dataset. This is done in spaced squared windows centred in the lines. In **Figure 5**, the extraction of the HOG descriptor in windows across a labeled power line is shown.

Finally, the obtained descriptor values in the previous stage are the input data for the classifier. The SVM classifier is trained with this input data using a sigmoid kernel.

The detection mode has to be used after a training mode. The objective of this stage is to detect the power lines using the previously trained classifier.

This begins with segmenting and detecting lines as in the previous mode. After that, HOG descriptors are computed across the detected lines using squared windows as were done in training mode. This information is gathered for the classifier.

In **Figure 6**, the detection of all linear elements using a conventional line detection method is shown. The results of the machine learning method are shown in **Figure 7**.

Finally, the SVM is evaluated with the obtained descriptor data. Line segments which pass this evaluation are power line candidates. Another possibility is to use deep learning methods and contextual information in order to improve the detection [1].

2.2 Catenary detection

Most of the works on power line detection are focused in straight line detection. Nevertheless, the electrical infrastructure is composed of catenaries which are

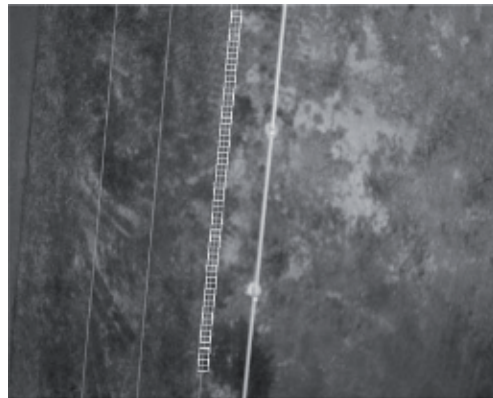


Figure 5.
Extracting HOG descriptor in lines.

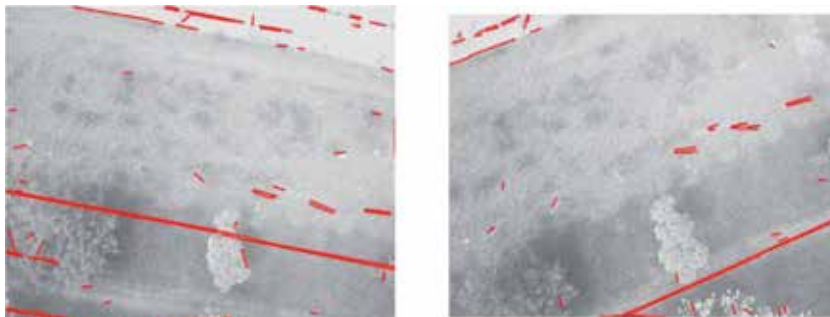


Figure 6.
Line detection in the scene.

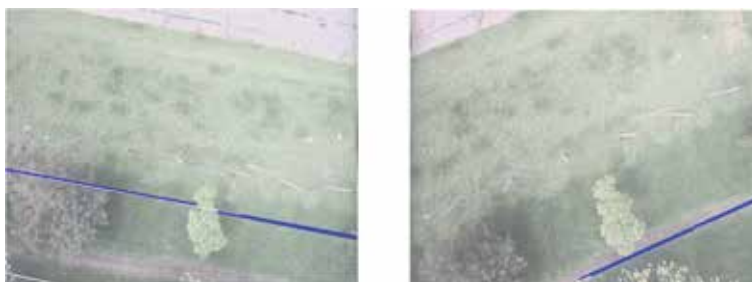


Figure 7.
Result of a machine learning method.

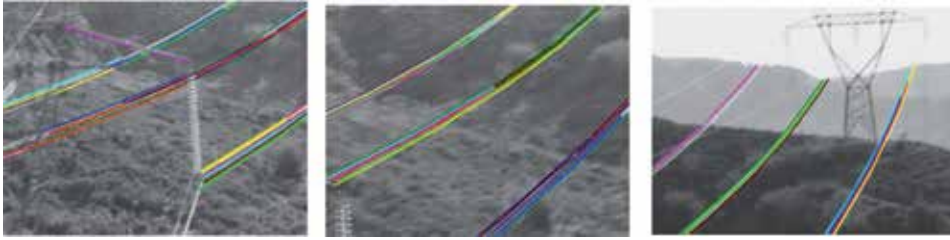


Figure 8.
Catenary detection based in a segment concatenation.

generated when a flexible cable is suspended between two poles or towers. This type of object appears in images of electrical infrastructure taken from non-top-down views, which could be obtained using manned aircraft or UAVs. Different methods for catenary detection that includes the use of matching filters, line segment pool and a graph-cut model as is shown in [17] exist, also using geometrical considerations and data structures of segment concatenation [18]. The results of catenary detection based on a segment concatenation are shown in **Figure 8**.

3. Tower detection process

The transmission towers are important elements of the electric transmission system. They require maintenance of its components such as the isolators and the power line connections.

The tower detection process is done mainly using computer vision techniques based in machine learning methods such as neural networks, SVM [19, 20] and recently deep learning [1]. The process requires a training stage. In this case a classifier is trained using a set of labelled images. A manual tool is used for labelling, this is for selecting the region of interest (ROI) where the tower is located as shown in **Figure 9**. In the selected ROI, a set of descriptors is extracted. The descriptors are the input to the classifier. After that, a detection stage operates with frames of videos. The linear information of the scene can be obtained using line detection methods. This can be useful to simplify the scene. The tower detection process is composed of two stages, training and detection, as shown in **Figure 10**. The result of the tower detection process is in **Figure 11**.



Figure 9.
The ROI selection of an electrical tower.

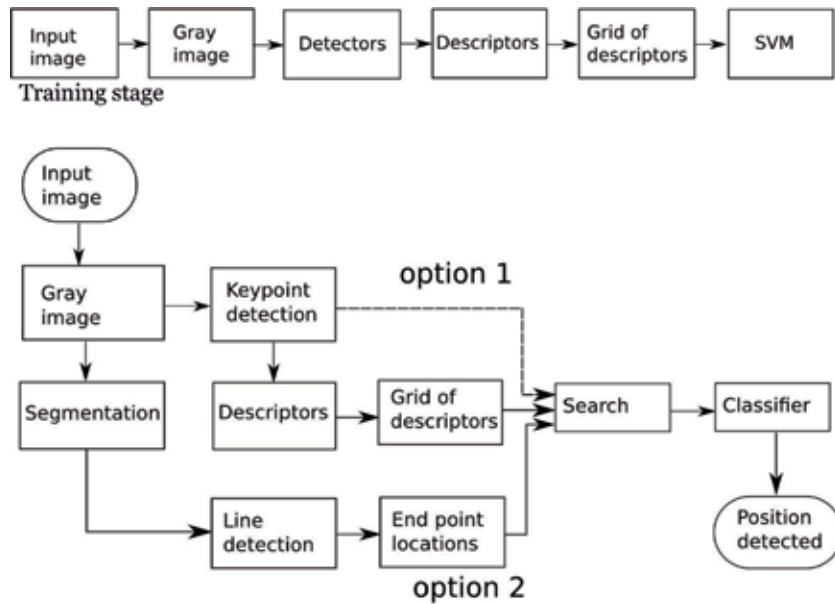


Figure 10.
Training and detection stages for tower detection.



Figure 11.
Tower detection examples using SVM and a grid of descriptors.

For an autonomous inspection system based on UAV, the tower can be a distinctive element for the navigation process. However, it is an element that may be at risk of collision. Autonomous systems must be prepared to use towers as a reference area and also to avoid collisions with them.

The recent advances in computer vision methods for object detection towards the use of deep learning methods. These algorithms can be implemented on onboard computers provided with GPU (graphics processing unit) for accelerating computation [1].

4. Autonomous navigation process

Vision-based autonomous navigation for UAVs is a complex process that requires short computing times and accurate measurements in order to provide suitable and safe control commands to the device. The UAV navigation requires real-time measurements to produce a response within a specified time (at least 100 ms); otherwise, severe consequences including failure may affect the device. The simulation of a control system for a fixed-wing UAV that uses vision-based navigation for power line tracking is presented in [21]. In a previous work, the



Figure 12.
Simulation of autonomous navigation.

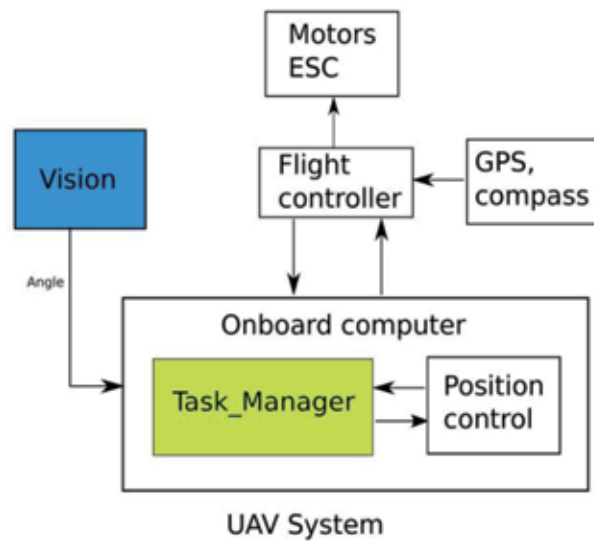


Figure 13.
UAV system.

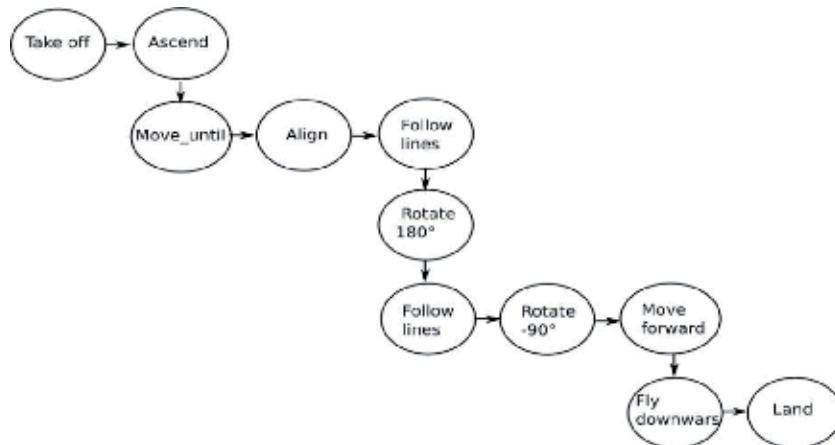


Figure 14.
Autonomous mission process stages.

simulation of a visual-based navigation process for power line following in a 3D environment using a closed loop control was presented in [22].

Two pictures of the simulator of autonomous navigation using power line detection are shown in **Figure 12**.

This camera provided images that are suitable for the line detection process. The frame rate permits closed loop control. The UAV system consists of a set of related components that are shown in **Figure 13**. The main components of the system are the UAV flight platform; the flight controller; the sensors that include GPS and inertial measurement unit (IMU) that includes three-axis magnetometers, gyroscopes, accelerometers and compass; camera; and the onboard computer to run the developed software. In this system, the flight controller receives setpoints from the onboard computer and sends sensed information to it. The vision sensor (camera) sends frames of images to the onboard computer.

Different kinds of missions for power line following and terrain inspection can be established. The main stages of a complete mission are shown in **Figure 14**.

5. 3D reconstruction of electrical infrastructure

Effective and efficient generation of 3D models from a set of 2D images is a well-studied problem in the literature and the principle of numerous computer vision applications. The keypoint detection and the 2D descriptor extraction are the first steps in the reconstruction process followed by the matching. There are different 2D descriptors such as SIFT, ORB, BRISK and FREAK that can be used in the context of 3D reconstruction using structure from motion (SFM). From the study [3], it can be concluded that it is possible to use the aforementioned descriptors in electrical tower reconstruction context. Also, the results shown that the SIFT descriptor presents the best performance in the generated cloud of points, but it spends more time than using other descriptors. Another good option is the use of the ORB descriptor. In **Figure 15**, a result using SIFT is presented.

Current developments tend towards the use of other types of sensors such as LIDAR whose information can be merged with information from cameras with different spectra.

Also it is important to develop an online process of object recognition by using simultaneous localization and mapping (SLAM). This can help to improve the object detection stage in order to obtain a more robust navigation system.



Figure 15.
Results of 3D reconstruction of electrical infrastructure.

6. Conclusions

Real-time power line detection is a challenging problem that must be performed using different methods such as edge detectors, machine learning methods and 3D computer vision. The main problems inside this are the image correction due the abrupt movements of the UAV, the difference of backgrounds found while flying and illumination changes. The tower detection using deep learning methods is recommended for a robust detection. The proposed vision strategy could help monitor the environment of power lines in order to prepare preventive maintenance for reducing risk of tree branches that can affect the electrical infrastructure.

As future work, a technique based on SLAM could be useful to deal with complex scenes in order to improve the process and extract 3D information as an online process using an onboard computer.

It is mandatory to focus the future work in collision avoidance systems that allow to protect both UAV and electrical infrastructure in order to minimize the risk of damages during inspection process or autonomous navigation. Motion prediction is necessary for path planning in autonomous systems, and risk assessment for intelligent vehicles is fundamental to improve the safety.

The development of a system with a fixed wing platform could be useful for long-distance inspections. Finally, the study of the effects of oscillation of the detected angle between the UAV and the power lines can be considered in order to improve the control strategy using methods such as filtering.

Acknowledgements

This work was supported by the INV-ING-2995 project of the Vicerrectoria de Investigaciones—Universidad Militar Nueva Granada.

Author details

Alexander Cerón^{1*}, Flavio Prieto² and Luis Mejias³


¹ Multimedia Engineering Program, Universidad Militar Nueva Granada, Bogota, Colombia

² Department of Mechanical and Mechatronic Engineering, Universidad Nacional de Colombia, Bogotá, Colombia

³ Australian Research Centre for Aerospace Automation, Queensland University of Technology, Brisbane, Australia

*Address all correspondence to: alexander.ceron@unimilitar.edu.co

IntechOpen

© 2019 The Author(s). Licensee IntechOpen. This chapter is distributed under the terms of the Creative Commons Attribution License (<http://creativecommons.org/licenses/by/3.0>), which permits unrestricted use, distribution, and reproduction in any medium, provided the original work is properly cited. 

References

- [1] Hui X, Bian J, Zhao X, Tan M. Vision-based autonomous navigation approach for unmanned aerial vehicle transmission-line inspection. *International Journal of Advanced Robotic Systems*. 2018;**15**(1):1-15. DOI: 10.1177/1729881417752821
- [2] Ceron A, Prieto F, Mondragon I. Onboard visual-based navigation system for power line following with UAV. *International Journal of Advanced Robotic Systems*. 2018;**15**(2):1-12. DOI: 10.1177/1729881418763452
- [3] Agudelo J, Ceron A, Prieto F. Evaluation of 2d descriptors for 3d reconstruction of electrical infrastructure. *International Journal of Imaging & Robotics*. 2018;**18**(2):101-115
- [4] Jones D. Power line inspection—A UAV concept. In: *Autonomous Systems*; 2005
- [5] Li Z, Walker R, Hayward R, Mejias L. Advances in vegetation management for power line corridor monitoring using aerial remote sensing techniques. In: *Proceedings of the First International Conference on Applied Robotics for the Power Industry (CARPI)*; IEEE; 2010. pp. 1-6
- [6] Hamid UZA, Saito Y, Zamzuri H, Rahman MAA, Raksincharoensak P. A review on threat assessment, path planning and path tracking strategies for collision avoidance systems of autonomous vehicles. *International Journal of Vehicle Autonomous Systems*. 2018;**14**(2):134
- [7] Lefèvre S, Vasquez D, Laugier C. A survey on motion prediction and risk assessment for intelligent vehicles. *ROBOMECH Journal*. 2014;**1**(1):1
- [8] Duda RO, Hart PE, Park M. Use of the hough transformation to detect lines and curves in pictures. *Graphics and Image Processing*. 1972;**15**(1):11-15
- [9] Burns B, Hanson AR, Riseman EM. Extracting straight lines. *IEEE Transactions on Pattern Analysis and Machine Intelligence*. 1986;**PAMI-8**(4):425-455
- [10] Akinlar C, Topal C. EDLines: A real-time line segment detector with a false detection control. *Pattern Recognition Letters*. 2011;**32**(13):1633-1642
- [11] Grompone von Gioi R, Jakubowicz J, Morel J-M, Randall G. LSD: A line segment detector. *Image Processing On Line*. 2012. pp. 35-55. Available from: <http://www.ipol.im/pub/art/2012/gjmr-lsd/>
- [12] Liu Y, Mejias L. Real-time power line extraction from unmanned aerial system video images. In: *2nd International Conference on Applied Robotics for the Power Industry (CARPI)*; September 2012. pp. 52-57
- [13] Liu Y, Mejias L, Li Z. Fast power line detection and localization using steerable filter for active uav guidance. In: *12th International Society for Photogrammetry & Remote Sensing (ISPRS2012)*; Vol. XXXIX; 2012. pp. 491-496
- [14] Yao X, Guo L and Zhao T. Power line detection based on region growing and ridge-based line detector, in Z. Sun and Z. Deng (eds), Vol. 255 of *Lecture Notes in Electrical Engineering*, Springer, Berlin, Heidelberg. 2013. pp. 431-437. Available from: <http://link.springer.com/10.1007/978-3-642-38460-8>
- [15] Ceron A, Prieto F, Mondragon I. Power line detection using a circle based search with UAV images. In: *2014 International Conference on Unmanned Aircraft Systems (ICUAS)*; 2014. pp. 632-639
- [16] Dalal N, Triggs B. Histograms of oriented gradients for human detection.

In: 2005 IEEE Computer Society
Conference on Computer Vision and
Pattern Recognition (CVPR); 2005.
pp. 1-8

[17] Song B, Li X. Power line detection
from optical images. *Neurocomputing*.
2014;**129**:350-361

[18] Ceron A, Mondragon IF, Prieto
F. Catenary detection based on segment
concatenation. *International Journal of
Imaging & Robotics*. 2018;**18**(2):1-12

[19] Martinez C, Sampedro C, Chauhan
A, Campoy P. Towards autonomous
detection and tracking of electric towers
for aerial power line inspection. In: 2014
International Conference on Unmanned
Aircraft Systems (ICUAS); 2014.
pp. 284-295

[20] Ceron A, Prieto F, Mondragon
I. Real-time transmission tower
detection from video based on a feature
descriptor. *IET Computer Vision*.
2017;**11**(1):33-42

[21] Mills SJ, Ford J, Mejias L. Vision
based control for fixed wing UAVs
inspecting locally linear infrastructure
using skid-to-turn maneuvers. *Journal
of Intelligent and Robotic Systems*.
2011;**61**:29-42

[22] Ceron A, Mondragon IF, Prieto
F. Towards visual based navigation with
power line detection. In: *Proceedings of
ISVC 2014, Lecture Notes in Computer
Science*. Springer; vol. 8887; 2014.
pp. 827-836

Extending the Limits of the Random Exploration Graph for Efficient Autonomous Exploration in Unknown Environments

Alfredo Toriz Palacios and Abraham Sánchez López

Abstract

The autonomous construction of environment maps using mobile robots is a fundamental problem of robotics; this is because virtually all tasks performed by robots need a representation of the working environment to operate. Although many works have addressed this problem known as SLAM, it still remains open; since most of the solutions do not consider a planner that allows the robot to explore autonomously the working environment or the works that consider it, they have developed slow algorithms that do not guarantee a total coverage of the environment or an optimal development of the exploration, which may result in maps of poor quality or definitely not usable given this lack of information. Thus, this work presents a new exploration method based on the random exploration graph (REG), which, unlike its predecessor, defines a systematic analysis of the next positions to be explored eliminating randomness in decision-making and thus minimizing the amount of movements that the robot must make to reach them and the time required to achieve total coverage of the environment. Additionally, a series of tests carried out on the proposed method are presented, and the results obtained in classical variables such as time and distance allow to validate the efficiency of our approach.

Keywords: SLAM, integrated exploration, path planning, unknown environments, random exploration graph

1. Introduction

Path planning is a well-known topic in the area of robotics whose main objective is to determine the best way for a robot to navigate autonomously in a work environment. Although many areas of robotics have benefited from research in this field, one of the most recent is its application to the problem of autonomous construction of environment maps, also known as integrated exploration or active SLAM, where the basic principle of operation consists of a mobile robot that must move through an unknown environment while constructing an environment map of it.

In this context, one of the first contributions can be traced to the work of Feder et al. [1], in which the authors describe an adaptive trajectory planning technique applied to the SLAM problem, where through the minimization of the inverse of the error covariance as an objective function, the next position is determined where the

robot must move with the intention of maximizing the information obtained, while it simultaneously localizes and constructs the environment map.

Commonly, the development of SLAM path planners requires dynamic and agile algorithms that can be adapted to new operating conditions in environments when obstacles are detected; with this in mind, many proposals have been developed by various researchers [2–10], being one of the most popular the sensor-based random tree (SRT) presented by Oriolo, Freda, and Franchi in [11]. This method is based on the random generation of robot configurations within a local security area detected by the robot's sensors, from which a compact tree-type data structure is constructed, which represents the road map of the area explored. In this structure, the leaves represent a previously reached robot position and their respective representation of the environment segment detected by the onboard sensors in that position called local safety region (LSR).

The SRT method randomly selects free borders detected at the current position of the robot where he can continue the exploration task; in case it is not possible to find one, the robot will automatically go to its parent node to look for new areas with exploration possibility. The process ends when the backspace behavior leads the robot to the root of the tree.

However, despite the popularity of the SRT scheme, it has certain problems that should be considered. The first of them lies in the ignorance of the state of the structure that is being built, where it is not possible to know if the nodes of the structure left behind contain more areas available for exploration, and therefore the total coverage of the environment cannot be guaranteed. The second problem depends on the first one, since not knowing which areas of the environment you remain unexplored, it is necessary for the robot to go back to parent nodes to find out if it is possible to continue exploring, which causes the structure to be traveled twice, and consequently the exploration time is very high.

From the above, a new method based on the SRT is developed by Franchi and others [4] for the multirobot case known as the sensor-based random graph (SRG). This method transforms the tree structure generated by the SRT method into an exploration network when the robot finds a safe way to travel between two nodes. In this method, a probability proportional to the length of the arc of the free edges that are in the node in which the robot is located is used to determine which will be the next position to explore; in addition, the way to verify the structure to establish the way to revisit zones already explored to continue the exploration is carried out by means of the generation of a tree of minimum expansion with all the adjacent nodes of the network, choosing that of the adjacent node with the greater weight with respect to the length of the free limits of the frontiers.

The SRG method presents similar problems to those of the SRT method: although the data structure is transformed into an exploration graph, the structure is not fully exploited to make exploration more efficient, because the way of revisiting nodes to verify unexplored areas creates a tree structure, which generates a discontinuous path that forces the robot to go through the parent nodes, ignoring the versatility of the graph. In fact, if the number of adjacent nodes and the number of nodes that conforms the environment are too large, the time to complete the exploration is increased. Also, like the SRT method, the robot decides the next position to explore without considering that the randomness of the selection causes too many orientation changes, which directly affects the odometric system.

More recently, Toriz et al. [12] presented a new approach known as the random exploration graph (REG), which optimizes map coverage in the exploration process. This method is based on the working principle of the SRT method and adapts it to build an exploration graph structure. Although this method has a probabilistic nature that can cause an excess of movements in the robot to complete its task and

increase the exploration time, one of its main advantages is the accumulation of knowledge acquired through the concept of border control, which stores information about areas that the robot left behind in the exploration process and that needs to be revisited to complete the exploration. This feature, plus the generated graph structure, allows an optimal return to unexplored areas to complete the exploration.

As it can be observed, the methods presented here maintain a random character to define the next position to explore, the problems found in these algorithms are the excess of time required to complete the task, and in some cases the uncertainty on the total coverage of the exploration area, which can have repercussions on partially constructed or low-quality maps, the reason why an integrated exploration strategy created from these methods would not be viable.

Thus, this work presents an approach to the problem of path planning of unknown environments based on the basic principles of the REG method; however, unlike this method, our proposal eliminates the randomness of the choice of the next frontiers to explore and, instead, relies on an analysis of the best frontier whose choice criterion is based on minimizing the amount of movements the robot has to make to reach it and maximizing the amount of information from the environment that will be acquired.

2. Extended random exploration graph

The exploration strategy presented in this research is a modified version of the REG algorithm, where the main difference lies in the way in which the robot will plan the exploration trajectory by performing a deterministic analysis of the next position to be explored; the algorithm is shown in **Figure 1**.

```

EXTENDED_REG_EXPLORATION
1. Node_Alg = 0
2. q_start = q_start
3. L_Nodes_Exp = Null
4. S_start = PERCEPTION(q_start)
5. for i = 1 to k_start
6.   S_curr = CURR_INTERSECTION(S_start, q_start, L_Nodes_Exp)
7.   F = FRONTIERS(S_curr)
8.   if F ≠ Null
9.     Node_Alg = Node_Alg + 1
10.    (F', θ_start) = FRONT_DET(F')
11.    F = REMOVE(F', F_start)
12.    q_start = DISPLACE(q_start, θ_start, r)
13.    MOVE_TO(q_start, q_start)
14.    S_start = PERCEPTION(q_start)
15.    F_start = VERIFICATION(F_start, S_start)
16.    F = F ∪ F_start
17.    if F ≠ Null
18.      L_Nodes_Exp = L_Nodes_Exp ∪ Node_Alg
19.    end
20.    G = ADD(G, Node_Alg, q_start, S, F)
21.    q_start = q_start
22.    S_start = S_start
23.  else
24.    (P, final_Node) = FIND_PATH(q_start, L_Nodes_Exp)
25.    for i = 1 to length(P)
26.      MOVE_TO(q_start, P(i))
27.      q_start = P(i)
28.    end
29.    L_Nodes_Exp = REMOVE(L_Nodes_Exp, final_Node)
30.  end
31. end
32. Return (G)
    
```

Figure 1.
 Extended REG algorithm.

The initial node considered in the algorithm will be the starting and finishing node, and as in the rest of the exploration structure, it will contain a position reached by the robot (in this case it will be the initial q_{init} position), as well as a representation of the environment surrounding it known as the local security region (LSR) where the robot will be able to navigate without the risk of colliding with any obstacle. With this node created, the cycle controls the exploration process.

Next, in each iteration k of the algorithm, the frontiers of the nodes adjacent to the current node are evaluated with the intention of verifying which free frontier segments with possibility of exploration of these are of the current LSR. The nodes that present positive intersections in this evaluation will be updated eliminating the free frontier segments of both the neighboring node and the current node, with the intention of not considering these frontiers in a possible return of the robot to continue with the exploration. In addition, the verification of intersections between nodes is used to modify the structure of the exploration graph by adding edges between nonadjacent nodes as long as there are safe roads to travel between them (see **Figure 2**). The described analysis is performed by the function CURR_INTERSECTION.

After the analysis of the frontiers of neighboring nodes covered by the new LSR and the modification of the exploration structure with new edges, the next step is to identify the remaining free frontiers F of the current position, which is performed by the FRONTIERS function. For each of the frontiers found, if they exist, an approximation point will be determined, which will serve to prioritize the free frontiers,

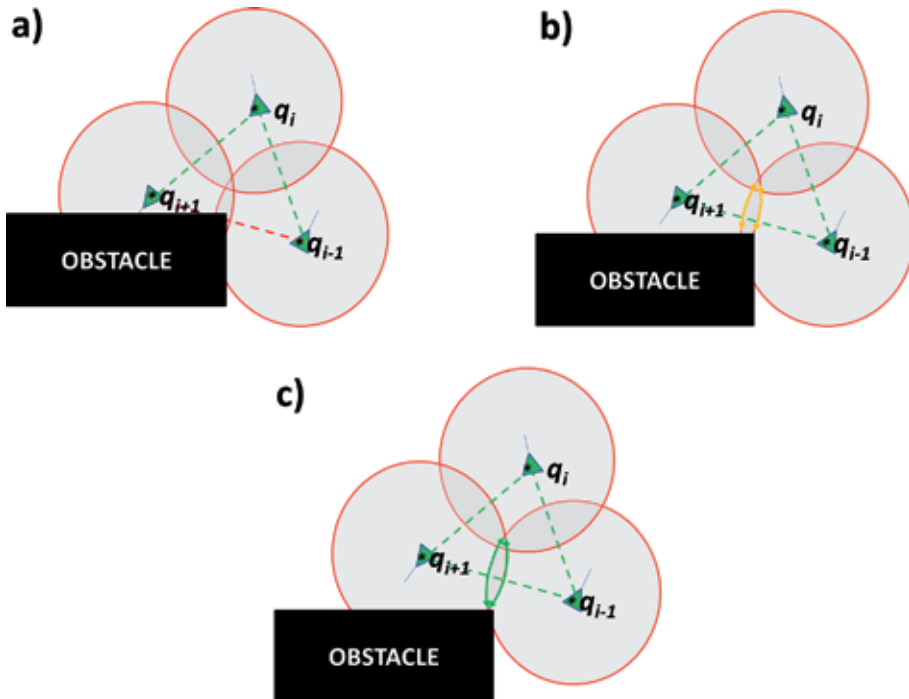


Figure 2.

Modification of the exploration graph structure through the insertion of new edges between nonadjacent nodes. (a) The insertion of the edge between q_{i-1} and q_{i+1} nodes is not possible (dotted red line) since there is no safe path between the nodes. (b) The insertion of the edge between the q_{i-1} and q_{i+1} nodes is not possible (dotted red line) since, although there is a collision-free path between the nodes, the intersection of the LSRs does not have enough space to navigate safely between the nodes. (c) The insertion of the edge between the q_{i-1} and q_{i+1} nodes is possible (dotted green line) since there is a collision-free path and enough space at the intersection of the LSRs to navigate safely.

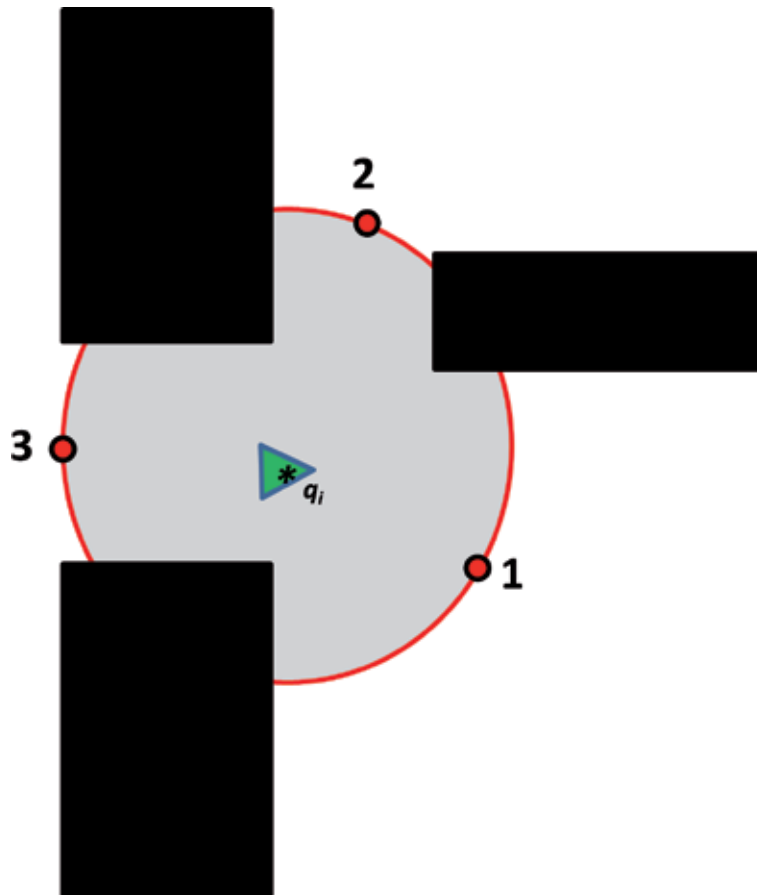


Figure 3.
Hierarchy of frontiers.

ranking them according to the effort required to reach them (FRONT_DET function) and choosing a new frontier to explore which has the highest hierarchy.

The approximation point is defined as the midpoint of the arc segment formed by the frontiers, if they can be covered in their entirety by the threshold defined by the LSR area (see **Figure 3**).

In the case that the criterion of choice of approximation point is not met, it will be redefined by taking the midpoint of the arc length proportional to the area that can be covered by the LSR, taken from the initial end of the border. With this new point chosen to continue the exploration, the frontier or segment of it, as the case may be, is removed from the group of free borders found by the REMOVE function (see **Figure 4**).

With the new frontier to explore chosen and the approximation point of it defined, the DISPLACE function will obtain the new q_{dest} position to visit to continue the exploration. This is done by taking a step of dimension $\alpha * r$ in the direction of the border approximation point, where the parameter α represents the defined radius of the LSR and the value $r < 1$ will guarantee that the new position will remain within it. Once the q_{dest} position is obtained, the MOVE_TO function will plan the path and take the robot to this new position.

In the q_{dest} position, the robot will calculate the surrounding space S_{dest} of this position (PERCEPTION function) and the VERIFIES function will determine precisely which is the real portion of the free frontier that was covered by this new LSR. In case the chosen frontier has not been fully covered, the remaining portion

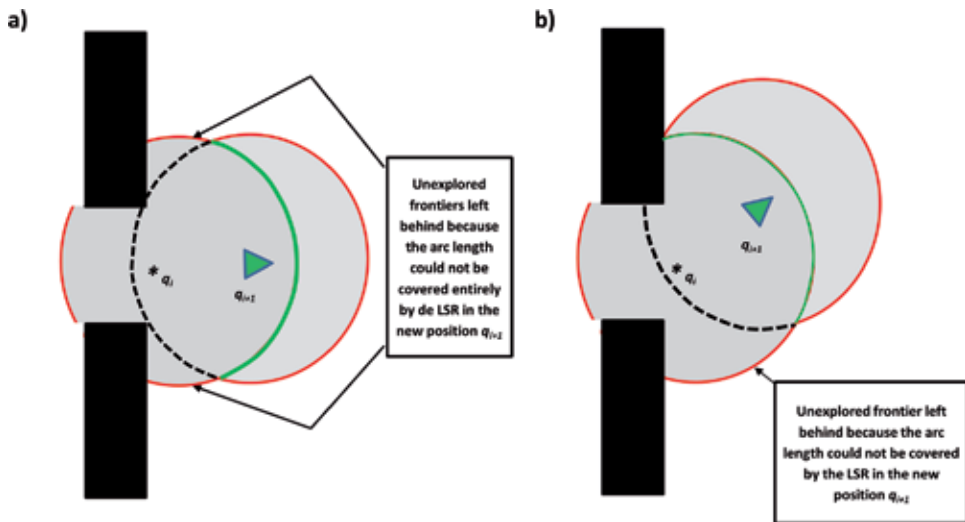


Figure 4. Criterion of approximation to the new frontier to explore. (a) The robot makes an incorrect approach to the new frontier, since the new LSR of the chosen position leaves two free frontiers in opposite directions. (b) Correct choice of the next position to explore, since, although the new RSL is unable to cover the border completely, no more than one free border is left.

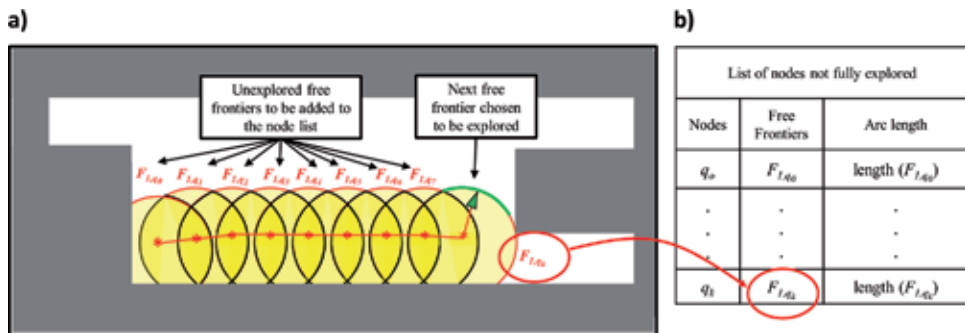


Figure 5. Frontier control. (a) Environment almost explored, where the arcs F_i and q_j represent unexplored free frontiers. (b) List of nodes not fully explored (frontiers control).

will be added to the list of free frontiers F of the previous node. Thus, if the F list of the node is not empty, its header will be added to the list of nodes with exploration possibility, also known as frontier control (see **Figure 5**).

After verification and validation of the structure with the new node, the ADD function will attach it to the exploration graph, and the objects on the map being constructed will be extended with the new information collected. At this point, the destination information (q_{dest} and S_{dest}) obtained at the previous point will become the current node information (q_{curr} and S_{curr}), and the described process will start again.

When the robot fails to find a new position to explore in the current node, i.e., there are no more free frontiers, one of the nodes contained in the frontier control will be chosen to continue the exploration, where the choice of it will be determined by the A* search algorithm in bidirectional way, where a path will extend from the current node to the frontier control nodes and from the nodes in the frontier control to the current position, ending when some path P is found (see **Figure 6**). At this moment the index of the node on which the trajectory was found will be removed from frontier control. This task is carried out by the FIND_PATH function.

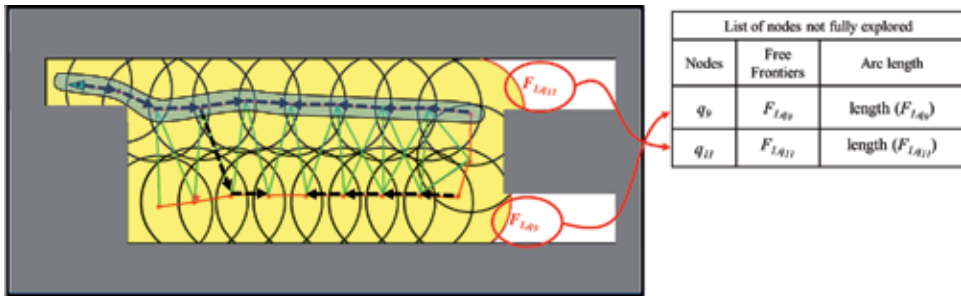


Figure 6. Bidirectional application of the A* algorithm from the current position of the robot to the nodes with possibility of exploration, stored in the frontiers control.

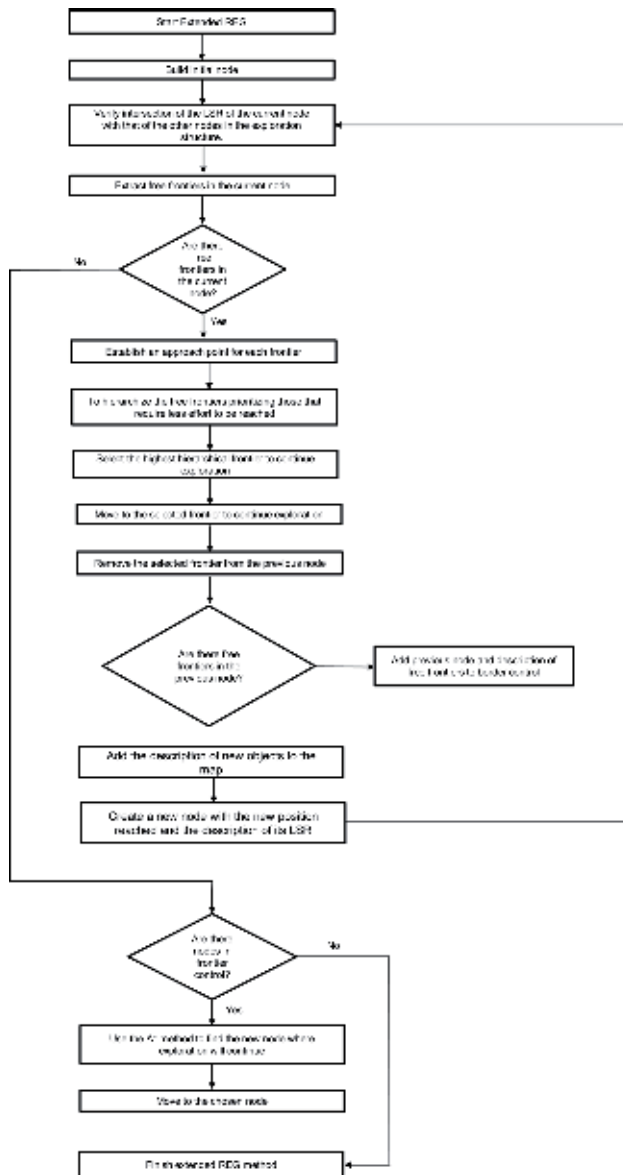


Figure 7. Flowchart of the extended REG method.

The MOVE_TO function will then use the path P obtained in the previous step to take the robot to the node from where scanning will continue. In this way, the method will continue executing the described process, until there are no more free frontiers in the current node, and the frontier control list is empty; at this point, the robot will look for a path to return to the initial node from where the exploration process starts. **Figure 7** shows the flow diagram of the extended REG algorithm.

3. Experimental results

Numerous experiments were carried out with the intention of validating the accuracy and consistency of the proposal made in this investigation; in addition, typical quantitative variables used in the field of exploration methods were analyzed, such as exploration time, distance traveled, and total environmental coverage, which were compared with data obtained by other methods such as SRT [11], SRG [6], and REG [12], which allows us to explain the efficiency of our method.

With respect to the integrated exploration paradigm, our exploration approach was designed to operate under the general concept of any SLAM method; however, for the tests performed, it was determined to use the method presented in [13] given the integral way of exploiting data from the work environment.

The tests were conducted using simulated information from a pioneer P3DX differential robot, which was equipped with a Hokuyo URG-04LX range sensor with a maximum detection range of 4 meters, an angular resolution of 0.360° , and a scanning angle of 240° . The environment used for the experiments is a modified version of the corridors of the Montpellier Computer, Robotics and Micro-electronics laboratory (LIRMM) (see **Figure 8**).

Figure 9 shows the exploration structure generated by the extended REG method after its application in the LIRMM environment; in it, the edges represent routes that the robot can navigate without the risk of colliding with obstacles in the environment.

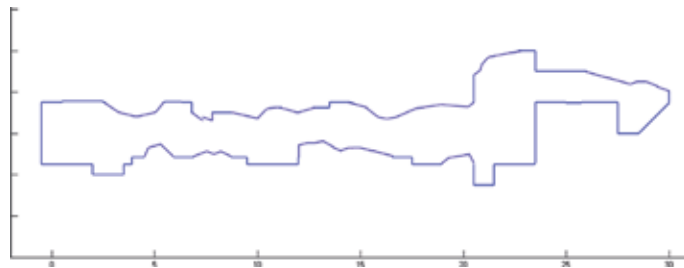


Figure 8.
The LIRMM environment.

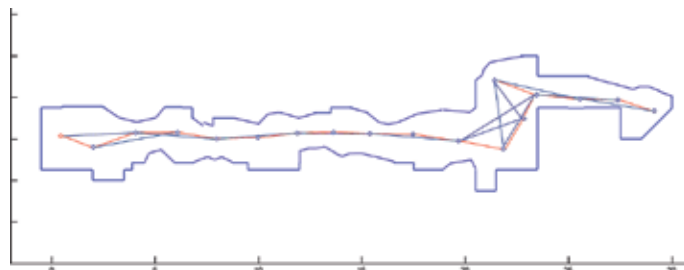


Figure 9.
Generated graph structure by the proposed exploration approach.

Tables 1 and 2 show the comparative results of the time and distance variables traveled by the robot using the SRT, SRG, REG, and Extended REG exploration methods; the results were obtained on the basis of 30 tests. In these tables, it is easy

LIRMM environment				
Exploration time (seconds)				
Test	Extended REG Method	REG Method	SRG Method	SRT Method
1	278.0889	315.7859	415.1445	563.1102
2	278.7979	326.7662	545.4457	687.7065
3	258.2204	359.3230	522.7711	441.5671
4	242.5923	318.7591	560.2500	688.0134
5	252.1377	402.3106	556.7573	519.7771
6	246.4645	334.3762	490.4706	502.1979
7	251.1057	294.8047	573.6789	584.2922
8	269.7181	336.8587	590.7163	666.9585
9	276.3011	380.5149	464.2052	650.8572
10	243.0794	310.7739	619.7049	503.9038
11	244.2341	416.5971	533.4251	665.0674
12	275.0934	364.7327	529.7478	577.1821
13	284.9026	374.9523	442.7496	569.8460
14	251.8885	294.3133	608.8775	453.4542
15	258.2455	337.2547	535.1509	475.1350
16	262.9808	309.5245	470.4473	626.2440
17	278.7238	340.1444	526.6756	636.6569
18	246.9795	378.1428	596.8990	515.8445
19	244.9627	327.7210	449.4658	683.2569
20	276.8152	384.1076	401.0013	606.8604
21	267.0117	305.4459	485.9701	505.5880
22	261.6335	358.1534	566.8682	420.1538
23	245.5880	330.3814	487.1188	570.1567
24	260.7357	406.2692	405.7856	426.6971
25	272.2311	406.2317	522.1408	475.3501
26	242.6921	369.3099	441.1361	573.6439
27	243.2405	329.8577	517.6172	532.1449
28	279.0752	383.5061	539.0328	609.7719
29	271.6649	302.1935	496.7664	675.1354
30	276.7029	417.5154	499.6830	672.9646
Average time	261.3969	350.5543	513.1901	569.3179
Standard Deviation	14.2286	37.9059	59.3018	84.9176

Table 1.
Time needed for the Extended REG, REG, SRT, and SRG exploration methods to explore the LIRMM environment on the basis of 30 tests

LIRMM environment				
Distance traveled by the robot (meters)				
Test	Extended REG Method	REG Method	SRG Method	SRT Method
1	94.2953	110.8750	176.5043	202.1030
2	97.0948	122.0881	171.5603	185.0873
3	93.5696	128.1114	148.7670	122.2305
4	92.8974	120.4839	154.3054	115.6293
5	95.2164	111.0441	99.9813	172.9572
6	96.4587	97.0754	161.0658	129.4353
7	89.4794	100.6069	122.4132	185.6566
8	97.8138	130.6982	135.4928	143.5254
9	88.1791	126.4050	112.2472	206.2968
10	90.1664	112.0377	137.2371	190.1586
11	88.9507	121.3078	120.6996	126.0833
12	96.3502	97.5515	128.1775	189.8909
13	98.2066	90.2293	176.2596	157.3321
14	89.9009	127.5927	119.5021	180.6779
15	91.3684	104.0339	174.5081	197.0456
16	92.2725	113.2718	133.4387	119.8085
17	93.6515	96.5836	165.1104	123.7504
18	88.6493	92.1664	164.9564	204.3196
19	97.8853	107.8139	127.0498	115.9971
20	98.4636	125.8068	158.0025	169.8498
21	97.9201	105.5806	127.9679	136.3876
22	95.8657	101.2719	152.5624	198.1987
23	96.7244	121.5712	153.0089	115.7825
24	93.0438	114.6411	117.7339	207.7524
25	96.3796	125.3939	103.3812	192.1662
26	88.3230	91.8653	127.6628	165.6248
27	96.4622	91.8655	160.8764	153.5368
28	92.7974	124.6801	154.4797	117.7001
29	89.3724	124.8849	106.7780	131.7636
30	95.9194	103.8811	104.1588	130.3949
Average distance	93.7893	111.3806	139.8630	159.5714
Standard Deviation	3.4125	12.9830	23.8407	33.4651

Table 2.
Distance traveled for the Extended REG, REG, SRT, and SRG exploration methods to cover the LIRMM environment on the basis of 30 tests

to observe that the Extended REG requires approximately 25% less time than the best average time of the other three methods, and about 16% in the best average distance was reported by the other three methods. In addition, it is possible to observe that

LIRMM environment				
Environment coverage (%)				
Test	Extended REG Method	REG Method	SRG Method	SRT Method
1	100%	100%	92.3592%	94.4365%
2	100%	100%	99.6659%	87.2937%
3	100%	100%	93.7106%	98.9930%
4	100%	100%	96.3776%	91.7059%
5	100%	100%	95.5086%	85.5518%
6	100%	100%	98.7745%	91.7032%
7	100%	100%	96.1068%	97.6451%
8	100%	100%	95.9189%	91.6015%
9	100%	100%	91.7190%	85.7556%
10	100%	100%	92.7108%	92.6386%
11	100%	100%	98.2033%	88.0735%
12	100%	100%	94.7589%	89.2148%
13	100%	100%	98.4398%	90.7828%
14	100%	100%	93.6729%	89.3881%
15	100%	100%	93.6892%	88.6274%
16	100%	100%	91.2083%	89.2020%
17	100%	100%	98.6001%	91.2047%
18	100%	100%	96.9909%	95.9539%
19	100%	100%	99.5792%	95.5916%
20	100%	100%	97.9685%	97.0562%
21	100%	100%	94.5170%	87.2147%
22	100%	100%	94.0025%	93.1977%
23	100%	100%	99.9579%	97.3336%
24	100%	100%	91.0922%	84.6677%
25	100%	100%	92.2726%	92.4071%
26	100%	100%	98.1241%	91.1557%
27	100%	100%	94.6410%	86.5926%
28	100%	100%	96.5149%	88.0764%
29	100%	100%	98.8809%	92.4875%
30	100%	100%	96.8469%	96.2568%
Average coverage	100%	100%	95.7604%	91.3937%
Standard Deviation	0%	0%	3%	4%

Table 3.
 Surface covered of the LIRMM environment for the Extended REG, REG, SRT, and SRG exploration methods on the basis of 30 tests

the standard deviation in both variables is very low compared to the other methods due to the deterministic way of choosing the next position to explore, which allows sustaining the affirmation that the method will always obtain the same results.

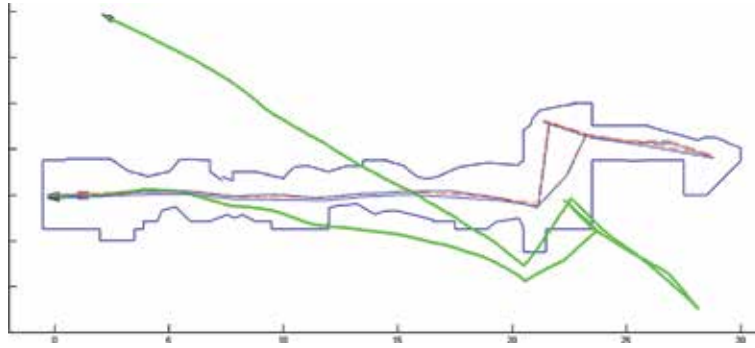


Figure 10.
Consistency test of the Extended REG method applied to the SLAM problem.

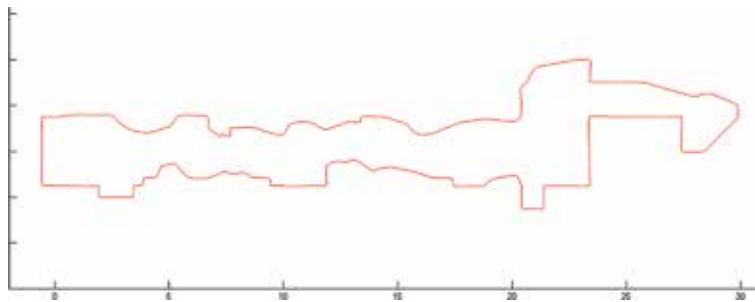


Figure 11.
Map obtained with the Extended REG method applied to the SLAM problem.

Moreover, since our proposal is based on the REG algorithm, one of the main benefits contained in the extension presented in this paper is the guarantee with a high degree of confidence that the environment will be fully covered in most cases, because it is possible to have a constant knowledge of the state of unexplored areas of the environment thanks to frontier control. Thus, to evaluate the coverage of the environment by the exploration method, this was divided into grids, which served to determine which of them had been explored (**Table 3**).

Finally, the algorithm of path planning for unknown environments presented in this article was developed with the intention of being integrated to SLAM algorithms to obtain an integral tool for the construction of autonomous maps. Although the Extended REG method could be used as a control module with any SLAM algorithm, for the tests performed, it was decided to use the method developed by Pedraza et al. [13] given the similarity of approaches when applying the methods in unstructured environments. The tests and results obtained are shown in **Figures 10** and **11**.

4. Conclusions

In this work, a strategy was presented for the problem of exploration of environments for SLAM; the approach presented is based on the REG algorithm introduced in [12], which builds a graph-like data structure that integrally exploits the experience acquired during the exploration process to perform this task efficiently. The main contribution of the exploration proposal made in this article is the use of a simplified criterion to find the next position to explore based on the hierarchy of free borders detected in an instant of time, which allows the elimination of unnecessary movements of the robot, increasing its efficiency. The main advantage of this

choice criterion is that the robot will travel short distances to the position closest to being explored, reducing the amount of time needed to reach them, which can be verified in the results of the tests performed to the method.

Also the Extended REG method is designed to be integrated in the context of a SLAM method, which facilitates the construction of environment maps simplifying the task of planning paths in unknown environments, which allows giving true autonomy to the robot responsible for obtaining the environment map eliminating the dependence on decision-making by a human operator. Finally, a series of simulations of the proposed integrated exploration strategy were carried out, which allowed us to validate our approach.

Author details


Alfredo Toriz Palacios^{1*} and Abraham Sánchez López²

1 Popular Autonomous University of the State of Puebla, Puebla, Mexico

2 Autonomous University of Puebla, Puebla, Mexico

*Address all correspondence to: alfredo.toriz@upaep.mx

IntechOpen

© 2019 The Author(s). Licensee IntechOpen. This chapter is distributed under the terms of the Creative Commons Attribution License (<http://creativecommons.org/licenses/by/3.0>), which permits unrestricted use, distribution, and reproduction in any medium, provided the original work is properly cited. 

References

- [1] Feder H, Leonard J, Smith C. Adaptive mobile robot navigation and mapping. *International Journal of Robotics Research*. 1999;18(7):650-668. DOI: 10.1177/02783649922066484
- [2] Campos FM, Marques M, Carreira F, Calado JMF. A complete frontier-based exploration method for Pose-SLAM. In: *IEEE International Conference on Autonomous Robot Systems and Competitions*. 2017. pp. 79-84. DOI: 10.1109/ICARSC.2017.7964056
- [3] Fermin-Leon L, Neira J, Castellanos JA. TIGRE: Topological graph based robotic exploration. In: *European Conference on Mobile Robots*. 2017. pp. 1-6. DOI: 10.1109/ECMR.2017.8098718
- [4] Meng Z, Sun H, Qin H, Chen Z, Zhou C, Ang MH. Intelligent robotic system for autonomous exploration and active SLAM in unknown environments. In: *IEEE/SICE International Symposium on System Integrations*. 2017. pp. 651-656. DOI: 10.1109/SII.2017.8279295
- [5] Ristic B, Palmer J. Autonomous exploration and mapping with RFS occupancy-grid SLAM. In: *Journal Entropy*. 2018;20:456-464. DOI: 10.3390/e20060456
- [6] Rodríguez-Arévalo ML, Neira J, Castellanos JA. On the importance of uncertainty representation in active SLAM. In: *IEEE Transactions on Robotics*. 2018;34:829-834. DOI: 10.1109/TRO.2018.2808902
- [7] Saeedi S, Nardi L, Johns E, Bodin B, Kelly PH, Davison AJ. Application-oriented design space exploration for SLAM algorithms. In: *IEEE International Conference on Robotics and Automation*. 2017. pp. 5716-5723. DOI: 10.1109/ICRA.2017.7989673
- [8] Sun X, Sun F, Wang B, Yin J, Sheng X, Xiao Q. Robotic autonomous exploration SLAM using combination of Kinect and laser scanner. In: *IEEE International Conference on Multisensor Fusion and Integration for Intelligent Systems*. 2017. pp. 632-637. DOI: 10.1109/MFI.2017.8170393
- [9] Valencia R, Andrade-Cetto J. Path planning in belief space with pose SLAM. In: *Mapping, Planning and Exploration with Pose SLAM*. Vol. 53. Pittsburgh, United States of America: Springer; 2017. p. 87. DOI: 10.1007/978-3-319-60603-3_4
- [10] Wang H, Zhang C, Song Y, Pang B. A perception-driven exploration hierarchical simultaneous localization and mapping for mobile robots adapted to search and rescue environments. In: *Advances in Mechanical Engineering*. 2018;10:1-18. DOI: 10.1177/1687814018765874
- [11] Oriolo G, Vendittelli M, Freda L, Troso G. The SRT method: Randomized strategies for exploration. In: *IEEE/RSJ International Conference on Intelligent Robots and Systems*. 2004. pp. 4688-4694. DOI: 10.1109/ROBOT.2004.1302457
- [12] Toriz A, Sánchez A, Bedolla JME. The random exploration graph for optimal exploration of unknown environments. In: *International Journal of Advanced Robotic Systems*. 2017;1: 1-11. DOI: 10.1177/1729881416687110
- [13] Pedraza L, Dissanayake G, Miro JV, Rodriguez-Losada D, Matia F, BS-SLAM: Shaping the world. In: *Robotics: Science and Systems*. 2007. pp. 1-8. DOI: 10.15607/RSS.2007.III.022

Section 3

Towards an Optimal Path
Planning

Model of the Optimal Maneuver Route

Jan Nohel, Petr Stodola and Zdeněk Flasar

Abstract

The chapter deals with the mathematical model for planning the optimal movement route, which has been implemented in the Tactical Decision Support System (TDSS). The model processes and evaluates the data contained in the five raster layers, which are tactically relevant for planning the movement route of troops or autonomous vehicles on the battlefield. The basis for calculating the optimal movement route is a ground surface layer, which is then modified by algorithmic and criterion relationships with the layers of hypsometry, weather attack, and the activities of enemy and friendly units. The result of mathematical model calculations is a time-optimized and safe movement route displayed on the topographic basis. The experiments realized have verified the function of the optimal movement route model when neither the reconnaissance group nor the autonomous vehicle was observed by the enemy. The total time of the UGV with the use of the TDSS to cover the route of maneuver was 67 minutes shorter than the real time of the BRAVO group movement with the use of the TDSS and 105 minutes shorter than the real time of the ALFA group without the use of the TDSS. The comparison of responses to the attack shows that the BRAVO group using the Maneuver Control System (MCS CZ) as part of the TDSS has destroyed the attackers faster by 71 seconds than the ALFA group without the use of the TDSS.

Keywords: autonomous vehicle navigation, optimal route of maneuver, off-road capability, passability, terrain analysis

1. Introduction

Over the past 10 years, a considerable progress has been observed in the field of autonomous systems in various fields of activity. Currently, autonomous systems are used and will continue to be used in all spatial dimensions, i.e., ground, aerial (space), as well as maritime ones. One of the criteria for the division of autonomous systems is a degree of autonomy. The system (vehicle) can be fully autonomous, when all the functions that the system has to carry out are controlled by a vehicle itself. The semiautonomous system is autonomous only in some of its partial functions, when the complex decision function is edited and controlled by the operator. In the case of ground autonomous systems

(Unmanned Ground System (UGS)), it is necessary to deal with two management processes in terms of their movement. On the one hand, it is a direct movement control in the field where the most important factors are microrelief and various types of obstacles and, on the other hand, the process of planning and creating the optimal movement route itself before completing the task itself.

In the past, the problem of searching for the optimal movement route was already dealt with using both vector and raster graphics. Based on the values of edges or raster cells, the shortest route between two points can be found using the mathematical algorithms described in [1, 2]. Some publications can also be found that describe models for moving different elements through the terrain. Based on passability parameters, they assess the movement possibilities for personnel and wheeled and tracked vehicles. These models can be found in [3–5]. The vector format of geographic data offers another route planning for autonomous vehicles. This format is commonly used by GPS receivers with the use of the road structure and graph theory. The graph of the road structure includes nodes and edges in the form of crossroads and roads. It is called “edge-defined,” which means that the only criteria are the edge value and the movement direction. The shortest path includes the sum of all edge values between the beginning and the end with the smallest value. Outside the network of paths, the vector model navigates directly to the target, without any analysis of the influence of the vegetation and the relief. Another planning strategy of movement for autonomous vehicles can be a “potential field” consisting of a limited space of artificial potential values. Autonomous vehicles operating in the area mentioned move from the position with the highest potential to the position with the lowest potential. However, it is very difficult to use the potential field in real-world situations.

Many articles deal with a series of “tracking strategies,” route planning, and obstacle avoidance in the case of autonomous vehicles. For example, [6] deals with obstacle avoidance in an urbanized environment and the comparison of techniques for the movement planning of autonomous and semiautonomous vehicles. The content of most articles aims at the movement planning strategies. These are characterized by route planning algorithms implemented in the planning process.

The tracking strategies, threat assessment, and route planning as part of the collision avoidance system are described in [7]. The most important part evaluates particular current methods in each collision avoidance strategy according to their advantages and disadvantages. The safety and fast resolution of collision situations is an important precondition for the efficient operation of fully automated vehicles.

The potential of unmanned marine vehicle (UMV) development is analyzed in [8]. One of the goals of the US Navy in the field of UMVs is to improve their autonomous movement planning and integrate the obstacle avoidance process at sea. The purpose of the UMV development mentioned is to prevent anticipated marine accidents and the future use of fully autonomous ships.

The cross-country movement analysis and the terrain passability testing are specified in [9]. Terrain passability is affected by many factors; it represents a key factor in achieving success in military operations. The geographic factors of the area of operations and the technical parameters of the vehicles define the capabilities of military units to move on the battlefield.

The optimal movement route model implemented in the Tactical Decision Support System (TDSS) can be used for planning and creating a movement route. The TDSS has been developed at the University of Defense in Brno, the Czech

Republic, since 2006¹. The implemented model of the optimal movement route uses a raster digital data model, map algebra algorithms, and associated criterion assessments of the effects of the situation to process the effects of the situation on the battlefield. The model raster has an optional resolution, which means it indicates how large area of a given terrain the cell represents. An important feature of each raster cell is its value (attribute), which is specified by a particular or continuous character of the represented terrain area. It may be a landform, a terrain slope, weather effects, the enemy activity, or the time of its covering in a predetermined manner. The raster format of the network graph allows the layers of individual situation variables to be flexibly updated and mathematically combined; the layers of the individual situation variables affect the process of creating the movement route. Depending on the importance or the character of information, each raster cell acquires an attribute from a minimum value to ∞ , which represents the time of covering the raster cell in hundredths of a second. The algorithm of the optimal movement route model then searches for the path between the two selected points with the lowest total sum of attribute values on the route; this allows the estimated total time of covering the route to be obtained. The TDSS uses the combination of Floyd-Warshall and Dijkstra's principle, described in [1, 10].

The model processes and evaluates tactical geographical information for three methods of troop movement:

- Dismounted movement
- Wheeled vehicles
- Tracked vehicles

Each method of the movement is influenced by specific characteristics of speed, terrain passability, and weather. The resulting movement route, evaluated by the model, is calculated with respect to the real terrain passability, the shortest time between the start and end points, and the safety. The enemy activity is the worst predictable part of the model due to its uncertainty and variant design.

2. Model concept

The concept of the optimal movement route model uses rasterized geographic data of the Digital Terrain Model and the Digital Relief Model for its work. The structure of the model is composed of several matrix layers that represent individual groups of horizontal (HF) and vertical (VF) factors of the passability (movement demands) of the area and safety. Each raster cell contains a numerical value of the difficulty of its covering (P_{np} , cost surface of passability), derived from the current state of the effects of task variables at a given position in the area. These are represented by HF and VF related to the difficulty of movement, which depend on the criterion evaluation of their occurrence characteristics, described in [11, 12].

When designing a movement route of forces and equipment, the model evaluates the following layers:

¹ The TDSS is an experimental platform for testing of mathematic algorithmic models, using raster representation of data, having been developed at the Department of Tactics at the University of Defense since 2006 by Lt-Col. assoc. prof. Petr Stodola, PhD, and Lt-Col. assoc. prof. Jan Mazal, PhD.

1. Ground surface layer (P_{np1} , HF_1)
2. Elevation layer (VF_2)
3. Weather layer (HF_3)
4. Enemy situation layer (HF_4)
5. Friendly forces and equipment layer of (HF_5)

The metrics of criterion evaluation are different for each layer in relation to its character and composition. The basic data for its calculation are cell dimensions, the average movement speed of a selected element on a given type of the ground surface that moves across the cell, and the resistance of the factor under consideration. The value calculated through the combination of P_{np1} and all layers of the model indicates the combined time of covering a given cell, influenced by all terrain and situation factors, in the form of the combined cost surface of passability (SP_{np}), shown in **Figure 1**.

2.1 Model layers

The calculation of the model combined cost surface of passability consists of several layers of the task variables that are defined in the following text:

1. Ground surface layer

The ground surface layer forms a basis for further analysis of the model. Its cost surface of passability (P_{np1}) consists of sublayers representing the types of ground surface as follows, described in [11–13]:

- a. Plant and soil cover

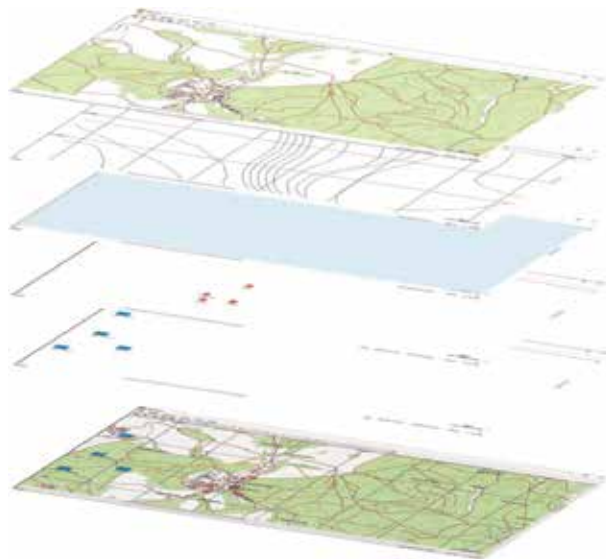


Figure 1. *The creation of the combined cost surface of passability (source: own).*

- b. Watercourses and water areas
- c. Communication over land and buildings
- d. Urbanized area

Based on its P_{np1} , the effects of other layers of the model are derived.

2. Elevation layer

The hypsometry layer is formed by topography, which enters the calculation of SP_{np} through the vertical factor (VF_2) of the terrain slope. Its definition can be formulated as a measure of demanding movement in the elevated terrain. $SP_{np1,2}$ is created by a multiple of P_{np1} with a value of VF_2 . It varies according to the type of movement as a vertical factor of the terrain slope for vehicles (VF_{2V}) and for dismounted units (VF_{2C}). The calculation of these factors is expressed by mathematical formulas (1) and (2). In the case of the movement of tracked or wheeled vehicles, it is possible to refer to the so-called linear influence of the terrain slope on the average speed of a given type of a vehicle. The vehicle engine load increases evenly with the rise in the terrain slope, and, under unchanged operating conditions, it causes a steady drop in speed. On the contrary, when driving downhill, the vehicle speed increases steadily. However, its gravity increase, given by the downhill driving and the pull of gravity, is usually broken by the driver using the braking system of the vehicle. The vertical factor of the terrain slope for vehicles (VF_{2V}) is expressed by the mathematical formula as follows:

$$VF_{2V} = K_{V2V} \times \omega + 1 \qquad VF_{2V} = \frac{1}{K_{V2C}} \qquad (1)$$

The limiting passable terrain slope is set for tracked vehicles in the range of -30° to $+30^\circ$ and for wheeled vehicles of -30° to $+20^\circ$, derived from [14–16]. Out of the range of these values, the terrain slope in the model is assessed as impassable, with $VF_2 = 0$. The course of VF_{2V} has a linear character given by constant value $K_{V2V} = -0.004$.

The difficulty of the movement of a dismounted element in the field has a nonlinear course as opposed to vehicles. The terrain slope (ω) affects the dismounted movement downhill or uphill differently depending on the topography and the safe movement controllability. Its difficulty in walking uphill increases exponentially as the slope increases. When walking downhill, it drops down up to 20° , when it is equal to the difficulty of movement on the flat ground. When walking downhill with the angle of slope of more than 20° , the difficulty increases again with the increasing slope. Such a course is caused by a degree of gravity that facilitates the movement at first. However, when the terrain slope is more than 20° , it forces the dismounted movement of individuals to brake in order to maintain a safe control over their movement. The influence of the terrain slope on the dismounted movement is expressed by the vertical factor of the terrain slope for dismounted movement (VF_{2C}). The coefficient of the vertical factor for dismounted individuals (K_{V2C}) is included in its calculation shown in **Figure 2**, which represents the degree of difficulty of the dismounted movement for a given terrain slope. Its values have been borrowed from the thesis developed by Lenka Mezníková, described in [17]. The limiting passable terrain slope for the dismounted movement is set in the range of -50° to $+50^\circ$.

Coefficient of vertical factor for walking(K_{V2C})

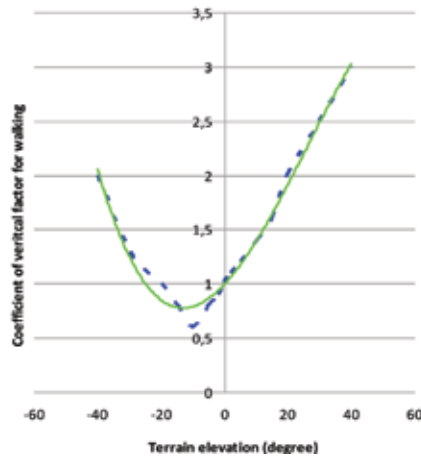


Figure 2.
Coefficient of vertical factor for dismounted movement (source: own).

The K_{V2C} curve, shown in the graph in **Figure 2**, has been put through the third degree polynomial curve to generate a regression equation as follows:

$$K_{V2C} = -0.0121\left(\frac{\omega}{10}\right)^3 + 0.0968\left(\frac{\omega}{10}\right)^2 + 0.3156\frac{\omega}{10} + 0.9933 \quad (2)$$

The value of the regression equation reliability is 0.9875.

3. Weather layer

In the weather layer, snowfall and rainfall are taken into account as direct effects on the terrain passability. Both of these effects are characterized by the overall impact of its occurrence in [18], which can be defined in the model based on the weather forecast or meteorological radar outputs. Snowfall limits the terrain passability on the entire terrain area. On the roads, it reduces the adhesion of their surface to the chassis of moving vehicles, even on a thin layer of snow.

To calculate the possibilities of passability in the field with a zero slope, the coefficients of the snow layer influence ($K_{3,1}$) related to particular types of moving elements were mathematically derived, as follows:

- For tracked vehicles: $K_{3,1P} = 0.01205$
- For wheeled vehicles: $K_{3,1K} = 0.0192$
- For the dismounted movement: $K_{3,1C} = 0.008$

The combination of the influences of the terrain slope and the snow layer thickness implements the coefficient of the snow-covered topography ($O_{3,1}$) in the calculation of $HF_{3,1}$, which is differentiated according to the type of a moving element. $O_{3,1}$ attains the following values:

- For tracked vehicles: $O_{3,1P} = 0.034$
- For wheeled vehicles: $O_{3,1K} = 0.0576$

- For the dismounted element: $O_{3.1C} = V_{F2C}$

For the movement of tracked and wheeled vehicles, the derived mathematical formula is used as follows:

$$HF_{3.1P/K} = 1 - (K_{3.1P/K} \times L_{3.1}) - (O_{3.1P/K} \times \omega) \quad (3)$$

For the movement of the dismounted element, the derived mathematical formula is used as follows:

$$HF_{3.1C} = 1 - (K_{3.1C} \times L_{3.1}) - (1 - O_{3.1C}) \quad (4)$$

The limiting passable snow thickness for the dismounted element is set for 90 cm of snow since a thicker layer of snow is negotiable with great difficulties or even impassable for the dismounted element.

The model of the movement route for forces and equipment evaluates the effects of rainfall only for tracked and wheeled vehicles that move off the paved roads. The limitation of the terrain passability due to rainfall is generally assessed in four steps based on the precipitation amount for the purpose of creating a movement route in the model. The degree of limitation of individual steps is derived from the reduction in vehicle climbing performance, which defines the approximated reduction in vehicle climbing performance up to 50% when moving on a muddy soil surface. The muddy soil surface is defined generally as a precipitation amount larger than 40 mm in 3 days. Based on the meteorological forecast or the measurement of the abovementioned precipitation amounts, the model user can set a horizontal rainfall factor ($HF_{3.2}$), which attains the values listed in **Table 1**.

4. The enemy situation layer

The enemy situation layer evaluates the safe passability of the area, depending on the possibilities of effective fire of his main weapons. It is created by the results of collecting the information on the enemy forces and equipment, which are defined in the model by their geographical position and the attributes of the tactical and technical characteristics of his weapons. From the location of their deployment, the area that is visible within the effective range of enemy weapon systems is then evaluated. Further, the model evaluates the danger area (which is impassable) of detected unexploded ammunition, improvised explosive devices (IEDs) or mine-fields, which is set based on the weight of detonating charge and the type of ammunition. The degree of danger expresses the degree of difficulty of covering the given area in the form of horizontal factor of the enemy situation (HF_4). The database of forces and equipment enables the rapid editing of enemy forces and equipment.

$HF_{3.2}$	Rainfall amounts
0 impassable	Larger than 80 mm
0.25	Larger than 60 mm
0.5	Larger than 40 mm
0.75	Larger than 20 mm
1 without an effect	Smaller than 20 mm

Table 1.
 The value of $HF_{3.2}$ with different rainfall amounts.

5. Friendly forces and equipment layer

The model of the optimal movement route evaluates the influence of availability of fire support executed by friendly forces and equipment based on their current position and effective range of the main weapon system. The model evaluates these facts as a supporting factor for the ability to pass through the area affected by the enemy activity via HF_5 . HF_5 expresses the degree of reduction in the impact of the enemy activity in terms of supporting the passage of the danger area of the task performance. The layer of friendly forces and equipment does not affect the passability of the area as a whole. It expresses only the ability or capabilities of friendly forces and equipment to support the maneuvering element by eliminating security risks. Thus, the combined cost surface of passability includes layers 1.4 and 5 only. The calculation of $SP_{np1.4,5}$ is then expressed by formula (5):

$$SP_{np1.4,5} = \frac{P_{np1,4}}{\min(1, HF_4 \times HF_5)} \quad (5)$$

In the areas where any combat activity of the enemy is not and even was not detected in the past, its influence on the passability in the model is not evaluated.

2.2 Combined cost surface of passability

The model of combined cost surface of passability (SP_{np}) is created by P_{np1} as a basis for its calculation and then by mathematical operations (division) of P_{np1} with HF and VF of individual layers. The SP_{np} calculation is then expressed by the mathematical formula as follows:

$$SP_{np} = \frac{P_{np1,4}}{VF_3 \times HF_3 \times \min(1, HF_4 \times HF_5)} \quad (6)$$

The result of the SP_{np} calculations is the difficulty of covering a given area in time affected by all the factors of the situation in the operation area shown in **Figure 1**.

3. Possibilities of the enemy activity influence

The enemy activity in the area of operation has the greatest influence on the planning of the movement route of forces and equipment along with the terrain passability. Estimating the future activity of the enemy is always a very complicated and intuitive matter for the analyst who processes it. Due to its uncertainty and variant implementation, it is impossible to create a mathematical algorithm that would accurately identify the intention of the enemy. However, it can be visualized based on the real terrain passability, including the weather attack, known deployment of enemy forces and equipment, and their activities in the past. The greatest deviations in the measurements were achieved outside paved roads, where hardly predictable impact of the microrelief, a driver's caution, and the dense vegetation of the terrain were evident.

3.1 Influence of detected enemy combat activity in the past

The past activity of the enemy includes the activity of his forces and equipment over the last 6 months, which can be divided according to the observed type of activity (laid minefields, barriers, IED, IDF, SAF, SVEST attacks, demonstrations, and other incidents). The geographical position, the type of activity or attack and its development, the frequency of repetition in the same areas, and the description of surroundings are critical for this kind of evaluation.

The degree of threat to the safe movement through the area can be expressed by the horizontal factor of enemy activity in the past $HF_{4,2}$, which can acquire the following average values:

- $HF_{4,2} = 0$, an impassable area, at a distance of 500 m from the site of the enemy activity, active minefields and barriers, and the repeated occurrence of attacks and incidents over the last 3 months
- $HF_{4,2} = 0.5$, at a distance of 1000 m from the site of the enemy activity and the repeated occurrence of attacks and incidents over the last 3 months
- $HF_{4,2} = 1$, without affecting the passability, at a distance of more than 1000 m from the site of the enemy activity, attacks, and incidents older than 3 months

3.2 Influence of the current deployment of enemy forces and equipment

This evaluation has already been described in a simplified fashion in the enemy situation layer. The model evaluates danger areas of the potential enemy conduct of effective fire depending on the visibility and effective range of the main weapons.

The degree of threat to the safe movement through the area may be expressed by horizontal factor of the enemy firepower $HF_{4,1}$, which attains the following values:

- $HF_{4,1} = 0$, impassable, enemy-observable area of an effective range of his weapon systems
- $HF_{4,1} = 0.5$, an area at a distance of 1 to 1.5 multiple of the effective range of the enemy weapon systems in a strip of the area observable by the enemy
- $HF_{4,1} = 1$, a passable area with minimal predictable threat, at a distance of 1.5 multiple of the effective range of the enemy weapon system in the area observable by the enemy

3.3 Databases of system information

The system input information must be structured and stored in thematic databases so that they can always be used quickly.

The information databases can be divided into:

- The TTD of friendly military equipment and weapon systems (including width, length, clearance height, weight, maximum range, terrain passability, carried weapon systems, and their effective range)
- The characteristics of performance parameters of the dismounted element (including the speed of movement at different slopes and on different terrain surfaces)

- An urbanized area (including location, population, livelihood, ethnic groups and their leaders with photographs, layout and characteristic of infrastructure, structure of state and municipal authorities, facilities, and important buildings)
- The TTD of enemy military equipment and weapon systems (including width, length, clearance height, weight, maximum range, terrain passability, carried weapon systems, and their effective range)
- Land mines and barriers
- IED attacks (date, time, location, type, description of the surrounding situation)
- IDF attacks (date, time, location, type, description of the surrounding situation)
- SAF attacks (date, time, location, type, description of the surrounding situation)
- Incidents (date, time, location, type, description of the surrounding situation)

Editing the new types of military equipment and weapon systems in the database, as well as creating a completely new database, is apparent.

4. Simulation of movement executed by enemy forces and equipment

The movement variant of the detected or predicted enemy units can be visualized in the terrain using the optimal route model and the TDSS. The editing and evaluation of the information related to all five layers identify the possibilities for performing the movement of the enemy. The specification of how to perform the movement to the system will complement the capabilities of a particular unit. The system, after selecting the initial deployment area and the projected objective area of the movement, will calculate the movement route optimized in terms of time and safety. However, an integral part of the simulated enemy movement will still be a qualified intelligence estimate of the enemy future intention, which will have to include the objective area or at least the direction of the enemy movement. Further, it will be necessary for the enemy to predict the deployment of particular friendly units so that the model could also include this factor in the calculation of the enemy movement route. Another suitable direction for the development of the TDSS will be a spatially specified and coordinated group movement of several units with the same goal. It will be necessary to specify the visualizations of movement routes of a larger concentration of enemy units with the same goal. It can provide commanders with an idea of a possible variant of the enemy activity in the whole area of responsibility of friendly forces and equipment.

5. Testing and verification of model functions

For the practical verification of the basic function and correctness of the mathematical processing and criterion evaluation of input geographical tactical information implemented in the TDSS, practical measurements have been made. The measurements have been focused on the correctness of the movement route

identification meeting the criteria of optimality in terms of the minimum time spent when covering and the calculation of the total time needed for its covering. In its implementation, most of the types of movement considered have been verified. Tracked vehicles were represented by BVP-2, wheeled vehicles by Tatra T815 (4×4), and the dismounted element by soldiers. The mean deviation of verified model results and the practical measurements besides the abovementioned extremes reached 2.74%, described in [11].

Supplemental measurements were carried out in experiments No. 1 and No. 2 relating to the movement of a reconnaissance group for the purpose of a concealed approach and the tracking of the object of interest. The same method of maneuver and approach was used in the experiment with a ground autonomous vehicle, the execution of which was calculated for the passability of wheeled vehicles. An off-road four-wheeler with a driver was simulating the vehicle, which solved the problems with the direct control of the vehicle, and the requirements for the terrain passability of wheeled vehicles were fulfilled. Experiment No. 3 was aimed at using the flanking maneuver model implemented in the TDSS. In all the cases, the enemy was made up of groups of individuals armed with hand weapons, taking up a fire position. For performing experiments No. 1 and No. 3, two groups were selected; each one consisted of four soldiers with comparable experience and skills. The commanders of both groups were soldiers who had the same level of experience in the decision-making process, terrain analysis, and leadership. All the experiments were carried out in daylight conditions in January when the temperature ranged from 2 to -2°C, without precipitation, on a frosted surface with a layer of snow cover of about 2 cm.

5.1 Experiment No. 1: Reconnaissance group movement

Both reconnaissance groups were given a task to move unnoticed and as quickly as possible to the object of interest to monitor it. The load carried by each group member included a personal weapon, individual protective equipment, and a backpack of a total weight of 20 kg. Both groups were given the task mentioned at the same time and in the same initial area. Then, their decision-making and planning process to accomplish the task followed; they planned the fastest and safest movement route to the object of interest. In the phase of approach to the object, both groups should have used the route concealed from the identified enemy units' observation in the area of maneuver and should have begun the immediate monitoring of the object. The ALFA reconnaissance group used only a printed topographic map, compass, and GPS receiver to plan and cover the movement route. The planning process of this group lasted 16 minutes. The ALFA group commander tried to estimate the conditions of the terrain passability, the visibility of the enemy, and protecting terrain features. The result of his rapid assessment was a movement route along the edge of the forest, which protected the group from the observation over a distance of more than 50 m. The route was 4190 m long (see **Figure 3**). The group covered the route in 113 minutes. During this movement, the group was not observed by the enemy soldiers. In the time of 118 minutes, the group took up positions in the vicinity of the object of interest and started its observation.

As a support for the decision-making process to create a movement route, the BRAVO reconnaissance group used the optimal movement route model, implemented in the TDSS, the possible application of which is described in [19]. The planning process of the BRAVO reconnaissance group took 7 minutes, including entering the identified enemy positions into the TDSS and the minimum necessary preparation to accomplish the task. Its route designed by the model is shown in **Figure 4**. When designing the optimal movement route, the TDSS calculated the

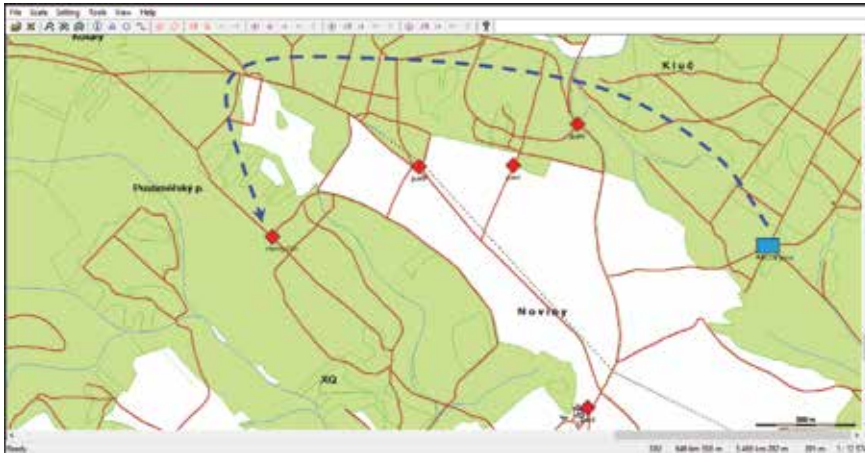


Figure 3.
The movement route of the ALFA group (source: TDSS).

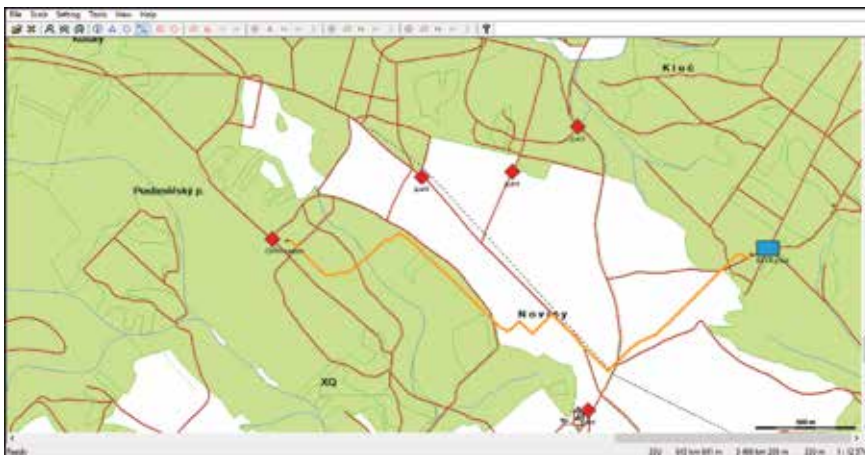


Figure 4.
The movement route of the BRAVO group (source: TDSS).

terrain passability characteristics, in which the system also included the possibilities of the enemy visibility. The priority was to lead the movement route off roads for safety reasons, which was achieved by the deliberate suppression of variable speeds on the routes in the TDSS. Through linking the calculations together, the system calculated the areas concealed from the identified enemy's observation. Subsequently, it used the areas identified in this way to create the fastest and safest movement route. The group covered the route (2963 m long) in 75 minutes. The time calculated using the TDSS to cover this route was 68 minutes. During this movement, the group was not observed by the enemy soldiers. In the time of 78 minutes, the group started observing the object of interest.

5.2 Experiment No. 2: Movement of an autonomous vehicle

Experiment No. 2 was carried out using the simulation of an autonomous vehicle in the form of a Yamaha Grizzly off-road four-wheeler (**Figure 5**) driven by one person and powered by a gasoline engine. The four-wheeler was selected due to similar terrain passability characteristics as a modern UGV. The need for direct



Figure 5.
The Yamaha Grizzly four-wheeler (source: own).

control and the influence of microrelief were eliminated thanks to the four-wheeler driver. The optimal movement route model implemented in the TDSS was used to plan and cover the UVG movement route. Entering the identified enemy positions in the TDSS and the minimum necessary preparation for the movement took 3 minutes. The UGV route was designed in the passability mode “for wheeled vehicles,” and its course can be seen in **Figure 6**. As in the BRAVO reconnaissance group, the TDSS assessed the passability possibilities of the vehicles in the field and calculated the areas concealed from the observation and fire of the identified enemy. Covering the proposed fastest and safest route (3419 m long) of the four-wheeler took 7 minutes and 25 seconds. During the movement, the vehicle at 124 cm high was not observed by the enemy. However, its engine running was audible, which could be replaced by a silent electric motor. The time calculated by the TDSS to cover this route was 7 minutes and 4 seconds.

5.3 Evaluation of experiments No. 1 and No. 2

As for the movement of reconnaissance groups in experiment No. 1, a noticeable difference in time required for planning the movement route was observed. When planning the movement route, the ALFA group commander used mainly his knowledge and experience and a printed military topographic map. He was not able

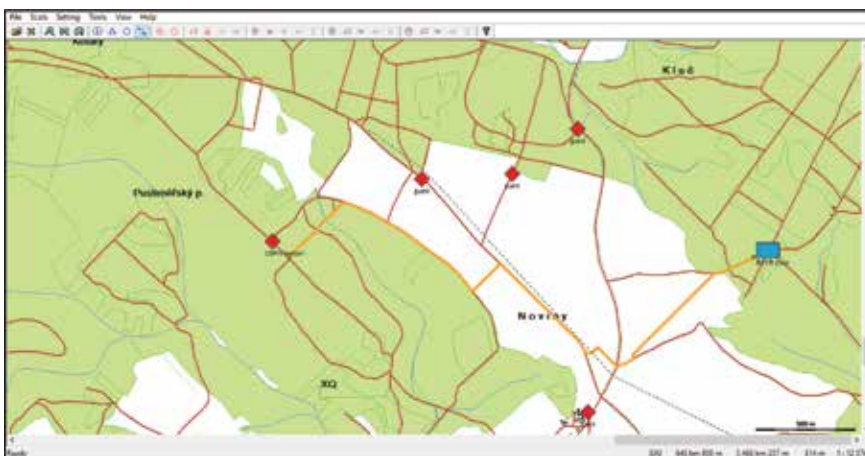


Figure 6.
Autonomous vehicle movement route (source: TDSS).

to accurately estimate the areas endangered by the enemy fire (by observation). Therefore, he directed the movement route through the forest vegetation, which provided the group with an estimated cover from observation from the ground. For planning the movement route, the BRAVO group commander took advantage of the optimal movement route model in the TDSS, which accurately calculated the areas concealed from the enemy's observation. Subsequently, the TDSS used these areas for planning the fastest and safest movement route, provided that the enemy does not significantly change his deployment or that he patrols the area. Its practical realization can be considered in terms of the necessity to fulfill the task as quickly as possible, with the acceptance of the abovementioned risk. In the case of an autonomous vehicle (four-wheeler), the route designed by the TDSS was the fastest and safest one for wheeled vehicles with variable speeds adapted to the type of vehicle (see **Figure 7**). The terrain passable for the Yamaha Grizzly off-road four-wheeler includes especially roads and open areas by the reason of its wheel undercarriage. Its height of 1240 mm is comparable to the height of the UGV, developed or used in modern armies (compare) [20]. The lower silhouette of the vehicle and the unmanned control make it possible to use even less concealed areas for the movement. The driver of the four-wheeler followed the proposed route and eliminated the impact of the microrelief on the terrain passability using the control mechanisms of the vehicle. In none of the experiments mentioned, the reconnaissance group or the four-wheeler was observed by the enemy. The movement of all elements was stopped in the area of the target object at a maximum distance of visibility. An additional change of the position of the observation post was subsequently done with the utmost care and minimum movement. In the case of four-wheeler approach, the guard of the target object would hear the sound of the vehicle engine but without locating the exact position. At that time, the four-wheeler appeared approximately 200 m from the object.

The experiments performed have proven the usefulness of the optimal maneuver model, especially when solving the situations requiring the fastest maneuver,

The screenshot shows a software window titled "Optimal route" with a close button (X) in the top right corner. The window is divided into several sections:

- Initial location:** X: 647 km 533 m, Y: 5 467 km 164 m, Z: 392.1 m
- Destination:** X: 645 km 69 m, Y: 5 467 km 209 m, Z: 404.0 m
- Distance:** By air: 2 464 m, Real: 3 419 m, Time: 0:07:04
- Buttons:** Edit initial location, Edit destination, Swap points
- Model parameters:** Type of vehicle: Wheeled vehicle (dropdown), Geodata precision: Extra high (dropdown), Load parameters, Save parameters
- Surface: roads:** Highway: 90.00 km/h, 1st class road: 90.00 km/h, 2nd class road: 70.00 km/h, 3rd class road: 60.00 km/h, Street: 40.00 km/h, Unsurfaced: 25.00 km/h, Other: 25.00 km/h
- Surface: vegetation:** Forest: 0.00 km/h, Pasture: 5.00 km/h, Field: 10.00 km/h, Other: 0.00 km/h
- Surface: other:** Water surface: 0.00 km/h, Build-up area: 0.00 km/h
- Buttons:** Close, Compute

Figure 7. Speeds of Yamaha Grizzly on individual types of surface in the TDSS (source: TDSS).

even at the price of the risk of revelation on the account of the enemy's unpredictable movement or the use of a hostile air reconnaissance. The reconnaissance of an important target, e.g., command posts or the location of fire support means, can be mentioned as examples. Using the TDSS optimal maneuver model in experiment No. 1, the total time from the receipt of the task to the attainment of readiness to fulfill it was reduced to 9 minutes. The calculation of the time to cover the movement route had a difference of 38 minutes from the real time of the ALFA group movement.

6. Maneuver control system

The optimal maneuver route model described in [11] represents the basis for optimizing the maneuver between the starting point and the target point of the maneuver. It can be used for dealing with different tactical situations and tasks on the battlefield including the UGV maneuver. One of them is an offensive maneuver performed by military forces and equipment; its technical term is flanking maneuver. The flanking maneuver represents an offensive maneuver of a part of the military unit, in which the detached forces attack on the flank and the rear of the enemy in the firing and tactical cooperation with the units attacking from the frontal direction. It is defined in [21].

One of the most significant benefits of this chapter is the flanking maneuver model, which represents the complement to the TDSS [11] in the form of the Maneuver Control System CZ application program. It is specified by the so-called invisible layer of the cost surface of passability in the form of an impassable (forbidden) area. This impassable area is in the form of a circle with a diameter equal to the distance "d" between the position of a friendly unit and an attacking unit of the enemy, but not more than 1 km. The attacking unit is divided into two independent elements, i.e., a firing group and an assault group. The TDSS suggests the maneuver route of the firing element to the nearest edge of the visibility area of the target enemy, but not more than 1 km from his position. The 1 km distance is specified in the model due to the expected maximum distance of the direct fire by handguns and mounted weapons. The firing group of the unit should be able to hold the enemy under fire at this maximum distance. Then, depending on the terrain, the assault group should be able to bypass this circular distance to the enemy and cover it. In the case of planning the offensive activity at a distance greater than 1 km, the TDSS will plan the movement route of the firing group to the nearest area with the direct visibility of the enemy (see **Figure 8**). Subsequently, it will plan the maneuver route of the assault group maintaining 1 km of the circular forbidden area. The reason is a real feasibility and success rate of the offensive maneuver in the direction of the enemy at a distance of 1 km or more while the firing group attacks on the identified enemy.

The maximum usability of the flanking maneuver in the TDSS can be considered when dealing with a response to attacking the unit by a weaker enemy, in the case of its inability to leave the attacked area completely (see **Figure 9**). Such a situation can occur, for example, in the case of multiple injuries of friendly forces or during the movement using combat vehicles. The solution of this situation can provide the enemy with the time, which he will probably use to change his position or to perform a direct attack without a direct pressure on his forces and equipment. The route of the flanking maneuver will be created outside the impassable circle, without including the layer of influence (the maximum effective range) of the target enemy. The reason for not including the target enemy's maximum effective range may be the absence of the fastest and safest route of movement to the area of his occurrence.

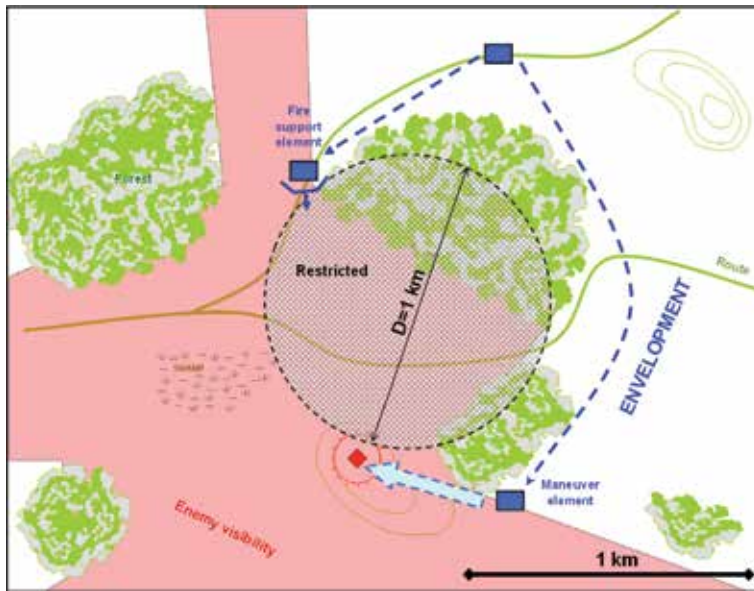


Figure 8.
The planned flanking maneuver route at a distance of more than 1 km (source: own).

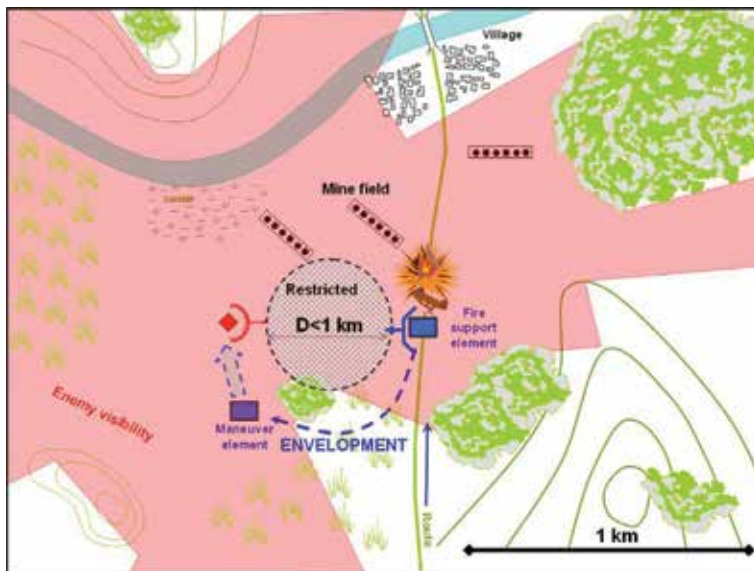


Figure 9.
The flanking maneuver route in response to the attack (source: own).

6.1 Experiment No. 3: Response to the attack

The experiment was carried out in a broken and partially forested terrain. The motorized unit was moving along the paved road. When passing through a partially open area, it was attacked by shooting handguns from an almost perpendicular direction to the paved road from a distance of approximately 230 m. The incapacitated vehicle with a severely injured driver remained at the scene of the incident. The attacker was interpreted as a group of men armed with handguns. During the

response to the attack, the unit had to provide the primary emergency treatment to the injured driver.

The commander of the attacked ALFA unit, using standard means to support decision-making (radio station and map), began to create an overview of the situation at the scene of the incident. He identified the position of the enemy based on the reports from his subordinates. He was well versed in the space distribution of his attacked unit, the attacking enemy, the open space in the shooting direction, the forest vegetation, and the relief of the terrain. The decision-making process to respond to the attack took him approximately 60 seconds. Its result was the approach maneuver of the assault group through a forest area to take up an advantageous fire position and to eliminate the enemy (see **Figure 10**). Executing the maneuver (428 m long) took 6 minutes and 50 seconds, including destroying the enemy and securing his positions.

Using the TDSS and its maneuver control system application, the commander of the attacked BRAVO unit defined the enemy's position and entered the calculation of the flanking maneuver approximately 30 seconds after the attack. Subsequently, the TDSS calculated the cost surface of passability in the area of the attack and proposed the fastest and safest route of the flanking maneuver to the position of the attackers with the use of mathematical algorithm. These calculations did not include visibility and the attackers' weapon range so that the system could plan the route in their position. Approximately 40 seconds after attack, the assault group started the flanking maneuver along the route in the direction of the enemy's position.

The route led to the position of the attackers through the forest vegetation passing into the open plain (see **Figure 11**). At the edge of the forest, the assault group took a hastily prepared firing position and almost immediately started destroying the enemy by fire. Then, it destroyed the enemy and secured his positions. The time to cover the route (369 m long) was calculated by the TDSS for 5 minutes and 3 seconds, which represented the difference of 36 seconds compared to the actual time of BRAVO unit. The delay of the real maneuver was caused by the destruction of the attackers by fire, which preceded the occupation of the target position itself.

6.2 Evaluation of experiment No. 3

When comparing both variants of experiment No. 3, a significant difference can be observed in both the speed of orientation and the decision-making process of the

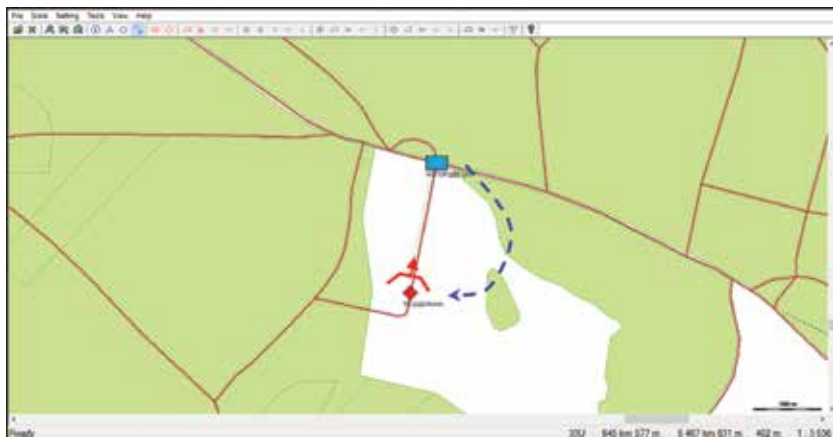


Figure 10.
The movement route of the ALFA group (source: TDSS).

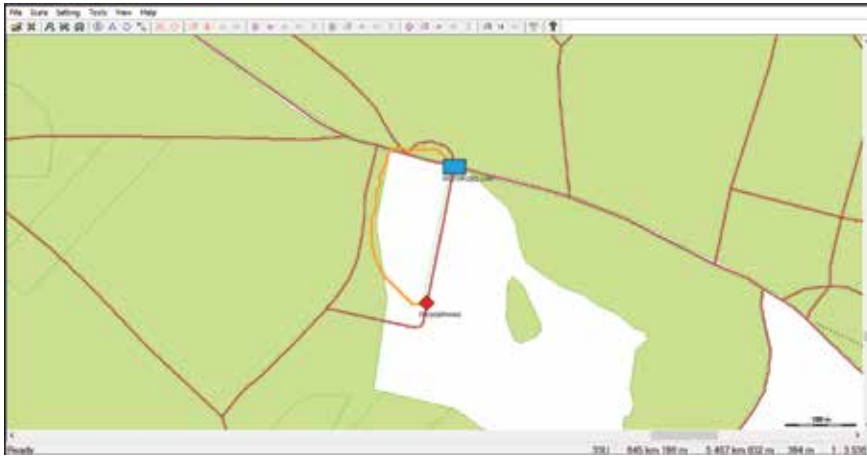


Figure 11.
The movement route of the BRAVO group (source: MCS CZ, TDSS).

attacked unit commander, as well as in the mode of maneuver execution. The difference in time of the commencement of the flanking maneuver to the enemy's position shows that the assault group of the BRAVO unit started more than 20 seconds earlier than the ALFA unit.

The terrain in the attacked area did not enable executing the direct attack, and, therefore, both units used the flanking maneuver. The maneuver route of the ALFA unit was displaced to the area where the commander expected the most advantageous and safest fire position. On the contrary, the BRAVO unit carried out the flanking maneuver using the fastest and safest route. The maneuver speed of the BRAVO unit created an effective pressure on the enemy's activity; he had to partially switch his attention to the damaged vehicle. At approximately 5 minutes and 40 seconds, after the commencement of the attack, the assault group of the BRAVO unit began firing on the enemy's position. The comparison of both responses to the attack shows that the BRAVO unit destroyed the attackers by 71 seconds faster than the ALFA unit. From the abovementioned facts, it can be stated that if the enemy did not abandon its position immediately after the commencement of the attack, he would be completely destroyed by rapid response of the BRAVO unit.

7. Conclusion

The abovementioned text has described the structure of the optimal movement route model implemented in the TDSS and its further possible use within the Maneuver Control System application. The practical benefit is a total of three experiments, in which two groups of soldiers and an autonomous vehicle simulation have been used. The results of the experiments have shown that the optimal movement route model is functional and very effective from the viewpoint of time demands for creating a movement route and the method of deploying military forces.

The optimal movement route model, implemented in the TDSS, has proven its usefulness even when planning the movement route of autonomous vehicles. In its calculations, it combines the assessment of all terrain and safety characteristics of the operational area; it also focuses on the possibilities of the passability of wheeled vehicles in the terrain. The passability of the routes calculated has been verified and confirmed during the experiments. Nevertheless, in the case of autonomous

vehicles, there is still a need for direct control in the terrain due to the accidental occurrence of microrelief forms and obstacles. The implemented model represents a basis for planning the movement route before the task fulfillment itself. The experiments realized have verified the function of the optimal movement route model when neither the reconnaissance group nor the autonomous vehicle was observed by the enemy. The total time of the UGV with the use of the TDSS to cover the route of maneuver was 67 minutes shorter than the real time of the BRAVO group movement with the use of the TDSS and 105 minutes shorter than the real time of the ALFA group without the use of the TDSS.

The TDSS calculation results are available in the order of seconds from the definition of all the tactical situation variables and the commencement of the calculation. This speed of calculation significantly minimizes time demands of the unit commanders' decision-making process. The functionality of the system has been verified in response to the enemy attacking a moving unit, the consequence of which was one incapacitated vehicle with a severely injured driver. The tactical situation of experiment No. 3 has been created precisely for the situation that demonstrates the most appropriate use of the TDSS. These are especially the situations with great time demands for creating an optimized decision, when friendly forces are endangered by the enemy. To achieve a successful solution with minimal death toll and loss of material, the decision must be taken as soon as possible after the attack of the enemy. The comparison of responses to the attack shows that the BRAVO group using the Maneuver Control System (MCS CZ) as part of the TDSS destroyed the attackers by 71 seconds faster than the ALFA group without the use of the TDSS. The optimal maneuver route model and the MCS CZ implemented in the TDSS represent the appropriate support tools for the command and control process in the military operation. They can also be used for planning a maneuver route of logistic support units and equipment if these units use UGVs for their activities in a military operation. Another possibility for using other types of autonomous vehicles is in military amphibious operations. The MCS CZ can be easily adapted to amphibious operations by adding a layer of the water surface. The standard part of the MCS CZ analyzes the terrain passability during the approach of the vehicle to the water surface. The added layer of the water surface will evaluate the character of the bottom along the coast as an approach route to the sea or to the river. The influence of direction and power of a water stream as a passability factor for amphibious vehicles as well as the standard or planned shipping lanes would also be included in this special water layer. The abovementioned MCS CZ update will reduce the risks of autonomous amphibious vehicles during the approach to the water surface and shipping.

Author details

Jan Nohel^{1*}, Petr Stodola¹ and Zdeněk Flasar²

¹ Department of Intelligence Support, University of Defense, Brno, Czech Republic

² Department of Tactics, University of Defense, Brno, Czech Republic

*Address all correspondence to: jan.nohel@unob.cz

IntechOpen

© 2019 The Author(s). Licensee IntechOpen. This chapter is distributed under the terms of the Creative Commons Attribution License (<http://creativecommons.org/licenses/by/3.0>), which permits unrestricted use, distribution, and reproduction in any medium, provided the original work is properly cited. 

References

- [1] Risald R, Mirino A, Suyoto S. Best Routes Selection Using Dijkstra and Floyd-Warshall Algorithm. 2017. pp. 155-158
- [2] Delling D, et al. Engineering route planning algorithms. *Algorithmics of Large and Complex Networks: Design, Analysis, and Simulation*, Springer; 2009. pp. 117-139
- [3] Tarapata Z. Military route planning in battlefield simulation: Effectiveness problems and potential solutions. *Journal of Telecommunications and Information Technology*. 2003;2003(4): 47-56
- [4] Rybansky M et al. Modelling of cross-country transport in raster format. *Environmental Earth Sciences*. 2015; 74(10):7049-7058
- [5] Zhanga X, Duana H. An improved constrained differential evolution algorithm for unmanned aerial vehicle global route planning. *Applied Soft Computing*. January 2015;26:270-284
- [6] González D, Pérez J, Milanés V, Nashashibi F. A review of motion planning techniques for automated vehicles. *IEEE Transactions of Intelligent Transportation Systems*. 2016;17(4):1135-1145
- [7] Hamid UZA, Saito Y, Zamzuri H, Rahman MAA, Raksincharoensak P. A review on threat assessment, path planning and path tracking strategies for collision avoidance systems of autonomous vehicles. *International Journal of Vehicle Autonomous Systems*. 2018;14(2):134-169
- [8] Campbell S, Naeem W, Irwin GW. A review on improving the autonomy of unmanned surface vehicles through intelligent collision avoidance manoeuvres. *Annual Reviews in Control*. 2012;36(2):267-283
- [9] Bureš M, Dohnal F. Verification of the mathematically computed impact of the relief gradient to vehicle speed. *Ratio Mathematica*. Pescara Italy: Accademia Piceno. 2016;30(1):23-33. DOI: 0.23755/rm.v30i1.6. ISSN 1592-7415
- [10] Pradhan A, Kumar Mahinthakumar G. Finding all-pairs shortest path for a large-scale transportation network using parallel Floyd-Warshall and parallel Dijkstra algorithms. *Journal of Computing in Civil Engineering*. 2013; 27(3):263-273
- [11] Stodola P, Nohel J, Mazal J. Model of optimal maneuver used in tactical decision support system. In: *Methods and Models in Automation & Robotics (MMAR 2016)*. Mezzidroje, Polsko: West Pomeranian University of Technology in Szczecin; 2016. pp. 1240-1245. ISBN 978-150901866-6
- [12] Nohel J. The possibilities of information support in the planning of the maneuver of units. Dissertation thesis. Brno: University of Defence; 2015. p. 101
- [13] Řehák T. Analytické možnosti GIS nad rastrovými daty. Diploma paper, Západočeská university, Plzeň, [Internet]. 2008. pp. 56-59. Available from: https://kgm.zcu.cz/studium/Zave-recnePrace/2008/Rehak_Analyticke_moznosti_GIS_nad_rastrovymi_daty_DP.pdf
- [14] Talhofer V et al. *Vojenská topografie, military publication*, Department of doctrine VeV – VA, Vyškov; 2011. pp. 186-187. Pub-28-68-01
- [15] Bureš M, Dohna LF. Verification of the mathematically computed impact of the relief gradient to vehicle speed. In: *Ratio Mathematica*; 30/2016. pp. 23-33. ISSN 2282-8214. Available from: <http://e>

iris.it/ojs/index.php/ratiomathematica/article/view/6

[16] Chalupa M, Veverka J. Simulation of track vehicle passability. In: Engineering for Rural Development; 2018. pp. 2065-2070. ISSN 1691-5976. Available from: <http://tf.llu.lv/conference/proceedings2018/Papers/N318.pdf>

[17] Mezníková L. Analysis of the shortest path on orienteering maps. Diploma paper, ČVUT University, Praha; 2011. 57 p. Available from: <http://geo.fsv.cvut.cz/proj/dp/2011/lenka-meznikova-dp-2011.pdf>

[18] Talhofer V et al. Vojenská topografie, military publication, Department of doctrine VeV – VA, Vyškov; 2011. p. 192. Pub-28-68-01

[19] Stodola P, Mazal J. Tactical decision support system to aid commanders in their decision-making. In: Modelling and Simulation for Autonomous Systems (MESAS 2016). Rome, Italy: NATO modelling and simulation centre of excellence; 2016. pp. 396-406. ISBN 978-3-319-47605-6

[20] Titan Unmanned Ground Vehicle (UGV). Army Technology [online]. London: Verdict Media Limited, 2018 [cit. 2018-12-29]. Available from: <https://www.army-technology.com/projects/titan-unmanned-ground-vehicle-ugv/>

[21] FM 100-5 OPERATIONS. Washington DC: Department of the Army; 1993. pp. 7-11

Path Planning Optimization with Flexible Remote Sensing Application

Agoston Restas

Abstract

The purpose of the path planning optimization is to find the most favorable route between starting and arrival points based on defined criteria and target functions. The change in the characteristics of each route becomes complicated when there is an increase in the number of intermediate points. This study predominately analyses the monitoring of a limited area. The author demonstrates how the path of the autonomous systems will change in different conditions and further introduces the possibility of using mobile remote sensing systems. The test is performed firstly in 2D flat area, then 3D spaces, and then—taking a forest fire as an example—the ideal conditions changed to reality. The study reveals findings on efficiency, based both on professional and economic considerations. The utilization of remote sensing technologies was found to optimize the observation of the given area generating new problems, such as what is the size of the monitored area at a given moment and how can we increase it for the higher effectiveness. An increase in the size of the monitored area results into an efficient and functional autonomous system albeit generating a shorter and modified path. Mobile autonomous systems therefore can be replaced by stable systems; simultaneously under real conditions, they can be more efficient than stable ones.

Keywords: path planning optimization, remote sensing, professional and economic analysis, 2D and 3D analysis, test in ideal and real conditions

1. Introduction

The purpose of path planning is to be able to get from point of A to B in the most efficient way. Most often we look at criteria such as the speed of travel, the shortest possible distance, the comfort, or the economy, but sometimes there are special aspects such as the minimum time for a particular route to go, the exact date of arrival, or the cost-effectiveness of the travel. The method of acquiring the most efficient solution in a given criteria is called as the optimization process. There is an abundance of literature and studies dealing with this problem, such as a common problem [1], a special problem for ground [2] or aerial vehicles [3], and a problem of industrial robots [4] or public service [5], even the author's team [6] tried to analyze the problem, that results are basically used for this study.

Path planning between two or more points may have even other goals than just doing the route. For example, during the travel we can observe the immediate surroundings of the route. If we take into account the possibility of remote sensing, the

observed field can be wider and wider when passing the route. Following this logic, we can conclude that choosing a route is not merely premised on getting from one point to another one but rather on supervising and monitoring an area of responsibility. The purpose of the area monitoring is typical for safety reason, prevention and protection against criminals, swift forest fire detection, or offering first aid to victims in case of disaster.

Following the path or monitoring, the area can be done by the traditional way meaning that the trained staff uses a vehicle; conversely it can be done in advanced way meaning that the presence of staff on board of the vehicle is no longer required. The latter can be interpreted as using the autonomous system. One of the advantages of autonomous systems is that we can eliminate human error by applying it.

The effectiveness of the autonomous system should be examined under different conditions. For easier understanding, the best method is if we start with the simplest condition that means the least distracting circumstances. This can also be called as an ideal case.

The purpose of observing an area is to detect the unrequired event or incident as soon as possible. In general, the faster the autonomous system detects the event, the more effective it is to apply. We need to look at how to optimize the path planning of the autonomous system with flexible remote sensing methods.

2. Basics of path planning

2.1 Path planning problems between two points

The purpose of path planning is to find the best route according to the desired target function between two points. The target function may have different expectations, such as making the route as short as possible or as fast as possible (1). Assuming a two-dimensional plane area and ignoring any kind of disturbing circumstance, ideally shown in **Figure 1** (left) and assuming constant speed, it means in both cases the same path and the same time spent:

$$A \rightarrow B (s \Rightarrow \min; t \Rightarrow \min) \quad (1)$$

The simplest assumption in reality is very rarely found. In most cases the natural conditions make the simplest approach impossible, which means longer paths as shown in **Figure 1** (right) and longer access times. If the ideal path between the two points is not available, you have to choose from the other options available. The number of available options may vary between zero and infinity, but both lower and upper extremes should be excluded. At the theoretical starting point, the zero option means that there is no point in the task, and with the infinite possibility, we can only count on the theory. By excluding the two extremes, we find that the number of solutions varies from 1 to a large number. The only possible path, of course, does not give a choice. The first choice appears in case of two different paths

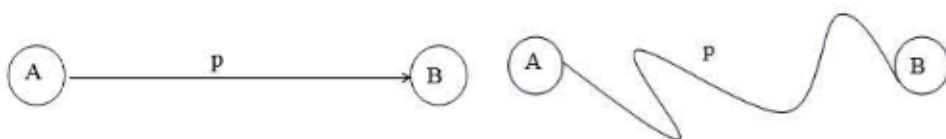


Figure 1. Path planning between points of "A" and "B" in ideal (left) and in natural (right) circumstances with only one option.

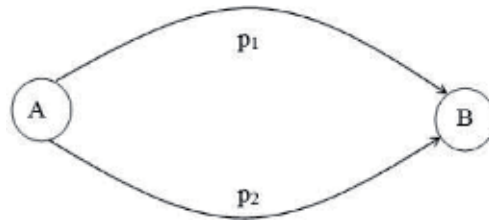


Figure 2.
Path planning options between points of “A and “B” with two different possible routes.

as shown in **Figure 2**. The quality of the different routes may be the same or different, but it is natural the better road quality allows faster progress, which means that it takes less time to do the same route length.

However, in case of different routes, choice is useless if there is no difference between them according to the target functions. The following options are available for two routes based on their length and quality:

1. The length and the quality of the two paths are the same ($s_1 = s_2$; $q_1 = q_2$).
2. The length of the two routes is different, but the quality is the same ($s_1 \neq s_2$; $q_1 = q_2$).
3. The length of the two routes is the same, but the quality is different ($s_1 = s_2$; $q_1 \neq q_2$).
4. The length and quality of the routes are different ($s_1 \neq s_2$; $q_1 \neq q_2$).

In general, the last one can be assumed. This gives new more opportunities, so the quality of the longer road can be better or worse than the shorter one and vice versa. In the latter case, when a longer road is combined with a poorer quality, it is clear this is not a choice. In the first case, when the quality of the longer road is better than the shorter one, you can get the following solutions:

1. The quality of the road is better, but not so much as to compensate the choice with time gains.
2. The quality of the road is better; however, its quality is able to compensate only for the loss of time resulting from the longer distance.
3. The quality of the road is so good that, despite the longer distance, we can achieve time gains.

The above is a mere combination of two different routes. It is easy to notice that changing the conditions makes the above more complicated. Example, if we increase the optional routes or the possibility of road quality per each new route but even with changing the quality along one route, the solutions increase exponentially. It is easy to notice that the above assumptions provide an ever-increasing choice, which is in the direction of infinity. However, a large part of the choices can be excluded, so all of those are certainly in a less favorable direction than the one that has already been examined before. As an example, all new routes with the same or worse route quality compared to a route of a given length can be excluded if they are longer than the examined one.

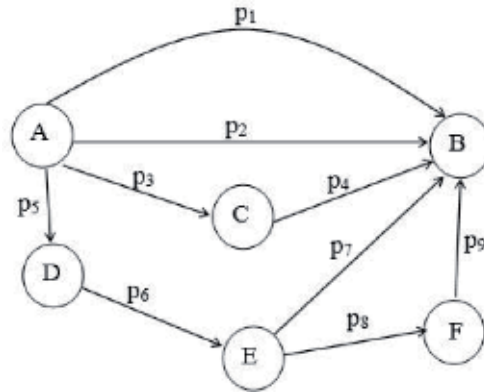


Figure 3.
An example for path planning between points of “A” and “B” in case of more options with pathway and with intermediate points.

Based on the above, it can be observed that in natural conditions there can be a significant number of solutions even between two points.

2.2 Path planning problems between several points

If we assume more than two points to be touched in the course of the route, we find that the number of options increases dramatically again as shown in **Figure 3**. Optimizing a multipoint path planning in a given plane area raises the travelling salesman problem (TSP) that has already been examined by many studies. At elementary level this question is raised hundreds years ago together with the trade development; however, as a classic scientific problem, it was mentioned firstly by Held and Karp [7] and Bellman [8]. They used dynamic programming approaches to find the solution.

Later other researchers followed these methods [9, 10], and others developed new ones offering other algorithms as well as time-dependent TSP [11] or TSP with time window and precedence constraints [12].

As new technologies appear in autonomous systems, like unmanned aerial vehicles (UAV) or drone applications, researchers found new problems and tried to give new approaches finding the best or optimized solution. Some of these studies focus only on the drone applications; others tried to combine drone application with the traditional delivery system [13, 14]. In these studies authors used different examining methods, as well as exact methods [15], heuristic methods [16–18], or approximation algorithm [14]. Bouman et al. cites a detailed summary about the above researches and results [19].

Based on the above, TSP is a very complex therefore not just natural condition, but also some idealistic assumption can generate a significant number of solutions.

3. The problem of path planning developed for area monitoring

3.1 Differences between effectiveness and efficiency

The overall goal of planning and optimizing routes is to solve practical problems in order to achieve the intended goal. This can focus only on one problem like transportation, e.g. the traveling salesman problem (TSP), in which the previous abovementioned logic can be continued, but the purpose can also be to select the path to optimize the observation of a particular area. Author calls it as the effective

patrolling path problem (E3P), where the selected area is under observation by the staff who make its supervision by continuous patrol. In this assumption the staff of the patrol can also be replaced by an autonomous system.

Obviously, the purpose of observing an area is to detect a particular event or phenomenon as early as possible. Early detection prevents the escalation of many unwanted events, for example, CCTV camera used for criminal prevention [20], aerial surveillance for forest fire detection [21, 22], or disaster escalation [23, 24]. The effectiveness of the prevention correlates to the early detection. The problem is that the patrol can see only a limited part of the supervised area, so the entire area can be divided in time into observed and not observed parts. However, the event or phenomenon can be noticed not only by the patrol but also by any other person in the area. Therefore, it is questionable who will be the first to detect the event, the patrol in duty or any other person spontaneously. This question focuses not only on the effectiveness of the applications but also on the efficiency of the autonomous systems. Patrol is costly, while spontaneous detection has virtually no cost. From the above, efficiency can be approached from several sides:

1. Performing the patrol, the average detection time is shorter than without patrol. In this case the autonomous system used for patrol is professionally effective; however, we do not take its costs in account.
2. Performing the patrol, the average detection time is shorter than without patrol; moreover, the costs of patrol will return. The latter means that the faster the detection of the event, the faster the response of the dedicated service to the event or phenomenon, which can raise the amount of the saved value or reduce the loss of the damage. In this case the saved value or the reduced damage balances or overtakes the total costs of patrolling. At this point, the application is effective not just professionally but even economically, meaning that using autonomous system is efficient.
3. The costs of patrolling can be reduced significantly while its benefit remains. In this case we are looking for different methods to further increase efficiency within a given budget, to make the use of limited resources more efficient.

Each of the above approaches requires different analyses to understand how to optimize autonomous systems with remote sensing application. Since the optimization in the reality means not only the mathematical solution but also the economical point of view, the latest author takes it in account too.

3.2 Path planning is effective in professional point of view

Previously it has been clarified that the purpose of patrol is to detect an incident or phenomenon earlier than it would be performing by other sources. Professional efficiency does not count with anything else, just to make the signal faster with a new system than without it. If the average signals performed by autonomous system are faster than without it, then the autonomous system is efficient from a professional point of view.

It is logical that, with increasing number of people present in a given area, the frequency and quickness of the report will increase statistically. The dispersion of signals from the larger population over time is broader; however, only one of the extreme values of the scatter is required, which is manifested by faster detection. Recognizing this, it can be concluded that the quickness of the report depends both on the number of people present and the population density of the area; moreover, both of them increase proportionally.

It is easy to see that in case of random but large number of event or phenomena, the average detection time of the autonomous system is equal to half of the patrolling cycle time (2). It is logical that with the increase in the density of the potential observers in the observed area, the advantage of patrol decreases. It happens because the standard deviation of the reports given by external persons decreases the amount of efficiency (3). This statement can be accepted as a logical conclusion:

$$\bar{t}_{Autonomous_report} = \frac{1}{2}t_{Autonomous_patrol} \quad (2)$$

$$\bar{t}_{Autonomous_report} < \bar{t}_{Civil_report} \quad (3)$$

- $t_{Autonomous_patrol}$: full time of the patrol, made by autonomous system
- $t_{Autonomous_report}$: average time of the report given by the autonomous system
- t_{Civil_report} : average time of reports, given by civilians

Based on the above, it can be concluded that, in the event of the occurrence of random but regular phenomena, the effectiveness of patrol in densely populated areas decreases, while in less populated areas, it increases. The rarer the population density of an area, the higher the effectiveness of patrol and vice versa: the more densely populated the area, the lower the effectiveness of patrol.

It can be concluded that patrolling can be advantageous or not advantageous, depending on the attendance and the population density of the area. Similarly, it means also the professional effectiveness or ineffectiveness. Till the average deviation of the signals given by external persons is higher than the average detection time of the autonomous systems during observations, the method is professionally effective, but no longer.

3.3 Path planning is effective in economic point of view

Economic effectiveness can be proven by counting the costs of patrolling and comparing the expected benefits of the application. In this case it is natural that the professional aspects—discussed in the previous point—are fulfilled. As a result, it is required to fulfill the professional efficiency, but this is not a sufficient condition to achieve economic effectiveness.

In case of forest fires, the response with and without patrolling had to be demonstrable in the difference of the damage caused by fire and the saved value. As a result of the previous indication, the damage is reduced to such an extent (4), which at least reaches but rather exceeds all costs of autonomous system patrol. We can approach this statement even from the opposite site that is saved value: it should expand to such an extent, which at least reaches, but rather exceeds, all costs of autonomous systems used for patrol (5). In this case, the advantageous of patrol exists not only in professional but even in economic view. The economically advantageous response also means fulfilling the condition of the national economy in broader interpretation:

$$\Delta K_{damage} > \Sigma C_{patrol} \quad (4)$$

$$\Delta M_{saved_value} > \Sigma C_{patrol} \quad (5)$$

- ΔK_{damage} : damage difference between patrolling response and non-patrolling response
- ΣC_{patrol} : total cost of patrolling
- $\Delta M_{\text{saved_value}}$: the difference of the rescued value between patrolling and non-patrolling

The operating costs of autonomous systems can only be paying back from an economic point of view if significant reductions in damage are detected by perceptions. Therefore, the total number of the perceptions during patrolling reaches or exceeds a certain level. This rate is due to the frequency of observations. The result is that a quicker detection also makes a quicker response; thus, the damage decreases, or the saved value increases, because of the escalation of the event. The total loss of damage must reach or exceed the total cost of the patrolling. The use of limited resources is efficient.

3.4 Description of the example area

The criterion of the efficiency is to get information about the change we want to detect as quickly as possible. On the one hand, this can prevent the occurrence of unwanted change (e.g. surveillance of the security area for crime prevention), and on the other hand, it can reduce the extent of change, such as the amount of resources needed for liquidation (e.g. flood management).

The negative effect caused by the phenomenon is minimal if it is detected immediately. In some cases, this may mean immediate detection (e.g. crime), while in others it is more time-consuming (e.g. forest fire detection). In this latter mentioned case, e.g. the author's experience and other sources [25–27] accept that detection within 15 min of the occurrence of a fire can be called effective. Apart from the extreme fire spread possibilities, the extent of the fire still allows for safe firefighting by using minimal power and tools.

For the purpose of path planning, we can create a large number of routes on the responsible area which should be followed by the staff during the patrol. Optimization requires the shortest route during the patrol with the same rate of observation time per a pixel of the given area. It can be observed that in ideal case pathway cannot cross itself during a cycle. Depending on the scale of the responsible area and the size of the observed pixel at the same time made by the autonomous systems, we can create many path configurations with the equivalent value as shown in **Figure 4**.

When judging the effectiveness of patrolling, the basic question is how fast the autonomous system can do a report on the detection of a problem at any location. Patrolling can be divided into a period of one cycle for a specific area of under “observation” and “non-observation”. The “blind area” can also be used for the non-observed area.

In the following, a sample area will be presented. Its parameters can be changed, so it can be adapted for other tasks as well. The area is a regular quadrilateral whose terrain condition does not limit the effectiveness of observation from the side. So it can be considered as a flat surface for the examination. The size of the examined area is 24 km × 24 km, making the whole area of 576 km².

According to the assumption, the autonomous system, which makes the patrolling, can run at different speeds on any route because of the nature of the area. It means the detection is done in two dimensions. An additional assumption is that the device installed on board of the autonomous system provides an angle of view that allows the simultaneous viewing of a 3 km × 3 km area at a given time.

Based on the above, we have the following data:

- $A = 576 \text{ km}^2$: total observation area.
- $A_{EA} = 3 \text{ km} \times 3 \text{ km} = 9 \text{ km}^2$ is the size of the pixel.
- α = focus angel of the camera.
- H_p = altitude of the patrol.
- v_p = patrol speed of the autonomous systems.
- A_o = size of the observed area in the given case.
- l = side length of a pixel.
- t_p = total cycle time of the patrol.
- L_p = total length of the patrol.
- t_o = observation time per a pixel.
- t_{blind} = non-observation time per a pixel (blind time).
- R_o = rate of observation and non-observation time per a pixel.

During the assumption the camera on board has an angle of view that allows a simultaneous viewing of a $3 \text{ km} \times 3 \text{ km}$ area at a given moment. In this test, we increase the speed of patrolling within reasonable limits, and next we increase the angle of view of the camera. Our aim is to determine how the observed and the blind area changes to an arbitrary point and what further conclusions can be drawn from the trend of change.

4. Path planning: taking into account remote sensing applications

4.1 Path planning in two dimensions with patrolling speed modification

During the examination a route which ensures that each territorial unit, the so-called pixel, was chosen and only detected once during the cycle time of the patrol. Paths can be displayed in several forms as shown in **Figure 4**, but the equivalent is essential in the case of the fulfillment of the previous condition. The initial speed of the patrolling of the autonomous system is taken to be 60 km/h , and then it increased by 30 km/h up to 180 km/h . To examine the differences, the author takes the values of **Table 1**.

Defining the values of the basic case, “A” means that the area $A = 576 \text{ km}^2$ divided into 9 km^2 ; taking $AA = 64$ units of floor area, we got the so-called pixels, which look like a chessboard. When an AA area unit has been flown at 60 km/h , the observation time is $t_o = l/v_{pA} = 3 \text{ km}/60 \text{ km/h} = 0.05 \text{ h}$, so that is 3 min . The length of the total route $L_p = 64 \times 3 \text{ km} = 192 \text{ km}$ long, which takes the next $t_p = L_p/v_p = 192 \text{ km}/60 \text{ km/h} = 3.2 \text{ h}$, that is, 192 min .

It can be seen from the values in the table that, by increasing the speed, the ratio of the observation time to the complete route is not changed ($R_o = 1/64$).

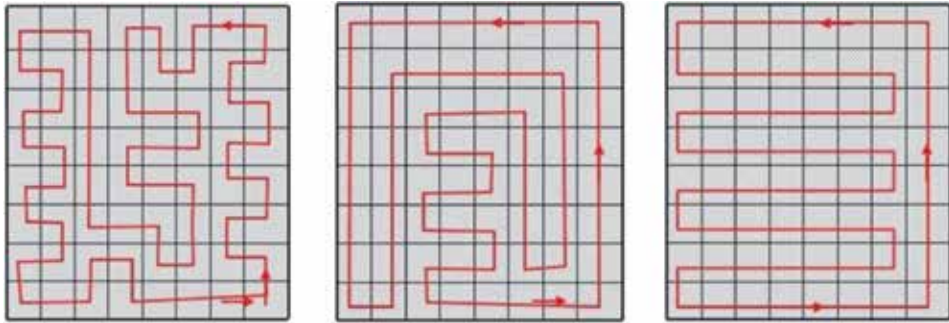


Figure 4. Examples of path planning with different pathway configurations for patrol. With constant patrol speed, the time of observation is equivalent in each pixel as well as equivalent to the length of total patrol route in each configuration.

Value event	v_p (km/h)	H_p (m)	α (°)	A_o (km ²)	l (km)	L_p (km)	t_p (min)	t_o (min)	t_{blind} (min)	R_o (-)
A	60	0	180	9	3	192	192	3	189	1/64
B	90	0	180	9	3	192	128	2	126	1/64
C	120	0	180	9	3	192	96	1.5	94.5	1/64
D	150	0	180	9	3	192	78	1.3	76.7	1/64
E	180	0	180	9	3	192	64	1	63	1/64

Table 1. Effects of changing speed of patrol for the observation time per a pixel and for the rate of observation and non-observation time.

The non-observation time frequency changes exponentially, the exponent is negative. In security checks, this result could be acceptable, but not in case of other examples like fire detection. The reason for this is that the fire increases constantly from the ignition time, so the burnt area changes exponentially. In the case of wildfires, it can be stated that the detection must be done within 15 min [25–27]. Continuing with the logic of the table, it can be calculated that it can only be provided at extremely high speed ($v_p > 720$ km/h). Based on the information above, it can be determined that by increasing the speed of the patrol, the efficiency of the detection cannot be increased (Figure 5).

The purpose of patrolling is to provide faster detection than the signals of the citizens. This allows police officers to investigate hot trail or firefighters to begin the intervention earlier. The result of it is a faster response and more saved values. If the patrolling can result faster signal, it can be considered as an effective method. Professionally, this approach is obviously true; however, the higher efficiency in the point of national economy view is not proven by this method. It is effective at national economy level only in that case if the increase of the saved values reaches or exceeds the all cost of the patrolling.

4.2 Using remote sensing: increasing the camera's angle of view

To optimize the autonomous system's path planning, we should examine what happens if the camera's angle view is changed. For it we have to take the values from Table 2. We suppose the speed of patrolling, the maximum value of the patrolling speed based on Table 1, so the value is 180 km/h. We should also take other special

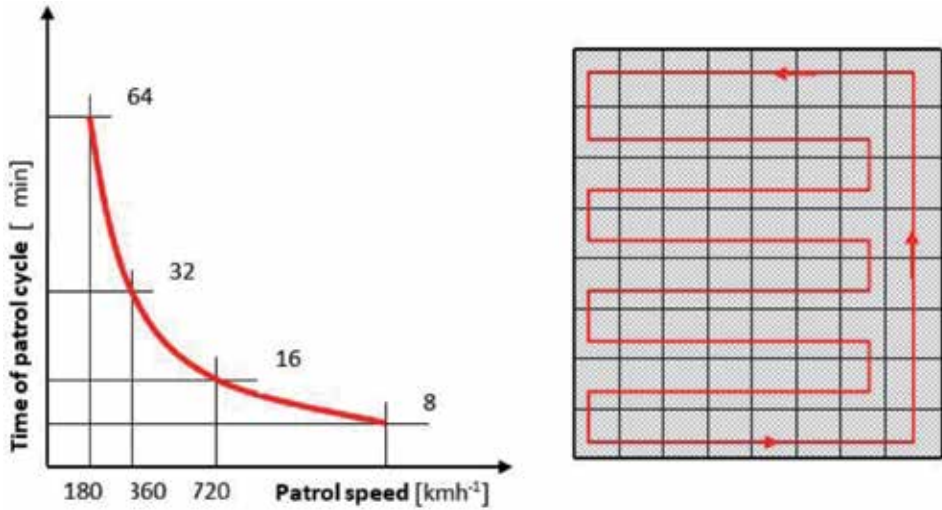


Figure 5. Correlation of patrol speed and time of patrol cycle (left) and a variation of patrol route planned for autonomous systems (right).

Value event	v_p (km/h)	H_p (m)	α_D ($^\circ$)	A_o (km ²)	l (km)	L_p (km)	t_p (min)	t_o (min)	t_{blind} (min)	R_o (-)
A	180	1500	90	9	3	192	64	1	63	1/64
B	180	1500	126	36	6	96	32	2	30	4/64
C	180	1500	151	144	12	48	16	4	12	16/64
D	—	1500	165	576	24	—	—	Cont.	—	64/64

Table 2. The effect of changing camera angle for the observed part of the area, demonstrating the theory with 1500 m path altitude.

circumstances regarding the camera’s view angle to understand the process better. Even if the patrol example in the previous subchapter was worked out at ground level, in **Table 2** the author counted with 1500 m altitude. It is performed to demonstrate with good visibility how the camera angle should change to be able to observe more than only one pixel at the same time.

The easiest way to change observation parameters is that to double the side length of the pixels, which means the territory becomes four times bigger than before. This process shows the development direction of the method. With this step we jump from the two-dimensional flat area to the three-dimensional space area that can be seen in the next subchapter even if in this moment this assumption serves only the more demonstrative understand.

It can be seen that by increasing the angle of view, the ratio of the time under observation increases exponentially comparing to the total flight time. Non-observation time reduces in the same way as well as the non-observed area but with the opposite direction as shown in **Figure 6**.

The 15 min criteria as the tipping point of the effectiveness can be satisfied at the case of line “C” in **Table 2** with $\alpha = 151^\circ$ camera angle. In this case the value of the rate of observed area and non-observed area is $1/4$. By increasing the observation angle, the observed area unit increased as shown in **Figure 7**.

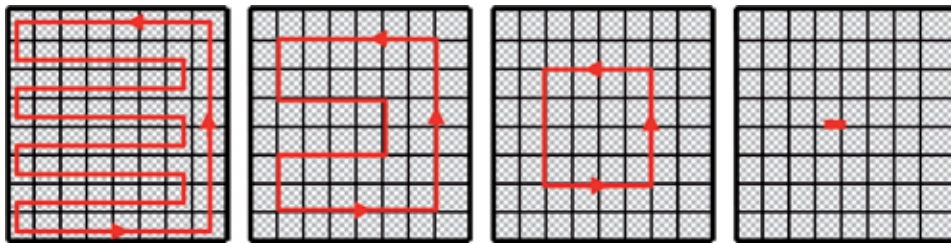


Figure 6.
The effect of changing camera angle for the flight path.

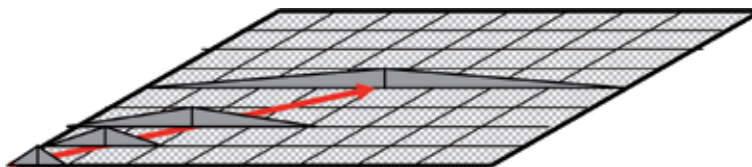


Figure 7.
Changing camera angle moves the flight path in to the centre of the observed area.

Since the sample area is delimited, the centre of the larger area unit—4 pixels, than 16 pixels—as well as the trend of the path change moves also toward to the centre of the area. In the “D” case of **Table 2**, we can see that, under certain conditions, by increasing the angle of view, the area can be monitored continuously. In conclusion, by increasing the camera’s angle of view, the efficiency of the detection can increase significantly.

Even if we used 1500 m altitude to better understand the process, it is easy to accept that the method works at non-zero but minimal altitude too. We can assume a 2–3 m high installed camera on autonomous systems like an unmanned ground vehicles (UGV), but in this case the change of camera angel is very minimal. Since the assumed speed is 180 km/h, it is much easier to take an aerial autonomous system like unmanned aerial vehicle (UAV) for this example. This assumption signs also the direction of the next examination.

4.3 Extending the possibility of patrolling by remote sensing to the third dimension

As a next step, we can unlock the criteria for monitoring in two-dimensional area or standard but relatively at low-altitude (1500 m) observation. Based on it we can examine how the results change if we extend the possibility of patrolling to the third dimension. In this case we use the aerial autonomous systems like UAVs or drones as it was explained in the previous subchapter where 1500 m altitude was used. In this example we assume the same observation area that is 576 km², the same maximum patrol speed that is 180 km/h, and the standard camera angle view that is 90°. However, we modify now the altitude of the flight path using 1500 m basic level—as it was in the previous subchapter—and raise it with double steps as well as 1500, 3000, 6000, and 12,000 m. Based on these conditions, the results are shown in **Table 3**.

It can be seen that by increasing the flight altitude, the ratio of the time under observation increases exponentially comparing to the total flight time. Non-observation time reduces in the same way but with the opposite direction as shown in **Table 3**.

Value event	V_p (km/h)	H_p (m)	α_D ($^\circ$)	A_o (km 2)	l (km)	L_p (km)	t_p (min)	t_o (min)	t_{blind} (min)	R_o (-)
A	180	1500	90	9	3	192	64	1	63	1/64
B	180	3000	90	36	6	96	32	2	30	4/64
C	180	6000	90	144	12	48	16	4	12	16/64
D	—	12,000	90	576	24	—	—	Cont.	—	64/64

Table 3.
The effect of flight altitude of autonomous system for flight path.

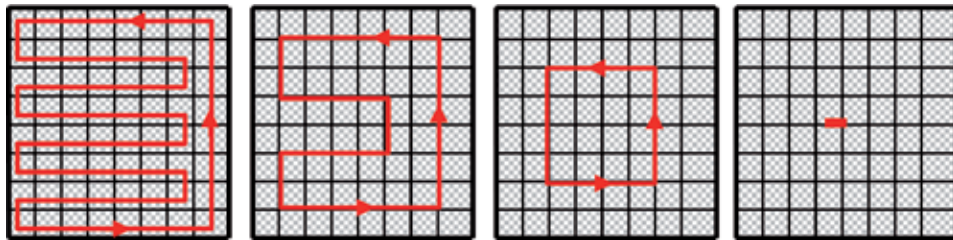


Figure 8.
Changing flight altitude moves the flight path in to the centre of the observed area.

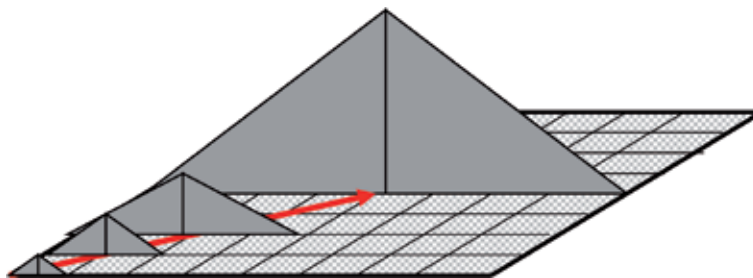


Figure 9.
Higher observation altitude means that the flight path will move to the centre of the given area.

Taking the forest fire detection as an example, the efficiency criterion is 15 min. This overflying time above the same point (pixel) can be assured at 6000 m flight altitude, ignoring the fact that the observation time ratio in this case is $\frac{1}{4}$. Increasing the observation altitude, the size of the observed area unit also increases. As the sample area is delimited, the centre of the larger area unit and the route of the patrol are moved toward the centre of the area as shown in **Figures 8** and **9**. In the “D” case of **Table 3**, we can see that by increasing the altitude, there is a point where the whole area can be monitored continuously.

Practically, the results are the same as we could see at the process of raising the camera angle view at the previous subchapter. Obvious changes of the flight paths are also the same in both cases as it can be seen in **Figures 6** and **8** as well as in **Figures 7** and **9**. Both in raising the flight altitude and the camera’s angle view the efficiency of the detection increases significantly.

According to the example, the continuous monitoring was materialized quite high, that is, at 12,000 m. The possibility of it can be carried out by a medium-altitude long-endurance (MALE) or high-altitude long-endurance (HALE) unmanned aerial vehicle (UAV) or system (UAS). Moreover, it can be served even by satellite-based monitoring systems.

The effect of raising the camera angle of the autonomous system or the flight altitude of the aerial autonomous systems, like drone, UAV, or UAS results in the same effect meaning that the path will move to the centre of the responsible area.

4.4 Comparing the mobile and stable remote sensing applications

The results from the increase of the flight altitude and of the camera angle, logically, will lead to further ascertainment. In both cases, the entire area can be observed simultaneously. This point locates in the centre of the area. From the data we can see that the speed value belonging to the centre point is zero. This is a very special situation: The camera of the autonomous system, as a monitoring device, does not require any movement, i.e. patrolling. The values in line “D” of **Table 2** and **Figure 7** show the increase of the camera’s angle view—which justifies the full observation of the area—can be ensured if the observation is not only from the same point but also from the same height! This statement proves that the application of the mobile autonomous system with the help of a stable or fixed installed autonomous system—in case of a flat area—can be theoretically triggered.

The characteristics of the function between the monitored pixels and flight altitude (left) or camera’s angle view (right) can be seen at **Figure 10**. In both cases we can see that there is a value where all pixels—which means the whole area—are under observation in the same time.

The comparison analysis based on economic base of the abovementioned ascertainment gives results as follows:

1. The camera, as a remote sensing device, would be present in both test lines, with approximately the same values in its technical parameters. Technically this would not cause a significant difference.
2. According to **Table 2**, the fixed-system monitoring rate is apparently full, so the comparison with the use of a mobile device is definitely a disadvantage of the latter.
3. While using a fixed installation system, we should choose the solution, when the camera does not see the whole area at the same time but detects it moving

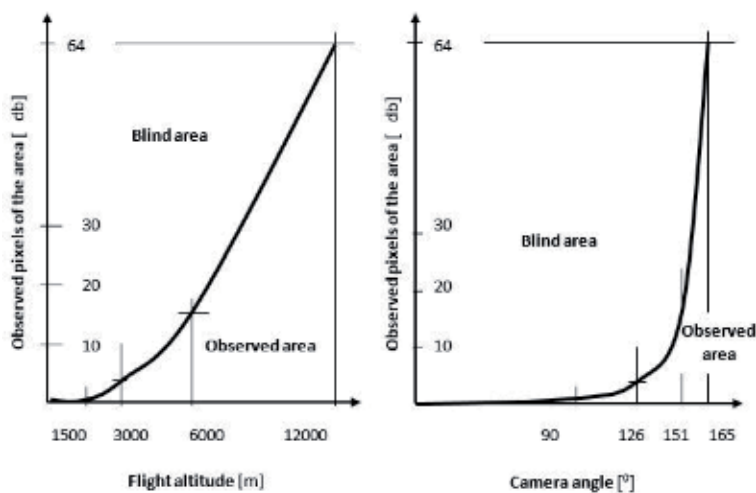


Figure 10. Rate of blind and observation area depending on raising the flight altitude (left) and the camera angle (right).

around. The advantage of this is that in its parameters, almost the same efficiency can be achieved with less power.

4. In the abovementioned case, the degree of efficiency can be calculated from the speed of rotation and the ratio of the angle of view, similar to the method used for speed testing.
5. The purchasing, operating, and personal costs of the autonomous system are very high. The investment costs of the fixed system are low. The continuous operation of the system is also low, practically free, because it does not require human intervention.

Of course, the abovementioned data are the extreme values of the mobile autonomous system's route planning. This can sometimes be an objective function, but that does not mean that it is always the only way to go, but this is the direction of increasing the efficiency by using remote sensing technology.

4.5 Examples with real circumstances

The result of the examinations above is a flat or an area which is almost flat. Aside from examining the advantages of using a fixed installed camera system and the possibilities of using an autonomous system, it is also important to examine their limitations.

4.5.1 Considering the articulation of the monitored area

The sample area allowed, for example, the detection of fire or its accompanying smoke, from the side. The latter is strongly influenced by the terrain. If there is only indirect fire detection, which is really a smoke detection (e.g. in a valley, a hill, or a fire behind a hill) in this case, the possibility of the detection is the rise of the smoke column above the mountain ridge and its visibility.

If the distribution of the terrain and the level differences are significant, the detection of smoke by a fixed monitoring system is also significant, but it may be delayed, which has an influence on the effectiveness. In this case, the efficiency of using a mobile autonomous system may again exceed the efficiency of fixed systems. [28]

The absolute criterion of the efficiency for the above mentioned case can be defined as the following: the non-observation time of using aerial patrolling is less than the average deviation of the appearance of smoke rising above the ridge due to fire development and reaching the detection threshold.

4.5.2 Considering extreme weather condition of the year

Examining the possibility of the fire detection in some periods, especially in dry seasons, the conditions of fire propagation become significantly more favorable. As a result of it, the burned area increases per unit of time. The damage will increase, the amount of power and tools for firefighting should be increased, and a higher alert state should be ordered. The time of the intervention will be longer, and costs will also increase. The firefighting units which are located far away from the fire department take a long time, the potential protection of the original location decreases, and the vulnerability of people and material goods increases. These factors also increase the risk of danger; the risks however can be reduced, if the fire department commences promptly with fire suppression efforts preferably in the early stages of the development of fire.

As a condition of this, in areas where stable fire monitoring stations are not required due to the low average risk level, it is advisable to shorten the average time of fire detection by using aerial or ground patrolling. To do this, we need to develop objective indicators which on the basis of the cost of patrolling can be recovered from an economic point of view. In this case, the interpretation of the return results from the quick firefighting of fires and the loss values.

In highly flammable periods, air reconnaissance may be more effective from an economic point of view than a stable observer station. The reason for this is that the probability of detecting air surveillance during these periods increases, so its unit costs are decreasing in relation to the number of “matches” meaning the number of detections. Due to the higher fire propagation, the unit costs are also reduced to the damages per unit time. Although it is difficult to measure, it has added benefit because people who are responsible for the fire take into consideration the air patrolling which also serves as a kind of deterrent.

5. Summarizing

This chapter examined a specific form of path planning. It has been stated that by increasing the number of the intermediate points and changing some characteristics of each path, the number of the possible options increases exponentially. It has already been confirmed by multiple literature sources, and it is part of the traveling salesman problem. The two-dimensional approach to the problem of the path planning to different points is abandoned. The chapter focused mainly on the problem of path planning in case of area observation. It further revealed that the optimization of path planning enables detection and observation of unexpected event during patrolling. If this activity is regular and targeted, we can call it patrolling and get to the effective path patrol problem (E3P). The author aimed to make an effective detection by using patrolling in a particular area.

E3P has been tested in several ways. The author assessed the effectiveness of the phenomena and the event of the detection from a professional and an economical point of view. An investigation on how to make use of the available limited resources more efficient was conducted. It has been determined that when we want to increase the speed, it is not practical to increase the efficiency, because of some objective reasons. However, by increasing the angle of view of the remote sensing system and introducing the possibility of aerial patrolling in different altitudes, the same results were achieved. Ideally, to monitor a two-dimensional particular area, the moving autonomous system can be replaced by a stable set of devices. However, apart from ideal conditions and taking three-dimensional area, we can conclude that mobile autonomous systems may be more efficient than stable systems. The optimization is entirely dependent on the on the target function we achieved and also on a particular condition system. This can usually be determined individually.

Author details

Agoston Restas
National University of Public Service, Budapest, Hungary

*Address all correspondence to: restas.agoston@uni-nke.hu

IntechOpen

© 2019 The Author(s). Licensee IntechOpen. This chapter is distributed under the terms of the Creative Commons Attribution License (<http://creativecommons.org/licenses/by/3.0>), which permits unrestricted use, distribution, and reproduction in any medium, provided the original work is properly cited. 

References

- [1] Amato NM, Wu Y. A randomized roadmap method for path and manipulation planning. In: Proceedings of the 1996 IEEE International Conference on Robotics and Automation; 1996. pp. 113-120
- [2] Sun CC, Jan GE, Lu C, Yang KC. Path planning on quadric surfaces and its application. In: Róka R, editor. *Advanced Path Planning for Mobile Entities*. London, UK: IntechOpen; 2017. DOI: 10.5772/intechopen.72573. Available from: <https://www.intechopen.com/books/advanced-path-planning-for-mobile-entities/path-planning-on-quadric-surfaces-and-its-application>
- [3] Kamrani F, Ayani R. UAV path planning in search operations. In: Lam TM, editor. *Aerial Vehicles*. Rijeka, Croatia: InTech; 2009. ISBN: 978-953-7619-41-1. Available from: http://www.intechopen.com/books/aerial_vehicles/uav_path_planning_in_search_operations
- [4] Barraquand J, Latombe J-C. Robot motion planning: A distributed representation approach. *International Journal of Robotics Research*. 1991;**10**(6):628-649
- [5] Bodnár L. Logistic problems of fighting forest fires based on case studies from Hungary. In: Linda MO, editor. *Proceedings of the 8th International Scientific Conference Wood and Fire Safety*. Zilina: EDIS Zilina University Publishers; 2016. pp. 23-32
- [6] Restás Á, Hinkley EA, Ambrosia VG. An approach for measuring the effectiveness of fire detection systems in different dimensions. *Bolyai Szemle*. 2014;**23**(3):283-296. ISSN: 1416-1443
- [7] Held M, Karp RM. A dynamic programming approach to sequencing problems. *Journal of the Society for Industrial and Applied Mathematics*. 1962;**10**(1):196-210
- [8] Bellman R. Dynamic programming treatment of the traveling salesman problem. *Journal of the ACM (JACM)*. 1962;**9**(1):61-63
- [9] Applegate DL, Bixby RE, Chvatal V, Cook WJ. *The Traveling Salesman Problem: A Computational Study*. Princeton, New Jersey, USA: Princeton University Press; 2011
- [10] Psaraftis HN. A dynamic programming solution to the single vehicle many-to-many immediate request dial-a-ride problem. *Transportation Science*. 1980;**14**(2):130-154
- [11] Malandraki C, Daskin MS. Time dependent vehicle routing problems: Formulations, properties and heuristic algorithms. *Transportation Science*. 1992;**26**(3):185-200
- [12] Mingozzi A, Bianco L, Ricciardelli S. Dynamic programming strategies for the traveling salesman problem with time window and precedence constraints. *Operations Research*. 1997;**45**(3):365-377
- [13] Condlife J. Drones get set to piggyback on delivery vans. *Technology Review*. 2016. Available from: <https://www.technologyreview.com/s/602316/drones-get-set-to-piggyback-on-delivery-vans/>
- [14] Steward J. A drone-slinging ups van delivers the future. *The Internet*. 2017. Available from: <https://www.wired.com/2017/02/drone-slinging-ups-van-delivers-future/>
- [15] Agatz N, Bouman P, Schmidt M. Optimization approaches for the traveling salesman problem with drone. *Transportation Science*. 2017;**52**(4):965-981

- [16] Murray CC, Chu AG. The flying sidekick traveling salesman problem: Optimization of drone-assisted parcel delivery. *Transportation Research Part C: Emerging Technologies*. 2015;54:86-109
- [17] Ferrandez SM, Harbison T, Weber T, Sturges R, Rich R. Optimization of a truck-drone in tandem delivery network using k-means and genetic algorithm. *Journal of Industrial Engineering and Management*. 2016;9(2):374-288
- [18] Ponza A. Optimization of drone-assisted parcel delivery [master's thesis]. Italy: University of Padova; 2016
- [19] Bouman P, Agatz N, Schmidt M. *Dynamic Programming Approaches for the Traveling Salesman Problem with Drone Networks*; Wiley Periodicals, Inc., 2018. DOI: 10.1002/net.21864. ISSN: 1097-0037
- [20] Carli V. Assessing CCTV as an effective safety and management tool for crime-solving, prevention and reduction; International Centre for the Prevention of Crime, Analysis Report, Montreal, Canada; 2008. ISBN: 978-2-921916-58-5
- [21] Yuan C, Zhang Y, Liu Z. A survey on technologies for automatic forest fire monitoring, detection and fighting using UAVs and remote sensing techniques. *Canadian Journal of Forest Research*. 2015;45(7):783-792. DOI: 10.1139/cjfr-2014-0347
- [22] Restas A. Wildfire management supported by UAV based air reconnaissance: Experiments and results at the Szendro fire department, Hungary. In: *First International Workshop on Fire Management*, Pinar del Rion, Cuba; 2006
- [23] Erdelj M, Natalizio E, Chowdhury KR, Akyildiz IF. Help from the sky: Leveraging UAVs for disaster management. *IEEE Pervasive Computing*. 2017;16(1):24-32
- [24] Restas A. Drone applications for preventing and responding HAZMAT disaster. *World Journal of Engineering and Technology*. 2016;04(03):76-84
- [25] Restas A. Optimizing drone applications at forest fire management based on economic effectiveness. In: *Forest Fire Research Abstracts Book*. Portugal: Coimbra; 2018. pp. 189-190
- [26] Martell DL, Drysdale RJ, Doan GE, Boychuk D. An evaluation of forest fire initial attack resources. In: *Interfaces*. University of Toronto, Ontario, Canada: The Institute of Management Sciences; 1984
- [27] Lenke O, Tomas P. Skúsenosti s likvidáciou lesných požiarov a vinich krajinách. *Crisis Management, Scientific-Technical Magazin of Faculty of Special Engineering at University of Zilina in Zilina*; Slovakia; 2003. ISSN: 1336-0019
- [28] Restas A. Szendro-type integrated vegetation fire management-based on remote sensing modules. *Wildfire Management Program from Hungary*. In: *5th International Workshop on Remote Sensing and GIS Applications to Forest Fire Management*, EARSeL Forest Fire SIG Meeting, Zaragoza, Spain; 2015

Distributed Optimization of Multi-Robot Motion with Time-Energy Criterion

Mohamad T. Shahab and Moustafa Elshafei

Abstract

This paper is an application of a special case of distributed optimization problem. It is applied on optimizing the motion of multiple robot systems. The problem is decomposed into L subproblems with L being the number of robot systems. This decomposition reduces the problem to solving a single robot problem. The optimization problem is solved via a distributed algorithm, utilizing subgradient method. A global objective function is set as the sum of individual robot objectives in time and energy. Constraints are divided into two sets, namely, robot-individual constraints and robots' interactions (collision) constraints. The approach is applied for the case of wheeled mobile robots: we are able to generate in parallel for each robot an optimized control input trajectory and then illustrate it in simulation examples.

Keywords: distributed algorithms, multi-robot systems, numerical optimal control, time-energy minimization

1. Introduction

Research in multi-robot systems is motivated by several notions; namely, some motivation can be put as [1]:

- It is complex for one single robot system to fulfill complex tasks. Instead, more than one system would simplify the solution.
- Tasks are generally distributed in nature.
- Multiple limited-resource robot systems are more efficient to deal with than a single powerful robot system.
- Speed of the task process increases through parallelism in multiple robot systems.
- Robustness increases as redundancy is introduced in multiple systems.

Until recently, the number of real-life implementations of multi-robot systems is relatively small. The reason is the complexity associated with the field. Also, the related technologies are relatively new. Emergence of autonomous driving vehicle

technology and market can push the boundaries in the field. As technology develops, new venues for application will open for mainstream use rather than only in research and development labs. Due to its promising applicability, autonomous cars and vehicles (or various intelligent transportation systems in general) sit at the forefront [2, 3]. To name a few, benefits include reducing congestions [4], increasing road safety [5], and, of course, self-driving cars [6]. Another application in civil environments is related to safety and security like rescue missions of searching for missing people in areas hard for humans to operate in [7] or searching for dangerous materials or bombs [8] in an evacuated building. Also, another area of application of multi-robot systems is in military area; research was done heavily in the fields of unmanned aerial vehicles (UAVs) and unmanned ground vehicles (UGVs) [9, 10].

Many approaches are developed to tackle the issue of *multiple* robot systems. Under the inspiration of biological systems and the need of technologies, many problems are defined as cooperative motions. Cooperative motion is discussed in [11–16]. Optimization in both time and energy has been tackled in the literature [17–20]. There is an opportunity to incorporate concept of time/energy optimization into the paradigm of multi-robot systems.

This paper investigates the solution of a time-energy optimal control problem for multiple mobile robots; namely, the paper is to study the problem as a nonlinear programming (NLP) problem. The main idea of the solution used here is to utilize distributed optimization techniques to solve the overall optimization problem. Solving for optimal time and energy of more than one robot system adds more burden on the problem; robot interaction with each other is added to the problem. This paper will focus more on the distributed aspect of the problem; more details about the numerical optimal control problem formulation can be found in [21]. In [21], the problem of controlling the motion of a single mobile robot is solved using the direct method of numerical optimal control (see [22]); this showed great flexibility in incorporating physical constraints and nonlinear dynamics of the system.

The rest of this section will define the global problem formulation. Discussion about distributed optimization and associated algorithm is presented in Section 2. Section 3 will apply the method on the multi-robot problem. Application to wheeled mobile robots and simulation examples are discussed in Section 4 followed by the conclusion.

1.1 Global problem formulation

We can present the discrete time global optimization (numerical optimal control) problem for L robots as follows:

$$\begin{aligned}
 & \min_{\{u^i, t_s^i\}_{\forall k, \forall i}} \sum_{\forall i} H(x^i(N)) + z^i(N) \\
 & \text{s.t.} \\
 & z^i(k+1) = z^i(k) + t_s^i(k) \cdot \{L(x^i(k), u^i(k), t_s^i(k))\} \\
 & x^i(k+1) = f_D(x^i(k), u^i(k), t_s^i(k)) \\
 & g(x^i(k), u^i(k), t_s^i(k)) \leq 0 \\
 & \Omega^i \left(\{x^i(k)\}_{\forall i}, \{u^i(k)\}_{\forall i}, \{t_s^i(k)\}_{\forall i} \right) \leq 0 \\
 & \forall k, z^i(0) = 0, x^i(0) = x_0^i, i = 1, 2, \dots, L
 \end{aligned} \tag{1}$$

with t being the time-independent variable, k being the time index in discrete domain, t_s^i being the sampling period, and N being the number of time discrete instants across the time horizon, i.e., $k = 0, 1, \dots, N$. The sampling period

corresponds to the length of time the system input $u^i(t)$ is kept constant (zero-order hold): we assume the system input to be

$$u^i(t) = u^i(k), \quad \text{for } t_k^i \leq t < t_{k+1}^i, \quad t_{k+1}^i = t_k^i + t_s^i(k), \quad t_0^i = 0, \quad \forall i$$

System behavior is governed by the nonlinear dynamic system in $f_D(x^i(k), u^i(k), t_s^i(k))$ with $x^i(k)$ as the robot i states an initial condition of $x^i(0) = x_0^i$. The above optimal control problem has a final state objective of $H(x^i(N))$ with the Lagrangian $L(x^i(k), u^i(k), t_s^i(k))$ information being embedded into a dummy state variable $z^i(k)$.

The above optimization problem can be viewed as having *two* sets of control variables; the first set resembles the discretized system inputs, $\{u^i(k)\}_{\forall k}$, and the other set consists of the variable sampling period, $\{t_s^i(k)\}_{\forall k}$. Let us have the Lagrangian for the problem be

$$L = x^T Qx + u^T Ru + \beta,$$

with β being the scalar weight on time. The performance is restricted by a collection of inequality constraints of robot-specific constraints $g(\cdot) \leq 0$ and robot-interaction constraints of $\Omega^i(\cdot) \leq 0$. The objective function is just the summation of individual objectives. In this paper, as it will be explained later, we consider only collision avoidance as robot-interaction requirement; however, the above formulation can also meet other considerations. It can be shown that the objective function in (1) corresponds to objective function of the form

$$\min \sum_{i=1}^L \left[H(x^i(t_f)) + \int_{t_0}^{t_f} x(t)^T Qx(t) + u(t)^T Ru(t) + \beta dt \right]$$

2. Distributed optimization

Here in this section, the concept of distributed optimization is explored. This area tackles optimization problems with *distributed* nature. Consider the following optimization problem:

$$\begin{aligned} \min_{\{u^i\}_{\forall i}} \sum_{i=1}^L J^i(u^i) \\ \text{s.t. } u^i \in \Omega^i, \text{ for } i = 1, \dots, L \end{aligned} \quad (2)$$

with $J^i(u^i)$ as the objective function and Ω^i the set of constraints. We can easily separate the problem into its corresponding *sub* problems. An i th subproblem is easily put as

$$\begin{aligned} \min_{u^i} J^i(u^i) \\ \text{s.t. } u^i \in \Omega^i \end{aligned} \quad (3)$$

Observing the global problem in (2), we can see that it is just equivalent to the combination of all the subproblems; it is easy to see that solving for each subproblem (3) *individually* will result in the solution for the whole global problem. Now, however, consider the following problem:

$$\begin{aligned} \min_{\{u^i\}} \sum_{i=1}^L J^i(u^i) \\ \text{s.t. } g^i(u^1, u^2, \dots, u^L) \leq 0, \forall i \end{aligned} \quad (4)$$

You see clearly that the above problem cannot be trivially separated into some subproblems due to the constraint $g^i(u^1, u^2, \dots, u^L) \leq 0$. This can be called a *complicating* constraint or a *coupling* constraint. In the next subsection, we discuss an optimization method that will help us in solving this kind of problems.

Decomposition in mathematics is the concept of breaking a mathematical problem into smaller subproblems that can be solved independently while not violating the original problem. Primary works of [23, 24] discuss multiple aspects of optimization in general while exploring specific classes as well; these works are excellent resources for reading and understanding. Viewing the applications of distributed optimization will convey the impression that they, however different, are all mostly very similar theoretically. Terms of *networked*, *distributed*, *decentralized*, *cooperative*, and the like are becoming all corresponding to somewhat similar problems. Other works related to this area and the area of multi-agent systems can be found in [25–29].

2.1 Subgradient method

Before going further, we discuss a method used in solving distributed optimization problem which will help us in solving the problem of this paper. This method is called subgradient methods [30]. These methods are similar to the popular optimization algorithms using gradient descent. However, they are extended to escape function differentiation. The works [31–33] also explore the method in the perspective of multi-agent systems.

Consider the typical problem:

$$\min_u J(u) \quad (5)$$

This typical problem can be solved using any *gradient descent* method. At iteration m of an algorithm, a solver, or an optimizer, can be constructed as

$$u_{(m+1)} = u_{(m)} - \alpha_{(m)} d_{(m)} \quad (6)$$

with $\alpha_{(m)}$ as a predefined step size. For a standard gradient method, the vector $d_{(m)}$ contains the gradient information of the problem. The simplest definition is to have

$$d_{(m)} = \nabla J(u_{(m)}) \quad (7)$$

However, for the subgradient method [33], we will have a *definition* of

$$d_{(m)} = p_{(m)} \quad (8)$$

with $p_{(m)}$, called *subgradient* of $J(u)$, being any vector that satisfies the following:

$$J(x) - J(u_{(m)}) \geq p_{(m)}^T [x - u_{(m)}], \forall x \quad (9)$$

The subgradient method is a simple first-order algorithm to minimize a possibly nondifferentiable function. The above definition escapes the requirement of a differentiated objective function. It is defined as finding any vector that makes the

optimization algorithm go to *better* value in a first-order optimality sense. Of course, when a gradient $\nabla J(u_{(m)})$ exists, we can compute the subgradient as the gradient. As it is a first-order method, it could have a lower performance than other second-order approaches. However, the advantage here is that it does not require differentiation. Also, and perhaps more importantly, it gives us flexibility to solve problems in a distributed manner as will be seen later.

Now observe the following constrained optimization problem:

$$\begin{aligned} \min_u J(u) \\ \text{s.t. } g(u) \leq 0 \end{aligned} \quad (10)$$

Let $g(u)$ be a vector of M constraints. Then, we can define the *dual problem*. Let us define the dual function of λ and u as

$$q(\lambda, u) = J(u) + \lambda^T g(u) \quad (11)$$

The vector λ of size M corresponds to the *multipliers* associated with each constraint. The dual problem relaxes the constraints of the original *primal problem* in (10) and solves for λ to maximize the *dual function*:

$$\begin{aligned} \max_{\lambda} q(\lambda, u) \\ \text{s.t. } \lambda \geq 0 \end{aligned} \quad (12)$$

The dual optimization problem is the pair of two optimization problems, namely, a maximization in λ as in (12) and a minimization in u . The pair resembles a maximization-minimization problem. You can visualize the solution of the problem as attacking the effect of constraint violation while solving for the original minimization problem concurrently.

Now, an algorithm for solving the dual problem utilizing subgradient method is discussed. Let us define

$$u(\lambda) = \arg \min_u \{J(u) + \lambda^T g(u)\} \quad (13)$$

The above definition is to clarify the minimum attained at any value of λ . So, with the above definition, at iteration m , with also denoting $u_{(m)} = u(\lambda_{(m)})$, we can safely have

$$q(\lambda, u_{(m)}) = J(u_{(m)}) + \lambda^T g(u_{(m)}) = \min_u \{J(u) + \lambda^T g(u)\} \quad (14)$$

Now, it is obvious from (14) that at iteration m , a subgradient of the dual function in (14) as function of λ can be computed as $p_{(m)} = g(u_{(m)})$. At iteration m of the algorithm, an update for the multipliers is constructed as

$$\lambda_{(m+1)} = P_{\lambda \geq 0} \{ \lambda_{(m)} + \alpha_{(m)} g(u_{(m)}) \} \quad (15)$$

The projection operator $P_{\lambda \geq 0} \{ \cdot \}$ is to ensure that the value of the update $\lambda_{(m)} + \alpha_{(m)} p_{(m)}$ is positive or enforced to zero. Also, observe the *ascent* update with the “+” sign rather than a descent update as it is a maximization. We can assume an initial $\lambda_{(0)} = 0$ or any other positive value. An optimal solution to the original problem in (10) will be attained as $m \rightarrow \infty$, with the optimal solution value of $u_{(m)}$.

2.2 The distributed algorithm

Recall the problem of combination of L subproblems in (2). Now, let us have the following global problem:

$$\begin{aligned} \min_{\{u^i\}} \sum_{i=1}^L J^i(u^i) \\ \text{s.t. } u^i \in \Omega^i, \forall i \\ g^i(u^1, u^2, \dots, u^L) \leq 0, \forall i \end{aligned} \quad (16)$$

As mentioned, the constraints $g^i(u^1, u^2, \dots, u^L) \leq 0$ are the complicating (or coupling) constraints. We can formulate the dual pair problems to be

$$\begin{aligned} \max_{\{\lambda^i\}} q(\{\lambda^i\}) \\ \text{s.t. } \lambda^i \geq 0, \forall i \end{aligned} \quad (17)$$

Put in mind that $\{\lambda^i\} = \{\lambda^1, \lambda^2, \dots, \lambda^L\}$. If we define the notations of

$$u = [u^1 \ u^2 \ \dots \ u^L]^T, \lambda = [\lambda^1 \ \lambda^2 \ \dots \ \lambda^L]^T,$$

then we can apply the *primal-dual* update from (13) and (15) at an iteration m as

$$\begin{aligned} u_{(m+1)}^* &= \arg \min_{\{u^i\} \in \Omega^i} \left\{ \sum_{i=1}^L \left\{ J^i(u^i) + [\lambda_{(m)}^i]^T g^i(u) \right\} \right\} \\ \lambda_{(m+1)} &= \mathcal{P}_{\lambda \geq 0} \left\{ \lambda_{(m)} + \alpha_{(m)} \cdot [g^1(u_{(m)}^*) \ g^2(u_{(m)}^*) \ \dots \ g^L(u_{(m)}^*)]^T \right\} \end{aligned} \quad (18)$$

We can see that the above pair of updates can easily be distributed; after the relaxing of the constraints, the primal problem can be separated. The facility of subgradients lets us propose that any iteration m for subproblem i has

$$\begin{aligned} u_{(m+1)}^i &= \varphi_{\min} \left(J^i(u_{(m)}^i) + [\lambda_{(m)}^i]^T g^i(u_{(m)}^1, u_{(m)}^2, \dots, u_{(m)}^L) \right) \\ \lambda_{(m+1)}^i &= \mathcal{P}_{\lambda^i \geq 0} \left\{ \lambda_{(m)}^i + \alpha g^i(u_{(m)}^1, u_{(m)}^2, \dots, u_{(m)}^L) \right\} \end{aligned} \quad (19)$$

The function $\varphi_{\min}(\cdot)$ is any algorithm minimizer for the primal problem constrained by $u^i \in \Omega^i, \forall i$. Observe that the primal update for each subproblem needs *only* the latest values of the other subproblem updates. During the computations of an iteration, computation of $u_{(m+1)}^i$ and $\lambda_{(m+1)}^i$ is done independent of each other; the updates above can be computed in parallel for each subproblem. The only information shared after each iteration is $u_{(m)}^1, u_{(m)}^2, \dots, u_{(m)}^L$ among all.

3. Distributed algorithm for multi-robot system

3.1 Problem formulation

Now, in this section we can apply the previous discussion into the problem of optimizing the motion of multiple robots. Recall the global optimization problem of motion of L mobile robots from (1)

$$\begin{aligned}
 & \min_{\{\mathbf{u}^i, \mathbf{t}_s^i\}_{\forall k, \forall i}} \sum_{i=1}^L H(\mathbf{x}^i(N)) + \mathbf{z}^i(N) \\
 & \text{s.t.} \\
 & \mathbf{z}^i(k+1) = \mathbf{z}^i(k) + \mathbf{t}_s^i(k) \cdot \{\mathcal{L}(\mathbf{x}^i(k), \mathbf{u}^i(k), \mathbf{t}_s^i(k))\} \\
 & \mathbf{x}^i(k+1) = f_D(\mathbf{x}^i(k), \mathbf{u}^i(k), \mathbf{t}_s^i(k)) \\
 & \mathbf{g}^i(\mathbf{x}^i(k), \mathbf{u}^i(k), \mathbf{t}_s^i(k)) \leq 0 \\
 & \Omega^i(\{\mathbf{x}^i(k)\}_{\forall i}, \{\mathbf{u}^i(k)\}_{\forall i}, \{\mathbf{t}_s^i(k)\}_{\forall i}) \leq 0 \\
 & k = 0, 1, \dots, N, i = 1, \dots, L, \mathbf{z}^i(0) = 0, \mathbf{x}^i(0) = \mathbf{x}_0^i
 \end{aligned} \tag{20}$$

You can see that the problem above is just the combination of L subproblems with superscript i corresponding to each robot. The objective function is just the summation of individual objectives. The coupling constraint of $\Omega^i(\{\mathbf{x}^i(k)\}_{\forall i}, \{\mathbf{u}^i(k)\}_{\forall i}, \{\mathbf{t}_s^i(k)\}_{\forall i}) \leq 0, \forall k$ is the only difference to the single robot problem. To simplify the notations, let us define

$$\bar{\mathbf{u}}^i = \{\mathbf{u}^i(k), \mathbf{t}_s^i(k)\}_{k=0}^N$$

The above definition is just to reduce the notation of robot input sequence. If we have, for example, two robot inputs $\mathbf{u}^i = [u_1^i \quad u_2^i]^T$ (e.g., wheel torques), then we have a total of $3 \times L \times N$ control variables of the optimization problem. We can condense notation of the global problem of multi-robot system without loss of generality to be

$$\begin{aligned}
 & \min_{\{\bar{\mathbf{u}}^i\}_{\forall i}} \sum_{i=1}^L J^i(\bar{\mathbf{u}}^i) \\
 & \text{s.t. } \bar{\mathbf{u}}^i \in \Xi^i \\
 & \Omega^i(\bar{\mathbf{u}}^1, \bar{\mathbf{u}}^2, \dots, \bar{\mathbf{u}}^L) \leq 0, \forall i
 \end{aligned} \tag{21}$$

with objectives

$$J^i(\bar{\mathbf{u}}^i) = H(\mathbf{x}^i(N)) + \mathbf{z}^i(N) \tag{22}$$

which are subject to the set of individual robot i constraints of

$$\Xi^i : \begin{cases} \mathbf{z}^i(k+1) = \mathbf{z}^i(k) + \mathbf{t}_s^i(k) \cdot \{\mathcal{L}(\mathbf{x}^i(k), \mathbf{u}^i(k), \mathbf{t}_s^i(k))\} \\ \mathbf{x}^i(k+1) = f_D(\mathbf{x}^i(k), \mathbf{u}^i(k), \mathbf{t}_s^i(k)) \\ \mathbf{g}^i(\mathbf{x}^i(k), \mathbf{u}^i(k), \mathbf{t}_s^i(k)) \leq 0 \\ \forall k, \mathbf{z}^i(0) = 0, \mathbf{x}^i(0) = \mathbf{x}_0^i \end{cases} \tag{23}$$

3.2 Distributed algorithm

Returning back to the primal-dual problem pair in Section 2, we can establish the algorithm updates according to the defined updates in (19). At each iteration m , we update each robot inputs and multipliers according to

$$\begin{aligned}
 \bar{\mathbf{u}}_{(m+1)}^i &= \varphi_{\min} \left(J^i(\bar{\mathbf{u}}_{(m)}^i) + [\lambda_{(m)}^i]^T [\Omega_{(m)}^i] \right) \\
 \lambda_{(m+1)}^i &= \mathcal{P}_{\lambda^i \geq 0} \left\{ \lambda_{(m)}^i + \alpha \Omega_{(m)}^i \right\}
 \end{aligned} \tag{24}$$

The minimizer update $\varphi_{min}(\cdot)$ is responsible to solve the single robot optimization (primal) problem according to the objective defined in (22) and subject to constraints in (23). In this paper, the minimizer update $\varphi_{min}(\cdot)$ is selected to be any state-of-the-art nonlinear programming (NLP) algorithm. Let us have the step size α for the dual update to be constant. This is sufficient for converging to a solution of the original problem [33]. You can read the algorithm updates in (24) at iteration m as each robot *independently* optimizes its whole motion throughout the whole time horizon $k = 0, 1, \dots, N$ while at the same time puts in mind the extra *cost* of cooperation/interaction with others introduced by the term $[\lambda_{(m)}^i]^T [\Omega_{(m)}^i]$ and so on.

3.3 Algorithm convergence

In this brief section, elaboration is put forth about how to practically use the algorithm. The ultimate goal is to optimize primal problem with no collision violation, i.e., reaching optimal dual (maximum) solution. At each global iteration, we only need to *improve* the primal problem values for the updated extra cost of the interaction constraint, $[\lambda^i]^T [\Omega^i]$. In this paper, a perfect solution is to optimize while maintaining $[\Omega^i]_{\forall k} \leq 0$. A logical property is to monitor the M-element vector of constraints for positive values, i.e., violations. So, a stopping criterion for the algorithm can be chosen to be some minimum change TolJ in the primal problem value:

$$|J_{(m+1)} - J_{(m)}| \leq \text{TolJ} \text{ with } J_{(m)} = \sum_{i=1}^L J(\bar{u}_{(m)}^i) \quad (25)$$

We can also *distribute* the stopping decision to individual robots by observing the change in individual objective values.

With condition (25) on its own, we cannot always be satisfying the collision requirement. So, this condition can be accompanied by a condition on the collision constraint violation. For all robots, elements of the complete constraint vector $[\Omega^i]_{\forall k}$ should be less than a relatively small positive value Tol Ω . So, for each robot, an extra stopping criterion along with criteria in (25) is to have

$$\max\left([\Omega_{(m)}^i]_{\forall k}\right) \leq \text{Tol}\Omega \quad (26)$$

Specific values of Tol Ω and TolJ depend on the nonlinear programming algorithm and/or the global desired requirements. Note that the behavior of the two tolerance parameters could be competitive with each other.

4. Application to wheeled mobile robots

4.1 System description

Figure 1 shows the individual robot system considered here. Robot state includes $x^i = [x \ y \ \phi \ \theta_R \ \theta_L \ v_R \ v_L]^T$ with both position (x, y) and orientation ϕ and $(\theta_R, \theta_L, v_R, v_L)$ as the right and left wheel angular positions and velocities, respectively. Robot input includes the respective wheel torques $u^i = [\tau_R \ \tau_L]^T$. You can have the details of the applied nonlinear dynamic model $f_D(x^i(k), u^i(k), t_s^i(k))$ based on the system model developed in [34, 35]. Details of discretization and

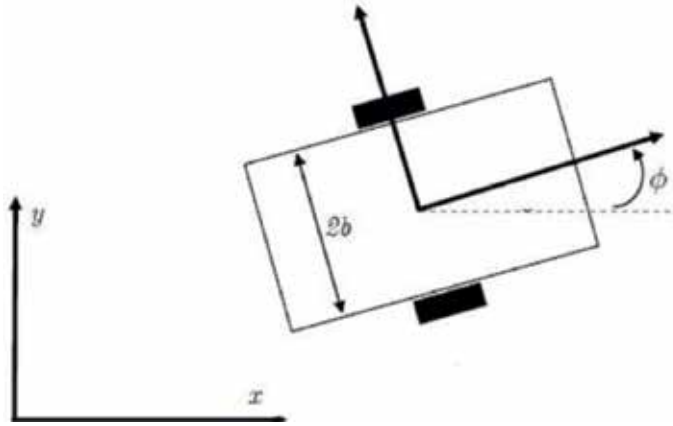


Figure 1.
 Wheeled mobile robot.

choice of parameters of the robot model can be found in [21]. As mentioned before, for choices of Q, R in Section 1, the Lagrangian for the problem is chosen to include the cost for energy spent by the torques of the wheels, the cost for kinetic energy spent by robot body, and the weight on time. Individual robot constraints include final desired configuration tolerance, torque limits, and the ensurance of zero final velocities (see more details in [36]).

4.2 Collision avoidance

Here, we will discuss the formulation and the structure of the coupling constraints. The robots can be designed to perform any cooperative strategy in their motion. Here, we only consider the global goal of optimizing the motion of each robot in time and energy while avoiding colliding with each other during the motion. Let us define the coupling constraint vector across the discrete time indexes as

$$\Omega^i(k) = \Omega^i \left(\{x^i(k)\}_{v_i}, \{u^i(k)\}_{v_i}, \{t_s^i(k)\}_{v_i} \right).$$

For the i th robot, it tries to avoid colliding with the rest of $L - 1$ robots at each of its time indexes k . Let us label elements of the constraint vector as $[\Omega^{ij}(k)]$. Each element is corresponding to a definition of constraint at time index k for all other robots, $j \neq i$. So, for each robot, the constraint vector $[\Omega^i]$ is of size $M = (L - 1) \times N$; of course, the multiplier vector λ^i in (24) is of the same size.

We define the collision avoidance by constraining motion of other robots to be outside a safety circle region around each i robot at the position (x^i, y^i) in the 2D plane:

$$(x^i(k) - \hat{x}^j(k))^2 + (y^i(k) - \hat{y}^j(k))^2 \geq p^2.$$

So, we can define each element of the constraint vector as

$$\Omega^{ij}(k) = p^2 - (x^i(k) - \hat{x}^j(k))^2 + (y^i(k) - \hat{y}^j(k))^2 \quad (27)$$

The radius of the safety region is chosen as p . Because of the definition of the sampling period variable, at each of discrete time step k , the actual time variable does *not* necessarily imply $t^i(k) = t^j(k)$ for all the other $L - 1$ robots. That is why you

see that the x- and y- coordinates in (23) of the j th robot are noted as (\hat{x}^j, \hat{y}^j) which are chosen to be calculated as linear interpolation of positions according to available actual times of $t^i(k)$ and $t^j(k)$.

4.3 Simulation examples

You can follow the whole distributed algorithm for the time-energy optimization of multi-robot system with collision avoidance in the flowchart in **Figure 2**. View the flowchart as the process for each individual robot (subproblem). We implement the algorithm in **Figure 2**. For the primal minimizer update in (24), the nonlinear programming (NLP) function of `fmincon` in MATLAB is used. We solved the problem for motion of $L = 3$ mobile robots. Utilizing the parallel capability in MATLAB, the distributed steps are solved independently utilizing three parallel processors. We choose number of instants $N = 40$; so, we are going to optimize 120 control variables for each robot. More details can be found in [36].

Example 1. In this example, exploration of the behavior of the algorithm is shown. The problem has the following desired values of initial and final positions and orientations for the three robots:

$$(x_0^1, y_0^1, \phi_0^1) = \left(0, -8, \frac{\pi}{2}\right), (x_f^1, y_f^1, \phi_f^1) = (0, 5, \pi)$$

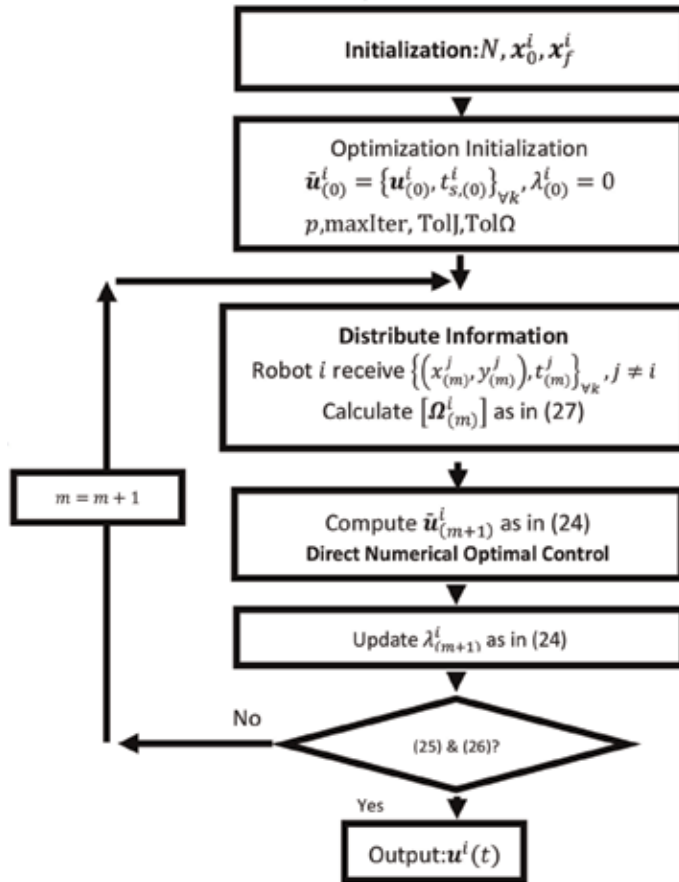


Figure 2. Distributed algorithm flowchart to optimize multi-robot motion.

$$(x_0^2, y_0^2, \phi_0^2) = (-10, -1, 0), (x_f^2, y_f^2, \phi_f^2) = \left(8, 5, \frac{\pi}{2}\right)$$

$$(x_0^3, y_0^3, \phi_0^3) = (5, 0, \pi), (x_f^3, y_f^3, \phi_f^3) = \left(-8, -1, \frac{\pi}{2}\right)$$

Here, robot 1 has equal objective weights of 5 on both time and energy, robot 2 has weights of 10 on energy and 1 on time, and robot 3 has 10 on time and 1 on energy. The maximum number of internal NLP iterations (primal update) is set to

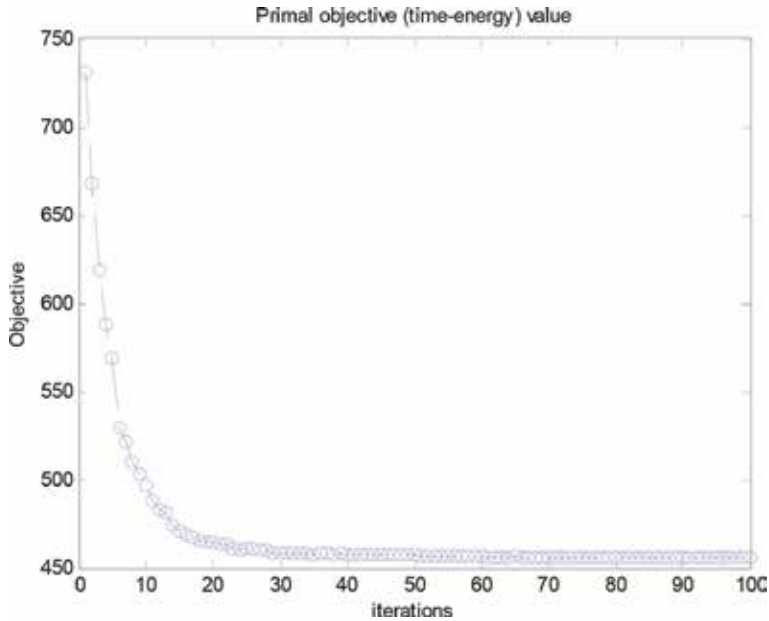


Figure 3.
 The time-energy objective values throughout global iterations (Example 1).

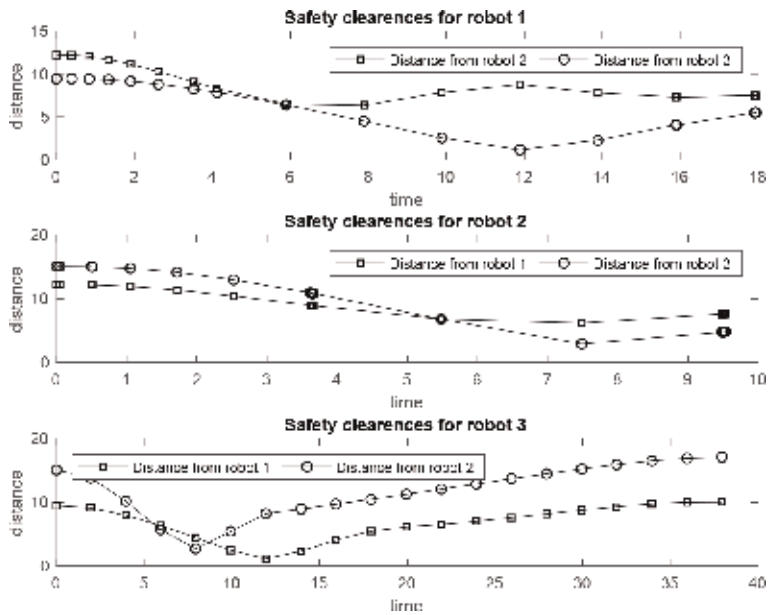


Figure 4.
 Collision avoidance (Example 1).

only 10. The step size is set to $\alpha = 0.1$. Maximum global iterations are allowed for 100 iterations. The safety circle radius is chosen to be $p = 2$.

Figure 3 contains the objective (time-energy) value evolution throughout iterations. You can see the stable convergence as the algorithm progresses. **Figure 4** shows each of the robots' safety clearances during the optimized motion. In **Figure 5**, snapshots of motion of the three robots at different time instants are depicted. This illustrates the collision avoidance attained throughout the optimized motion. Observe also how different are the speeds of each robot because of objective weights; note from **Figure 4** that each robot has a different final time for their motion. The algorithm has shown good performance at eliminating collision constraint violations. **Figures 4** and **5** show an instant (around $t = 12$) where robots 1 and 3 violate collision distance with very small value, but no collision occurs. This is because the maximum number of iterations of the algorithm is exhausted. This

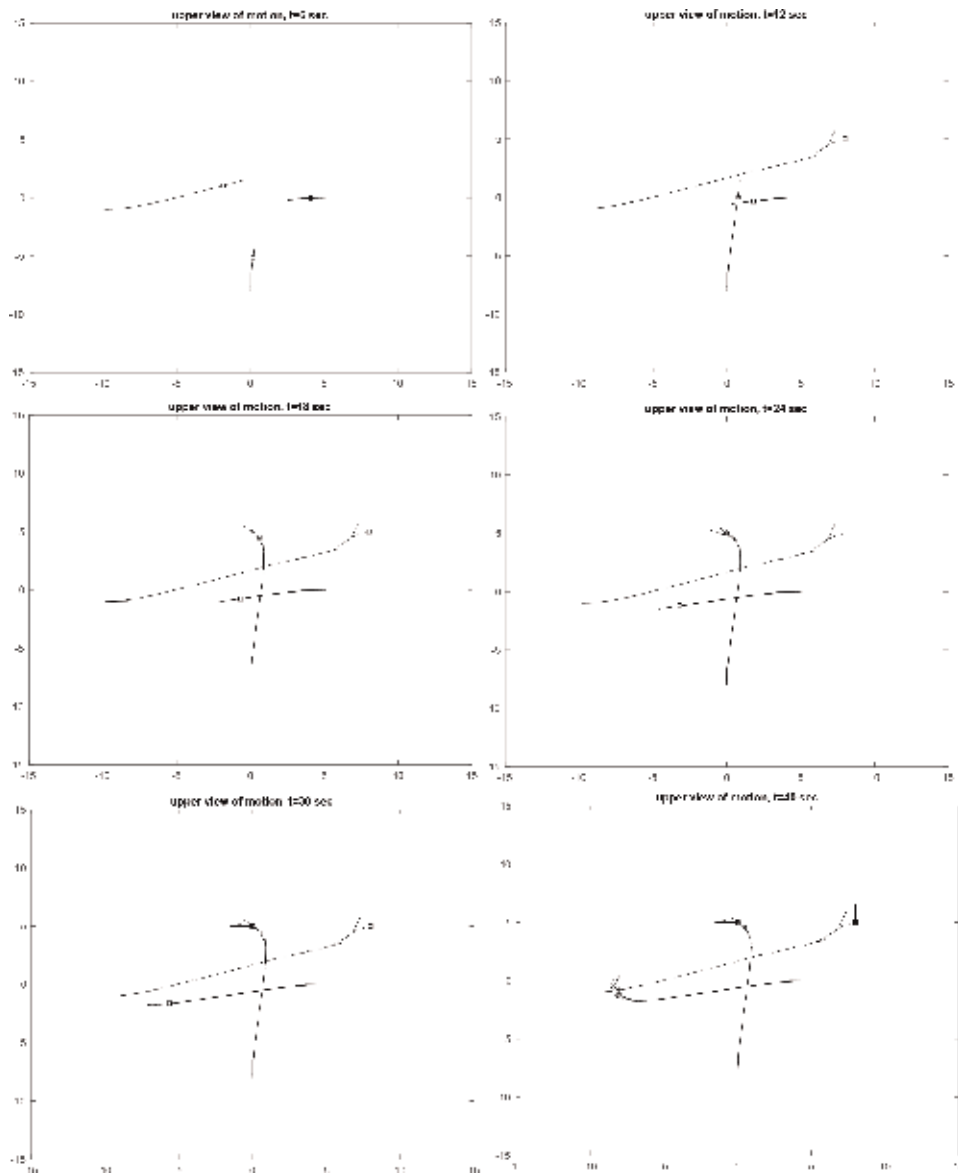


Figure 5. Snapshots of optimized motions at different instants (Example 1).

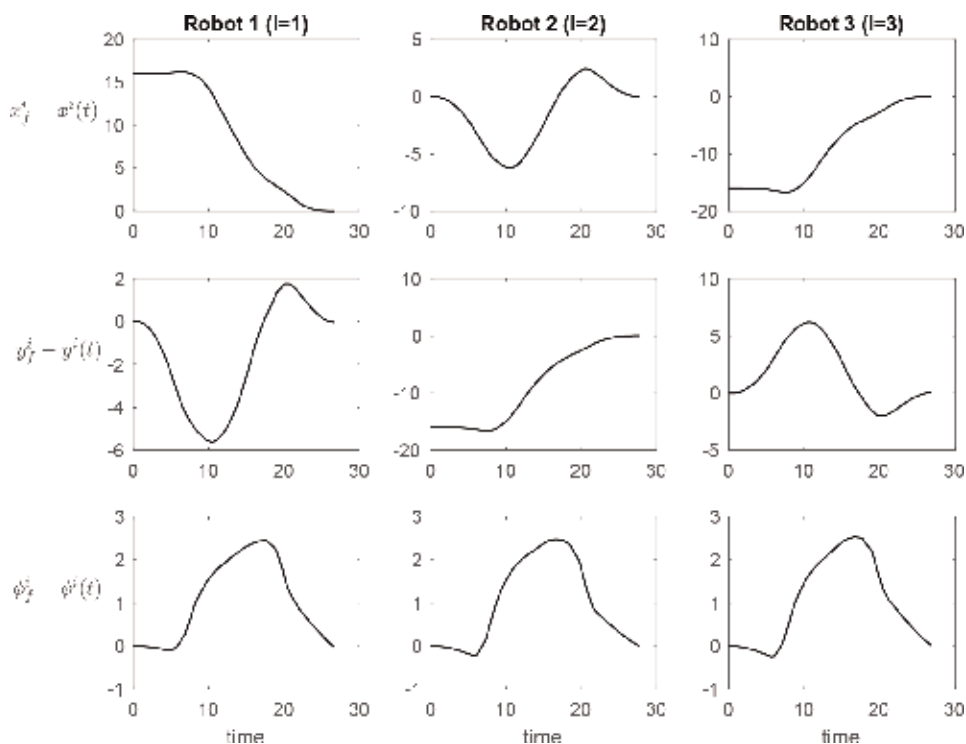


Figure 6. Optimized trajectories of the three robots: each row of plots shows x-coordinate error, y-coordinate error, and orientation error, respectively; each column of plots show robots 1, 2, and 3 errors, respectively (Example 2).

indicates the possibility for the motion to be optimized even more if collision constraints were relaxed or if more algorithm iterations were allowed. Initialization of the algorithm also plays a role in algorithm evolution.

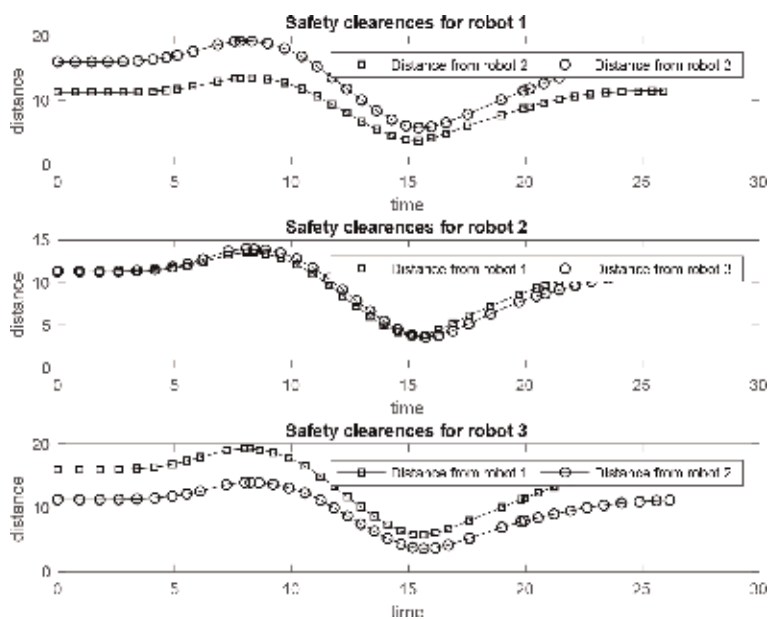


Figure 7. Collision avoidance (Example 2).

Example 2. This example illustrates more the satisfaction of the objectives. In this example the safety circle radius is put as $p = 3$. Here we choose the following initial and final positions and orientations for the three robots:

$$\begin{aligned}(x_0^1, y_0^1, \phi_0^1) &= \left(-8, 0, \frac{\pi}{2}\right), (x_f^1, y_f^1, \phi_f^1) = \left(8, 0, \frac{\pi}{2}\right) \\(x_0^2, y_0^2, \phi_0^2) &= (0, 8, 0), (x_f^2, y_f^2, \phi_f^2) = (0, -8, 0) \\(x_0^3, y_0^3, \phi_0^3) &= \left(8, 0, -\frac{\pi}{2}\right), (x_f^3, y_f^3, \phi_f^3) = \left(-8, 0, -\frac{\pi}{2}\right)\end{aligned}$$

After applying our approach, you can see the resulting optimized motions in **Figure 6**. In **Figure 6**, errors in x- and y-coordinates and orientation of each robot are shown with respect to time. It is clear that errors of zero are achieved. In **Figure 7** for each robot, constraint evaluations, i.e., safety clearance, are displayed for the other two robots throughout time. You can see that robots come close to each other sometimes but without violating the safety distance. This result is attained maybe because of special structure of initial and final positions and orientations. That could have given flexibility for the algorithm.

5. Conclusion

The paper investigated the time-energy minimization onto the multi-robot case. A global objective function is formulated as the sum of individual robot objectives in time and energy. Constraints are divided into two sets, namely, robot-individual constraints and robots' interaction constraints. The problem is decomposed into L subproblems with L being the number of robot systems. The subproblems are coupled with each other by the collision avoidance information. Applying a distributed algorithm solved the problem iteratively. The overall output gives optimized motions for all robots in time and energy while adhering and not colliding with each other. We applied our approach to the case of three wheeled mobile robots: we generated in parallel for each robot an optimized control input trajectory.

An extension to this study is to generate optimized motion trajectories and apply them experimentally. A possible area for experimentation is full-scale autonomous vehicles. Issues related to communication and distributing information during the parallel algorithm will need to be incorporated and investigated. Also, aspects of state estimation and localization of the robot system will come into the place which were not considered in this work. A possible other investigation is to distribute the problem further onto the time variable k ; this will lead the problem to the domain of distributed model predictive control. This will, possibly, pave the way to faster deployment into autonomous vehicles.

Acknowledgements

The authors would like to thank King Fahd University of Petroleum and Minerals supporting this work.

Author details

Mohamad T. Shahab^{1*} and Moustafa Elshafei²

1 Department of Electrical and Computer Engineering, University of Waterloo, ON, Canada

2 Zewail City of Science and Technology, October Gardens, 6th of October City, Giza, Egypt

*Address all correspondence to: m4shahab@uwaterloo.ca

IntechOpen

© 2019 The Author(s). Licensee IntechOpen. This chapter is distributed under the terms of the Creative Commons Attribution License (<http://creativecommons.org/licenses/by/3.0>), which permits unrestricted use, distribution, and reproduction in any medium, provided the original work is properly cited. 

References

- [1] Siciliano B, Khatib O, editors. Springer Handbook of Robotics. In: Springer Science & Business Media. Berlin/Heidelberg; 2008
- [2] Thrun S. What we're Driving At. The Official Google Blog. 2011. Available from: <https://googleblog.blogspot.com/2010/10/what-were-driving-at.html> [Accessed: 23 Jan 2019]
- [3] Ioannou P, editor. Automated Highway Systems. Boston, MA: Springer Science & Business Media; 1997
- [4] Kurzhanskiy AA, Varaiya P. Traffic management: An outlook. *Economics of Transportation*. 2015;4(3):135-146
- [5] Huang C-L, Fallah YP, Sengupta R, Krishnan H. Adaptive intervehicle communication control for cooperative safety systems. *Network, IEEE*. 2010; 24(1):6-13
- [6] Guizzo E. How Google's self-driving car works. *IEEE Spectrum Online*. 2011. Available: <https://spectrum.ieee.org/automaton/robotics/artificial-intelligence/how-google-self-driving-car-works>
- [7] Burgard W, Moors M, Stachniss C, Schneider FE. Coordinated multi-robot exploration. *IEEE Transactions on Robotics*. 2005;21(3):376-386
- [8] Ferranti E, Trigoni N, Levene M. Brick & Mortar: An on-line multi-agent exploration algorithm. In: *Robotics and Automation, 2007 IEEE International Conference on*. 2007. pp. 761-767
- [9] Beard RW, McLain TW, Nelson DB, Kingston D, Johanson D. Decentralized cooperative aerial surveillance using fixed-wing miniature UAVs. *Proceedings of the IEEE*. 2006;94(7):1306-1324
- [10] Das AK, Fierro R, Kumar V, Ostrowski JP, Spletzer J, Taylor CJ. A vision-based formation control framework. *IEEE Transactions on Robotics and Automation*. 2002;18(5): 813-825
- [11] Jadbabaie A, Lin J, Morse AS. Coordination of groups of mobile autonomous agents using nearest neighbor rules. *IEEE Transactions on Automatic Control*. 2003;48(6): 988-1001
- [12] Murray RM. Recent research in cooperative control of multivehicle systems. *Journal of Dynamic Systems, Measurement, and Control*. 2007; 129(5):571-583
- [13] Fax JA, Murray RM. Information flow and cooperative control of vehicle formations. *IEEE Transactions on Automatic Control*. 2004;49(9): 1465-1476
- [14] Olfati-Saber R. Flocking for multi-agent dynamic systems: Algorithms and theory. *IEEE Transactions on Automatic Control*. 2006;51(3):401-420
- [15] Gazi V, Passino KM. Stability analysis of swarms. *IEEE Transactions on Automatic Control*. 2003;48(4): 692-697
- [16] Desai JP, Ostrowski JP, Kumar V. Modeling and control of formations of nonholonomic mobile robots. *IEEE Transactions on Robotics and Automation*. 2001;17(6):905-908
- [17] Khoukhi A, Baron L, Balazinski M. Constrained multi-objective trajectory planning of parallel kinematic machines. *Robotics and Computer Integrated Manufacturing*. 2009;25(4):756-769
- [18] Bobrow JE. Optimal robot plant planning using the minimum-time criterion. *IEEE Journal of Robotics and Automation*. 1988;4(4):443-450

- [19] Sergaki ES, Stavrakakis GS, Pouliezios AD. Optimal robot speed trajectory by minimization of the actuator motor electromechanical losses. *Journal of Intelligent and Robotic Systems*. 2002;**33**(2):187-207
- [20] Sun Z, Reif JH. On finding energy-minimizing paths on terrains. *IEEE Transactions on Robotics*. 2005;**21**(1): 102-114
- [21] Shahab MT, Khoukhi A, Al-Sunni F. Time-energy optimal control of a mobile robot using direct numerical method. arXiv preprint arXiv:1312.7088; 2013
- [22] Chachuat B. *Nonlinear and Dynamic Optimization: From Theory to Practice*. Switzerland: Automatic Control Laboratory, EPFL; 2007
- [23] Bertsekas DP, Nedic A, Ozdaglar AE. *Convex Analysis and Optimization*. Belmont, MA: Athena Scientific; 2003
- [24] Stephen B, Xiao L, Mutapcic A, Mattingley J. *Notes on Decomposition Methods*. Notes for EE364B. Stanford, CA: Stanford University; 2007
- [25] Zhu M, Martinez S. An approximate dual subgradient algorithm for multi-agent non-convex optimization. *IEEE Transactions on Automatic Control*. 2013;**58**(6):1534-1539
- [26] Terelius H. *Distributed multi-agent optimization via dual decomposition* [PhD diss.]. Stockholm, Sweden: KTH; 2010
- [27] Bhattacharya S, Kumar V. *Distributed optimization with pairwise constraints and its application to multi-robot path planning*. *Robotics: Science and Systems VI*. 2011;177
- [28] Johansson B. *On distributed optimization in networked systems* [PhD diss.]. Stockholm, Sweden: KTH; 2008
- [29] Kuwata Y, How J. Decentralized cooperative trajectory optimization for UAVs with coupling constraints. In: *Decision and Control, 2006 45th IEEE Conference on*. 2006. pp. 6820-6825
- [30] Boyd S, Mutapcic A. *Subgradient methods*. In: *Lecture Notes of EE364b*. Stanford, CA; Stanford University
- [31] Nedic A, Ozdaglar A. Distributed subgradient methods for multi-agent optimization. *IEEE Transactions on Automatic Control*. 2009;**54**(1):48-61
- [32] Nedic A, Ozdaglar A, Parrilo PA. Constrained consensus and optimization in multi-agent networks. *IEEE Transactions on Automatic Control*. 2010;**55**(4):922-938
- [33] Nedic A, Ozdaglar A. Cooperative distributed multi-agent optimization. In Eldar Y, Palomar D, editors. *Convex Optimization in Signal Processing and Communications*. Cambridge: Cambridge University Press; 2010. pp. 340-386
- [34] Fukao T, Nakagawa H, Adachi N. Adaptive tracking control of a nonholonomic mobile robot. *IEEE Transactions on Robotics and Automation*. 2000;**16**(5):609-615
- [35] Yamamoto Y, Yun X. Coordinating locomotion and manipulation of a mobile manipulator. *IEEE Transactions on Automatic Control*. 1994;**39**(6): 1326-1332
- [36] Shahab MT. *Time-energy optimization of motion of multi-robot system* [master thesis]. Saudi Arabia: King Fahd University of Petroleum and Minerals; 2014

*Edited by Umar Zakir Abdul Hamid,
Volkan Sezer, Bin Li, Yanjun Huang
and Muhammad Aizzat Zakaria*

Path Planning (PP) is one of the prerequisites in ensuring safe navigation and manoeuvrability control for driverless vehicles. Due to the dynamic nature of the real world, PP needs to address changing environments and how autonomous vehicles respond to them. This book explores PP in the context of road vehicles, robots, off-road scenarios, multi-robot motion, and unmanned aerial vehicles (UAVs).

Published in London, UK
© 2019 IntechOpen
© JC DeLa Cuesta / unsplash

IntechOpen

